Cart3D Simulations for the First AIAA Sonic Boom Prediction Workshop

Michael J. Aftosmis

Applied Modeling & Simulations Branch
NASA Ames Research Center
Moffett Field, CA 94035
michael.aftosmis@nasa.gov

Marian Nemec

Science and Technology Corp.
Applied Modeling & Simulations Branch
Moffett Field, CA 94035
marian.nemec@nasa.gov

11 Jan 2014, National Harbor, Maryland, USA

Note:

- Full paper available on-line AIAA 2014-0558

- Presentation is Tuesday Jan 14 @ 3:30 in Applied CFD

Introduction – Cart3D

Meshing:

- Multi-level Cartesian mesh with embedded boundaries
- Insensitive to geometric complexity
- Adjoint-based mesh adaptation

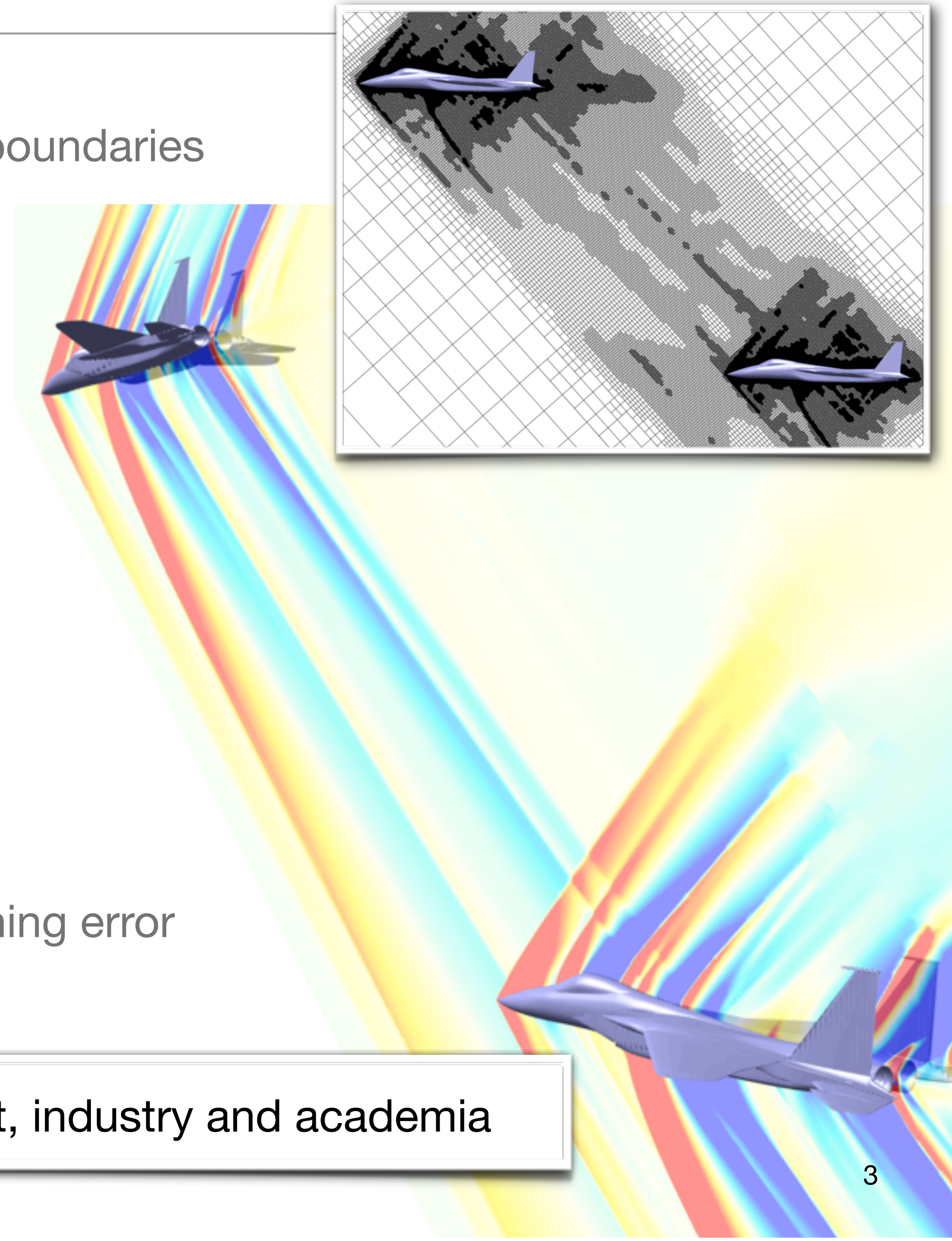

Inviscid flow solver

- Monotone second-order upwind method
- Tensor slope limiters preserve k-exactness
- Runge-Kutta with multigrid acceleration
- Domain decomposition for scalability

Output-based mesh adaptation

- Duality-preserving discrete adjoint
- Provides output correction & error estimate
- Adjoint-based mesh refinement using remaining error

Broad use throughout NASA, US Government, industry and academia

Boom problems with Cartesian Mesh Methods

Goal: Accurate prediction of near/mid-field pressure signatures

- Mesh adaptation to pressure sensor output

$$\mathcal{J}_{\text{sensor}} = \int_0^L \frac{(p - p_\infty)^2}{p_\infty} dl$$

- Mesh rotation to ~Mach angle
- Mesh stretching along dominant direction of wave propagation
- See: *AIAA 2008-0725, 6593 &* *AIAA 2013-0649*

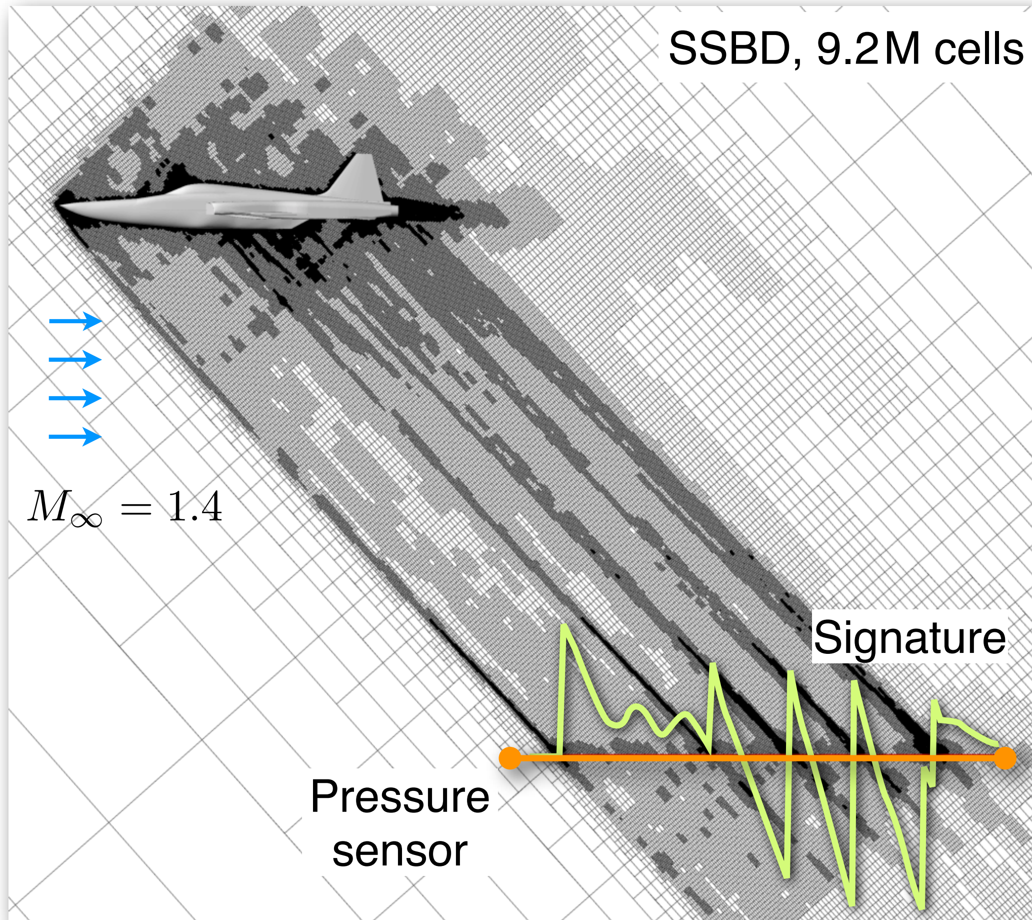

AIAA 2008-6593, Wintzer et al.

Nomenclature

Cylindrical coordinates used for sonic boom

x : Distance along sensor (axial distance)

h : Distance from axis (radius)

Φ : Off-track angle (azimuth)

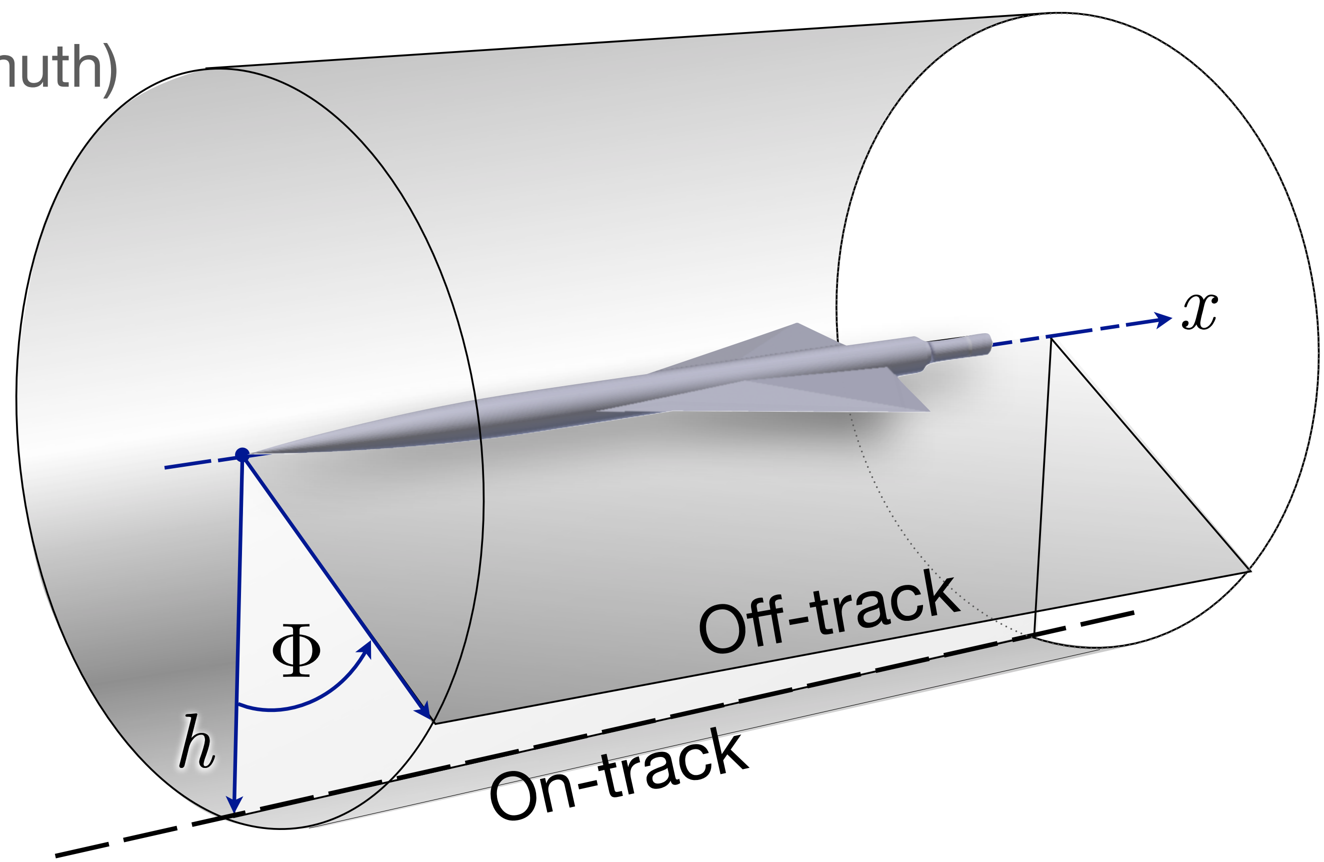

Results and Investigations

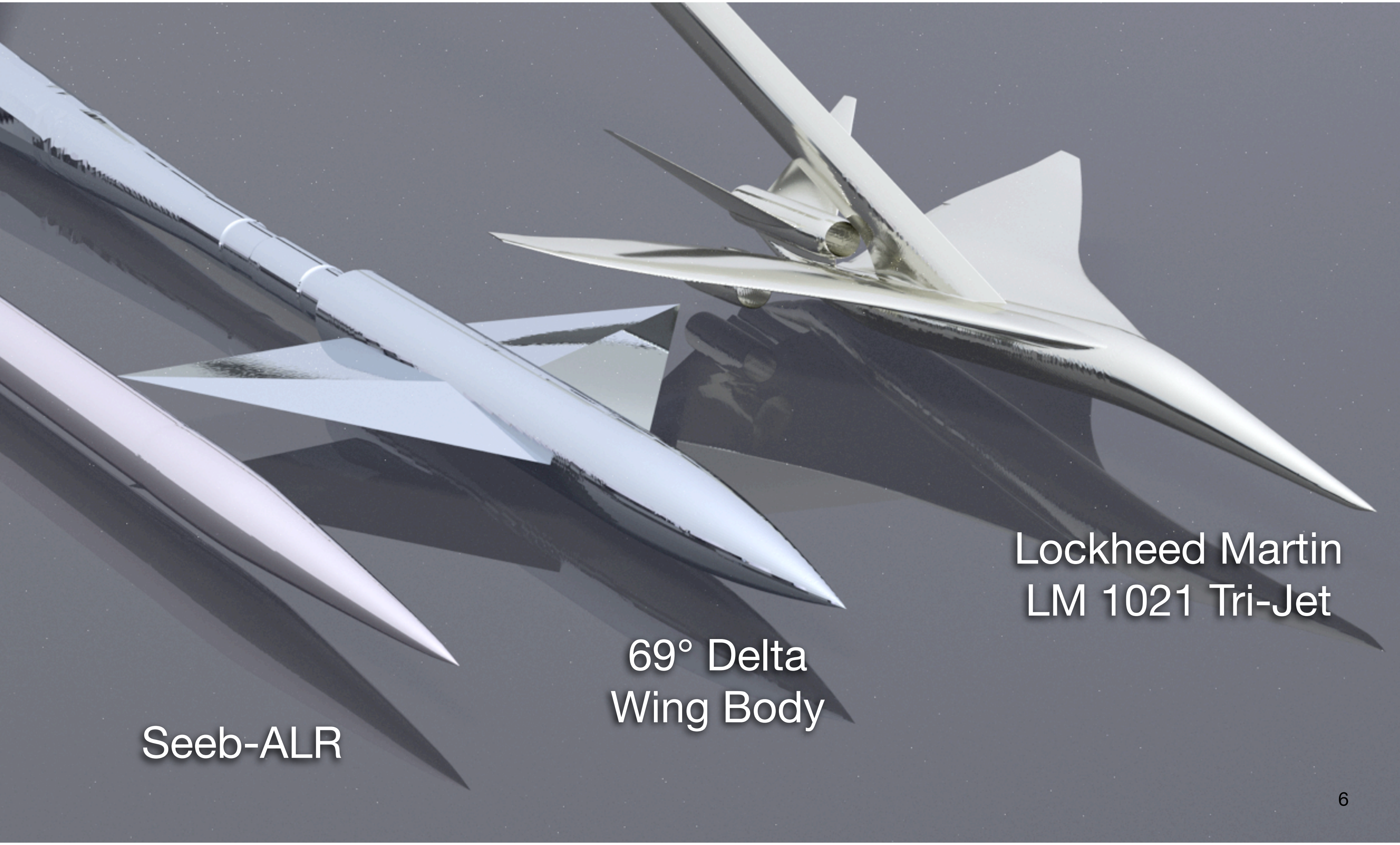

Results and Investigations

For each model

- Simulation results and computational resources
- Mesh & Error Convergence
- Investigations

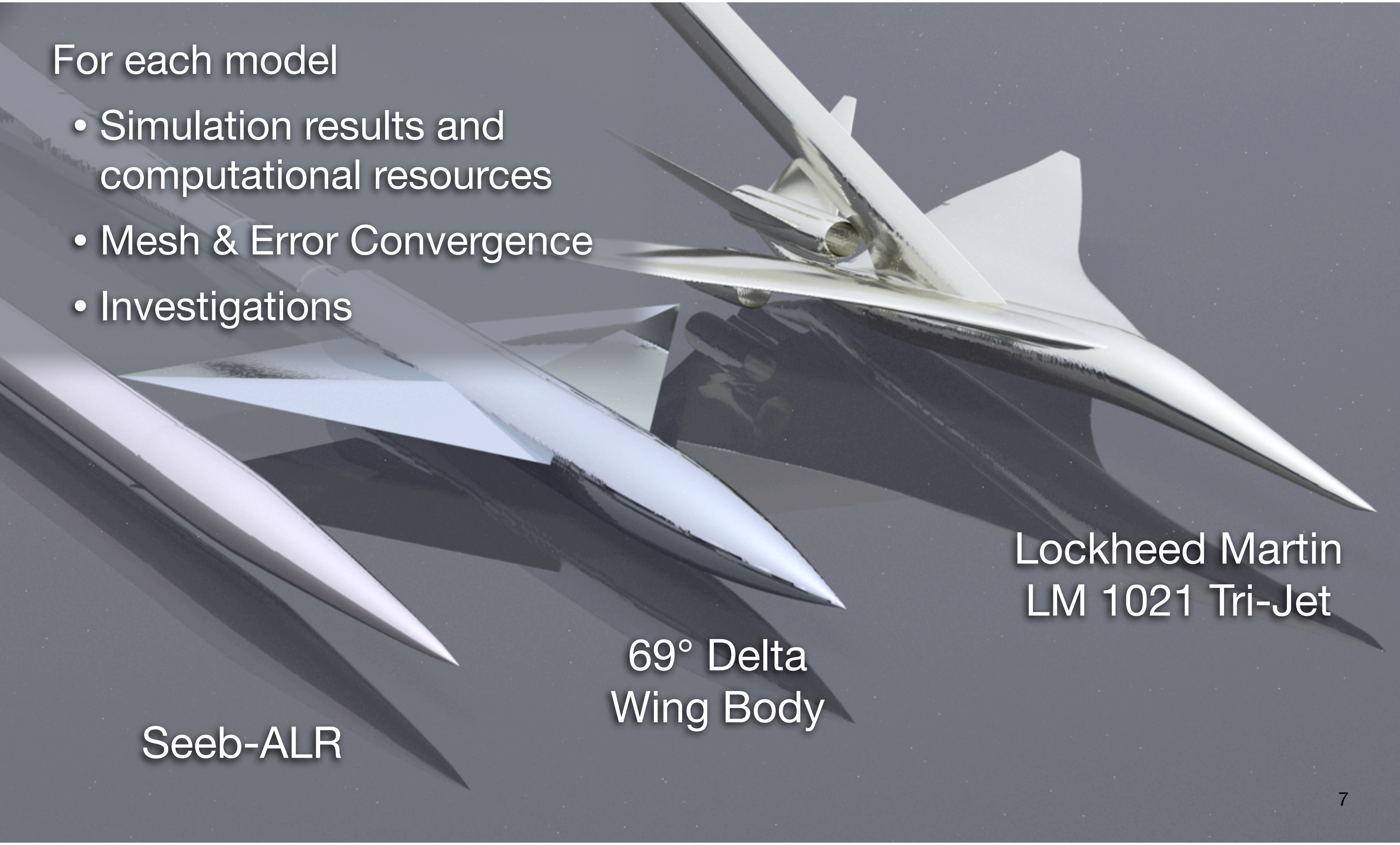

Case 1 – Seeb-ALR

$M_\infty = 1.6, \alpha = 0°$

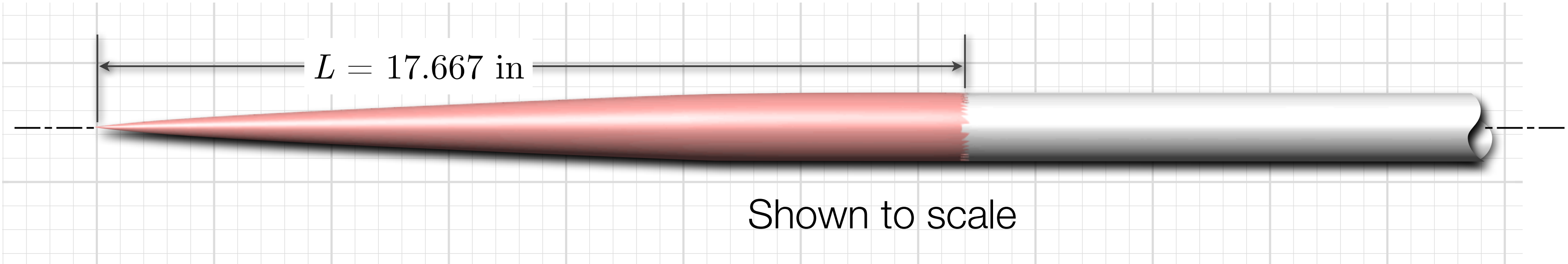

Case 1 – Seeb-ALR

$M_\infty = 1.6,\ \alpha = 0°$

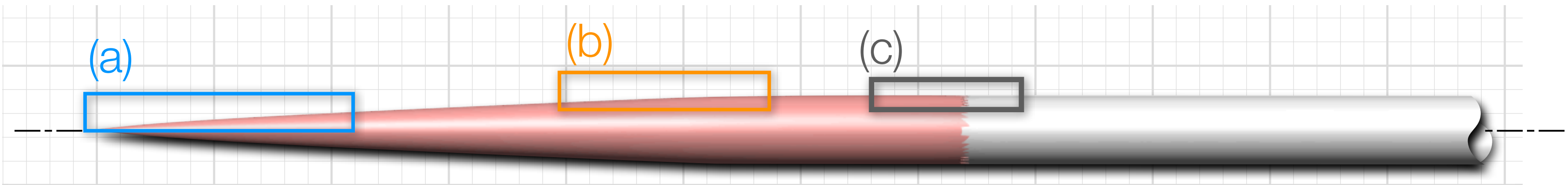

“As-built” geometry shown to scale

Detail with axial scale compressed 5x

(a) Slight inflection (concavity)

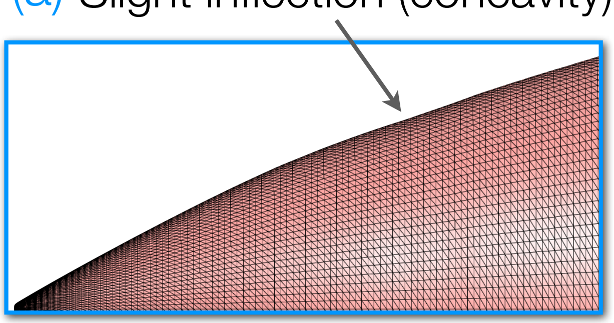

(b) Surface mesh at shoulder

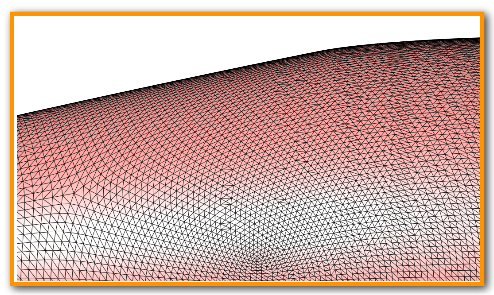

(c) Aft cylindrical juncture

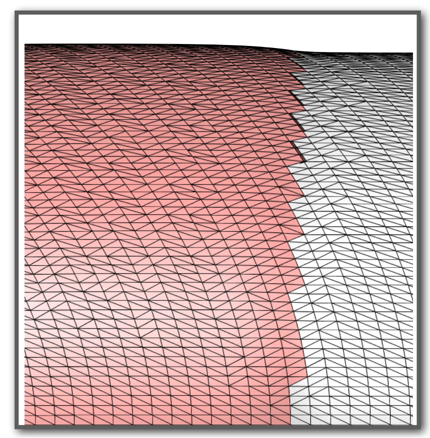

Seeb-ALR: Meshing

$M_\infty = 1.6$, $\alpha = 0°$, On-track @ $h = 21.2$ in. & 42 in.

Initial Mesh: 25k cells

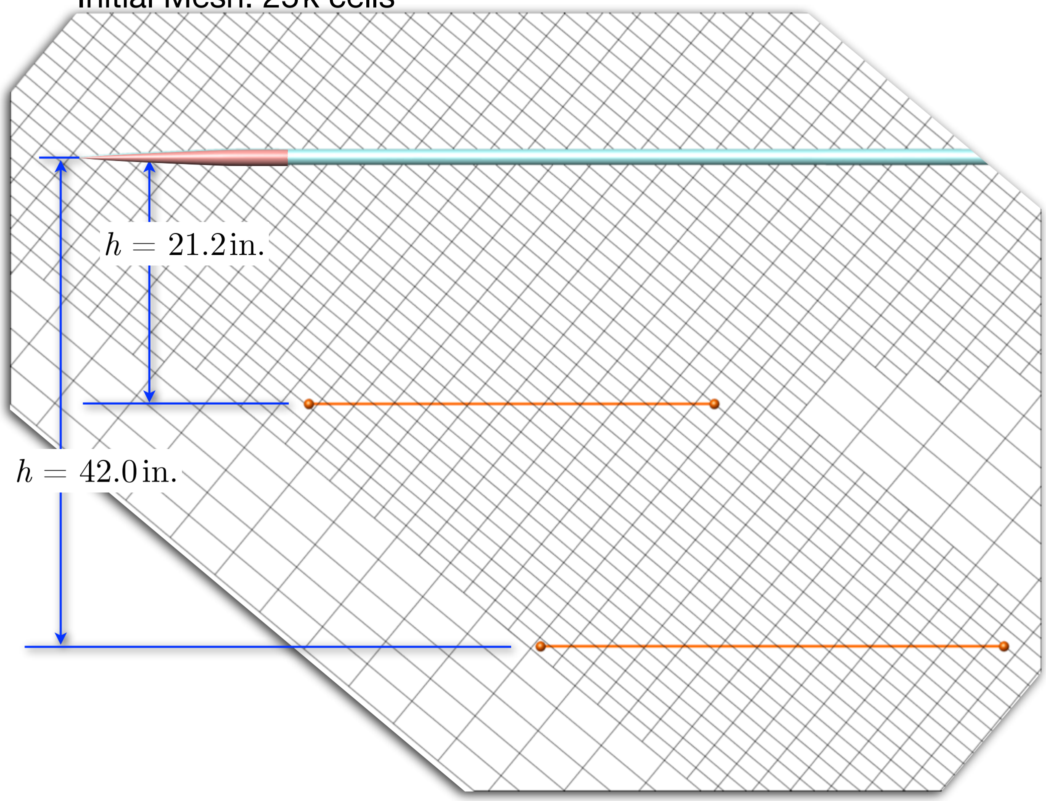

Seeb-ALR: Meshing

$M_\infty = 1.6$, $\alpha = 0°$, On-track @ $h = 21.2$ in. & 42 in.

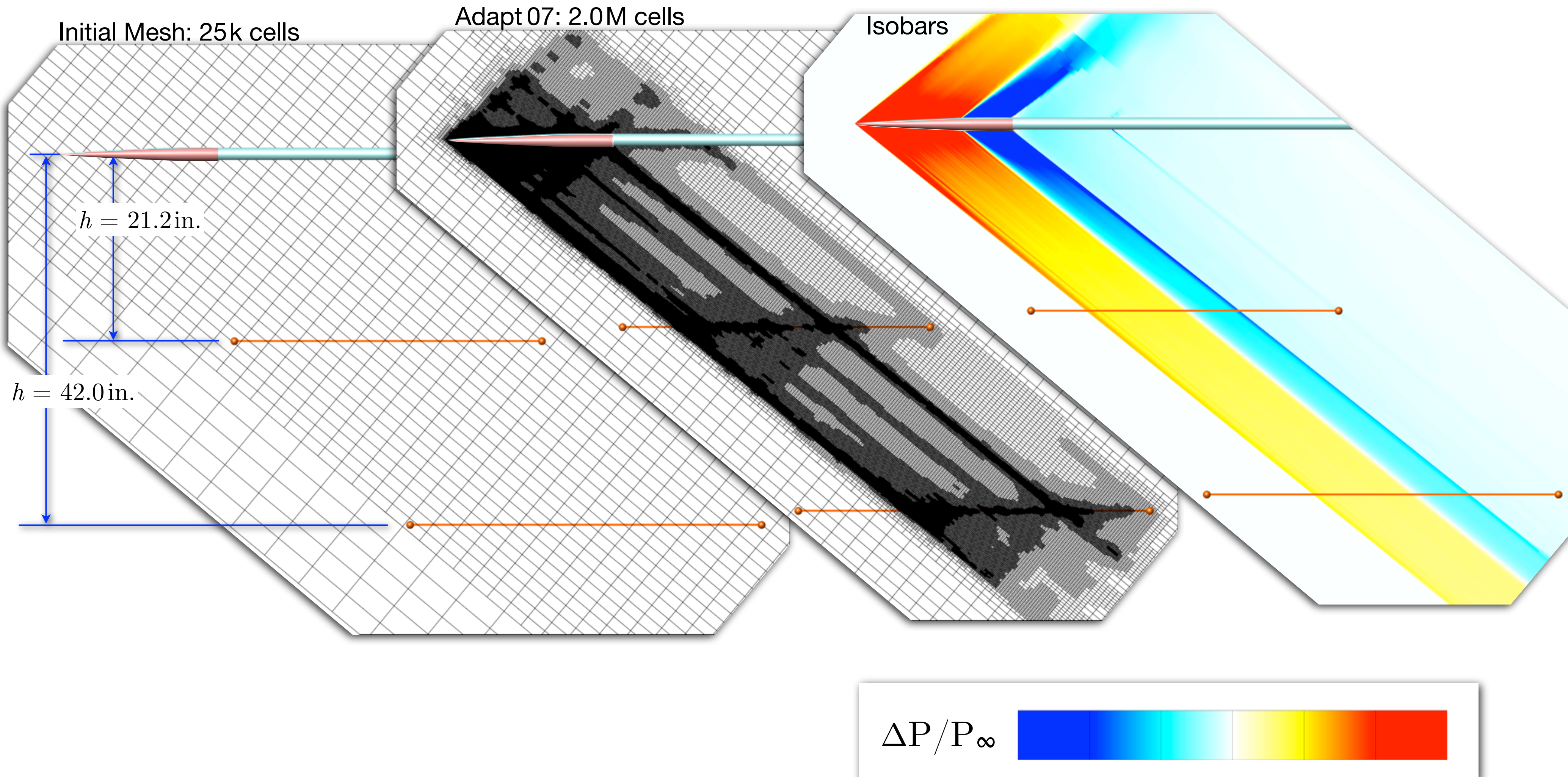

Seeb-ALR: Computational Work

$M_\infty = 1.6$, $\alpha = 0°$, On-track @ $h = 21.2$ in. & 42 in.

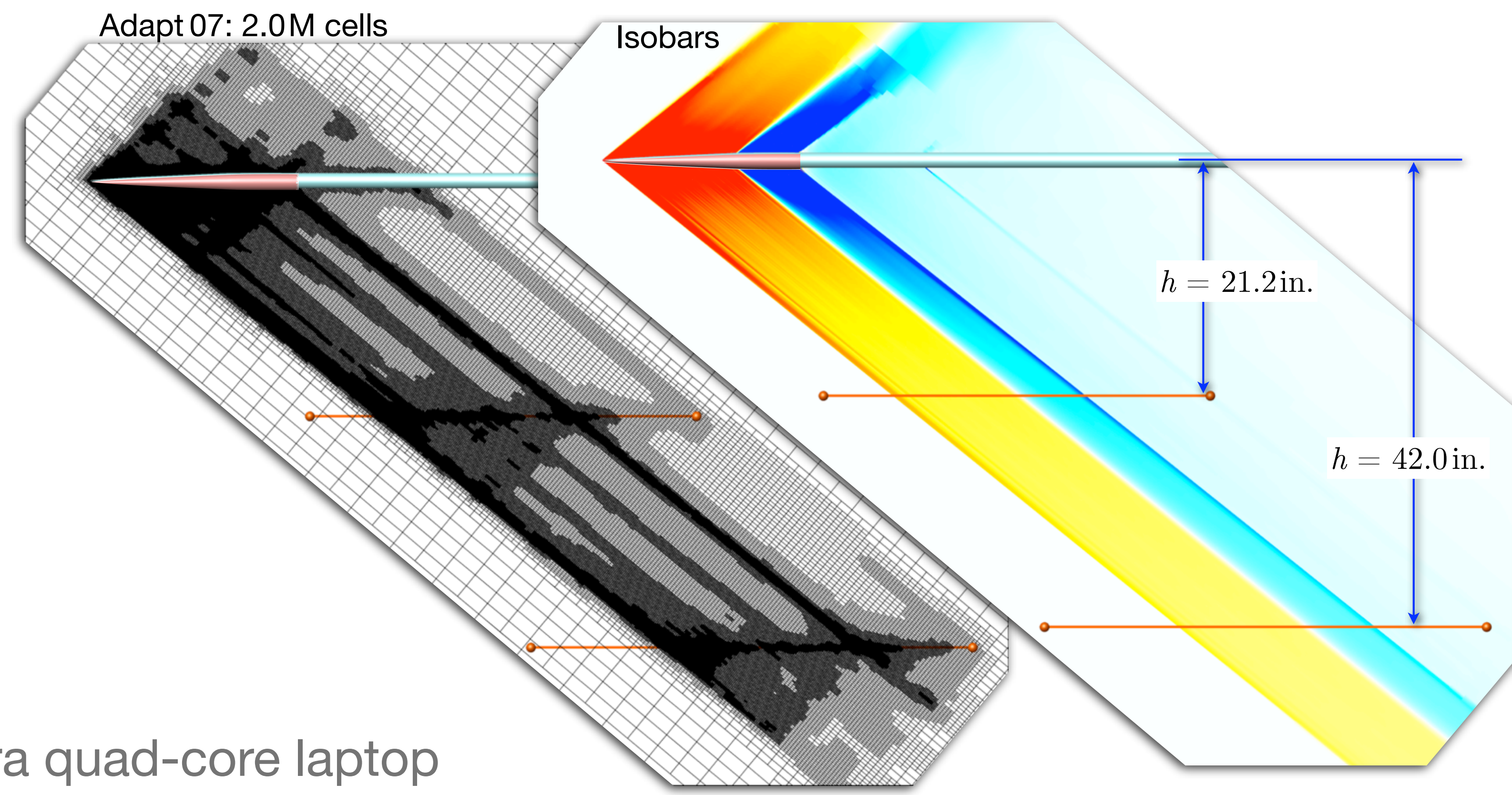

Resources

- Run on 2011-era quad-core laptop
- ~1 hr runtime (61mins)
- 3.6 GB of memory (max)

Seeb-ALR: Mesh Convergence

Convergence of pressure signature, $M_\infty = 1.6$, $\alpha = 0°$

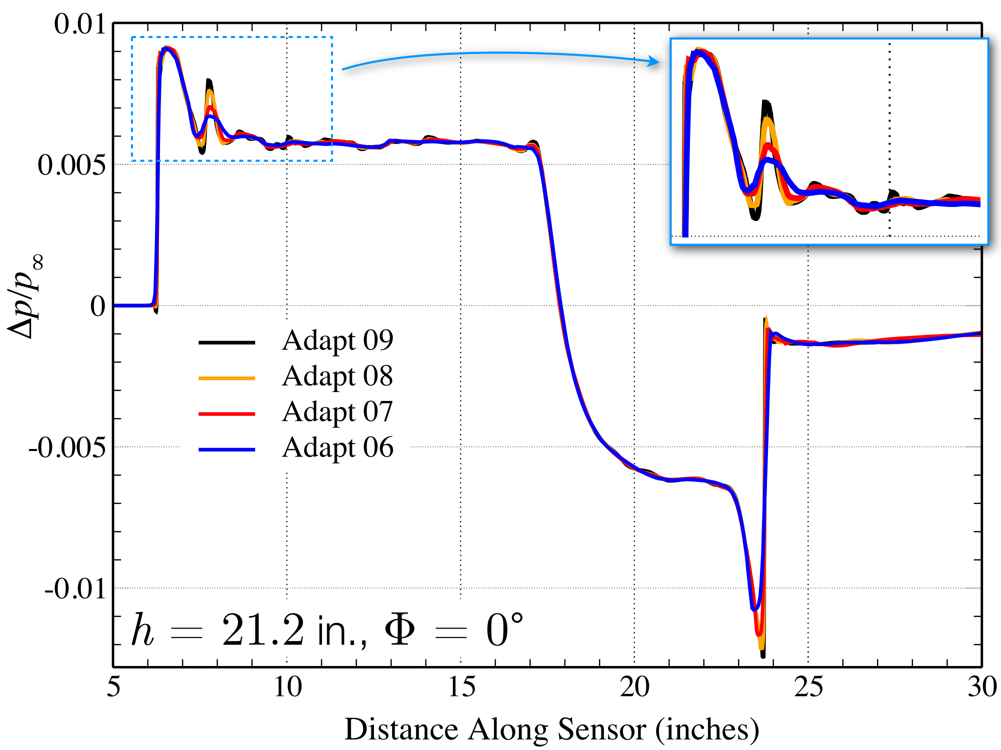

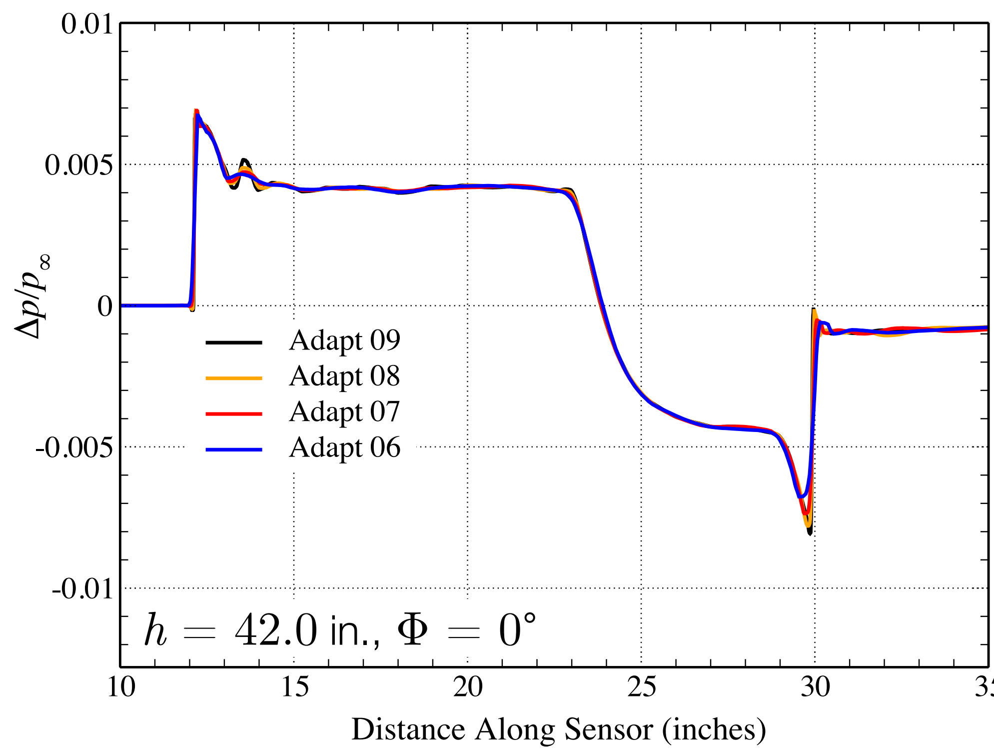

- Pressure signatures largely converged by 6th adapt cycle. - even at 42 in.
- Additional mesh resolution only sharpening shocks

Seeb-ALR: Mesh Convergence

- Results at 7th adaptation submitted to workshop
- Perform 2 more adaptations to assess degree of mesh convergence

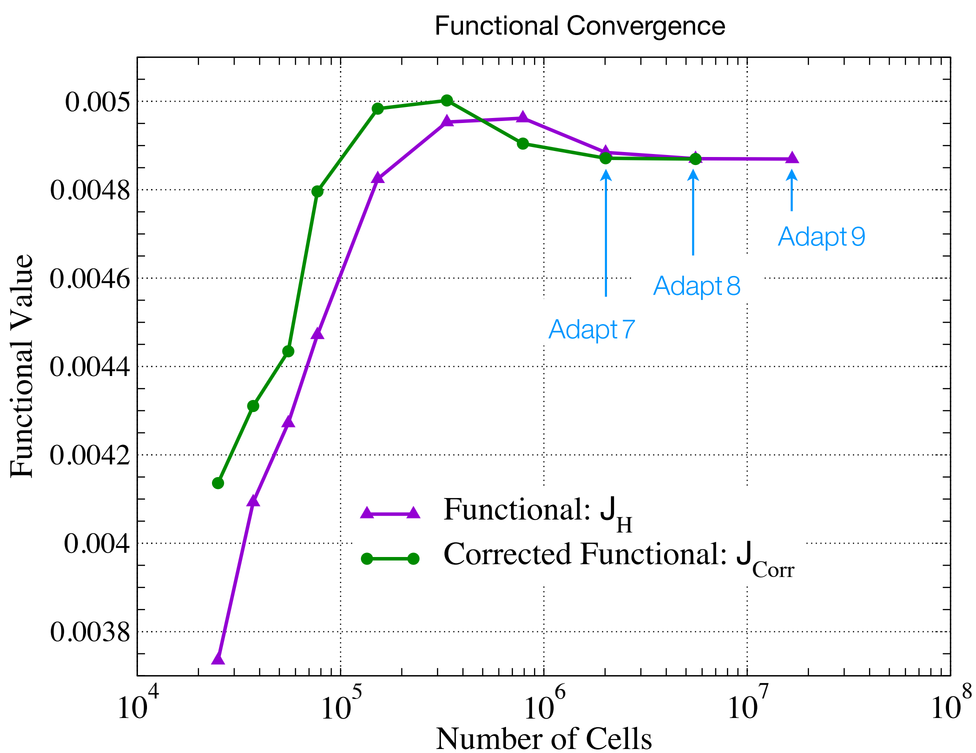

- Functional converges
- Correction *leads* functional
- Adjoint Correction vanishes

Seeb-ALR: Mesh Convergence

- Results at 7th adaptation submitted to workshop
- Perform 2 more adaptations to assess degree of mesh convergence

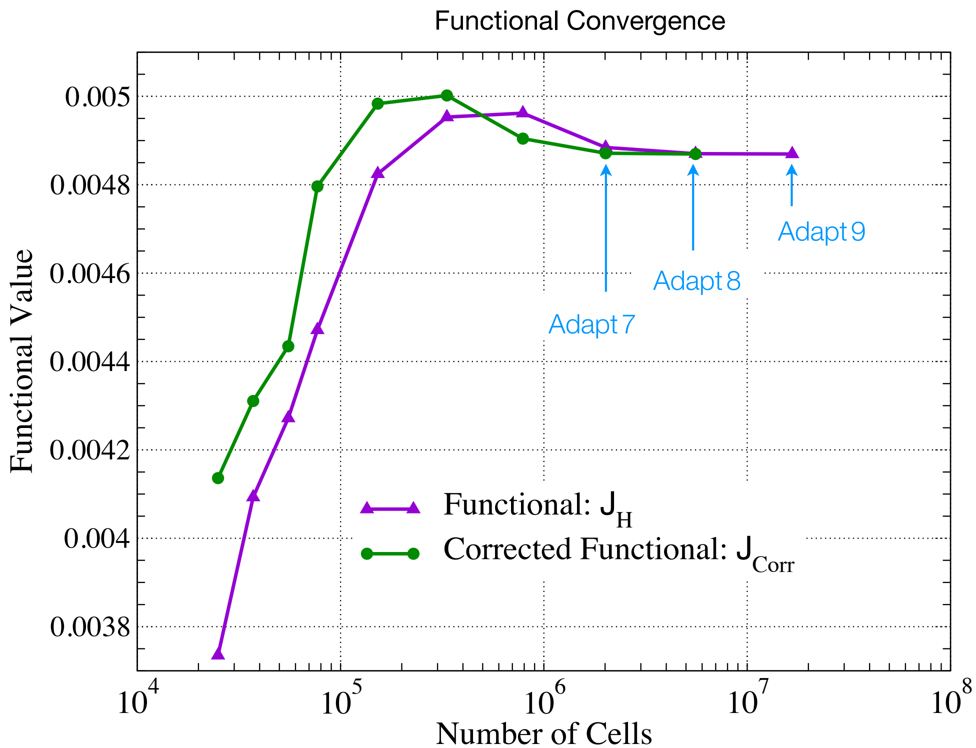

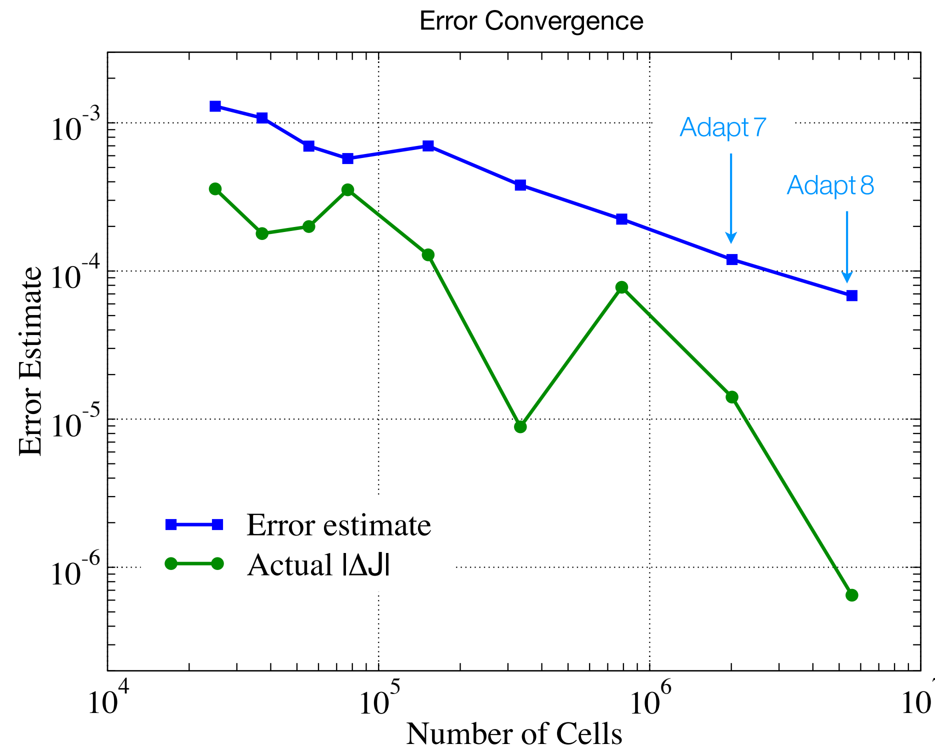

- Functional converges
- Correction *leads* functional
- Adjoint Correction vanishes

- Error-estimate bounds update |ΔJ|
- Remaining error converges asymptotically
- “Textbook” convergence

Seeb-ALR: Data Comparison

Comparison with linear theory, $M_\infty = 1.6$, $\alpha = 0°$

- Code-to-Code comparison used before exp. data was available

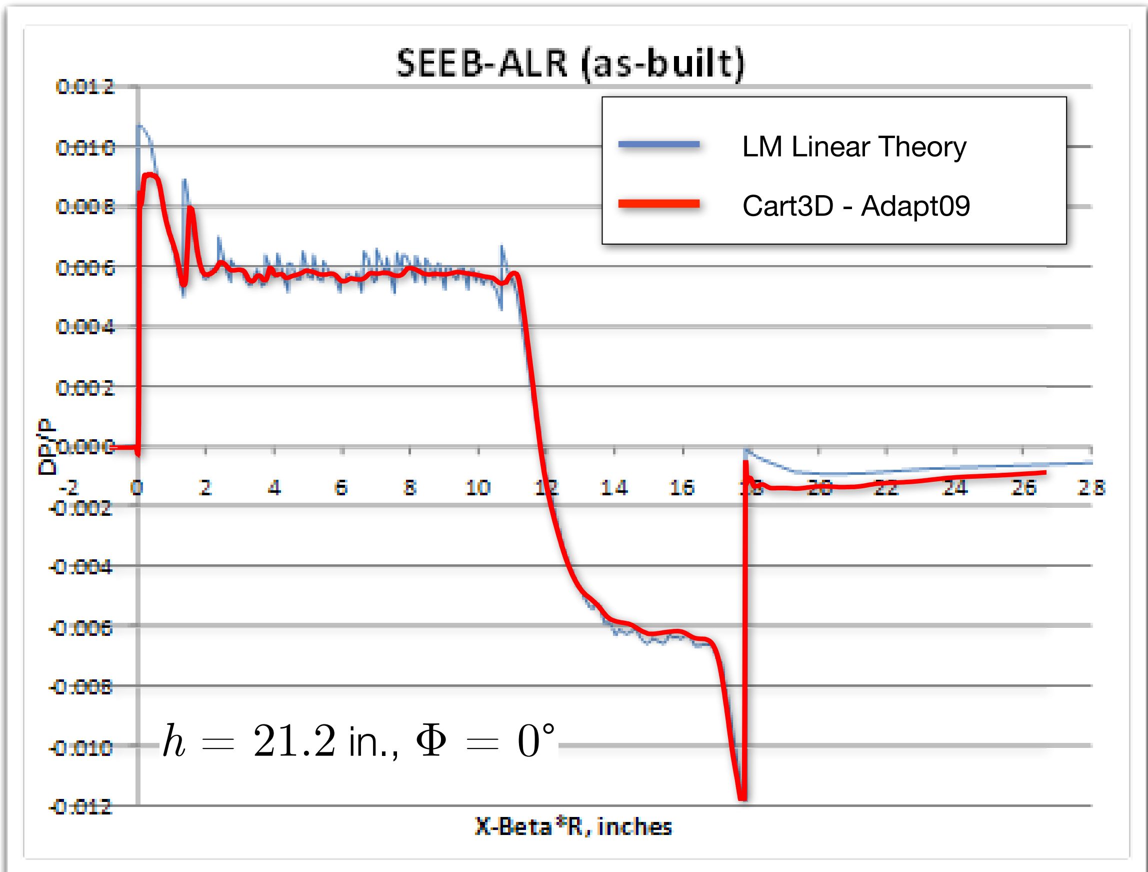

Morgenstern *et al.*, NASA CR–2013-217820, fig 18

Seeb-ALR: Data Comparison

Comparison with experimental data, $M_\infty = 1.6$, $\alpha = 0°$

- Closest data at $h \approx 20.6$ in., $\alpha =$ -0.3°, $\beta =$ -0.3°
- Excellent agreement in peaks and on flat-top, some differences in expansion

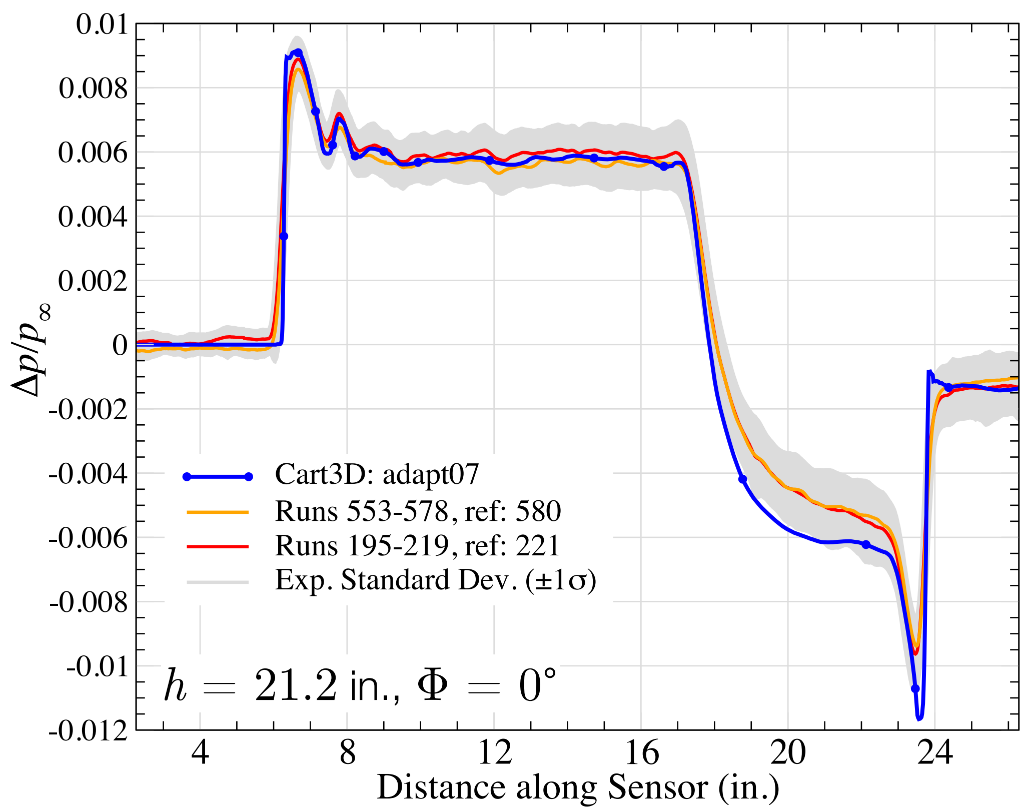

Seeb-ALR: Data Comparison

Comparison with experimental data, $M = 1.6$, $\alpha = 0°$

- Closes
- Excelle in
  expans

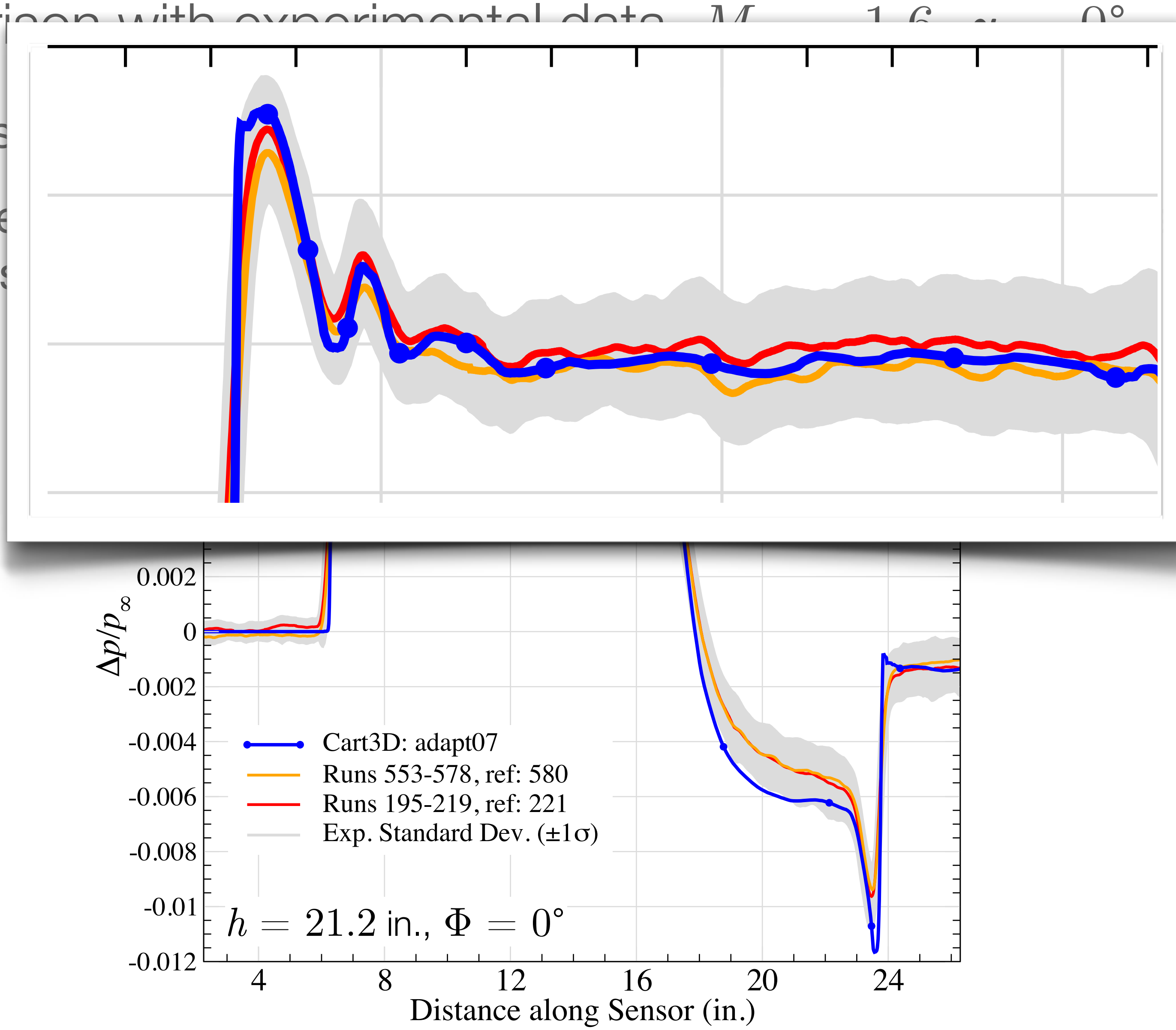

Seeb-ALR: Data Comparison

Comparison with experimental data, $M_\infty = 1.6$, $\alpha = 0°$

- Closest data at $h \approx 20.6$ in., $\alpha = -0.3°$, $\beta = -0.3°$
- Excellent agreement in peaks and on flat-top, some differences in expansion

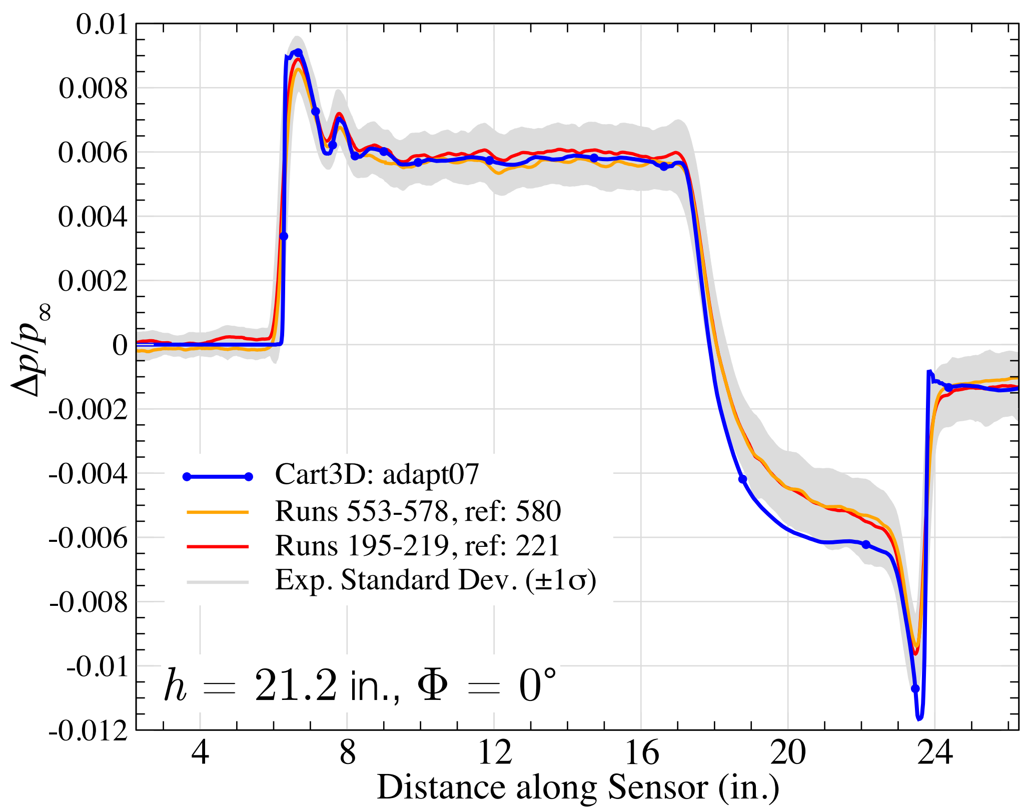

Seeb-ALR: Data Comparison

Comparison with experimental data, $M_\infty = 1.6$, $\alpha = 0°$

- Closest data at $h \approx 20.6$ in., $\alpha =$ -0.3°, $\beta =$ -0.3°
- Excellent agreement in peaks and on flat-top, some differences in expansion

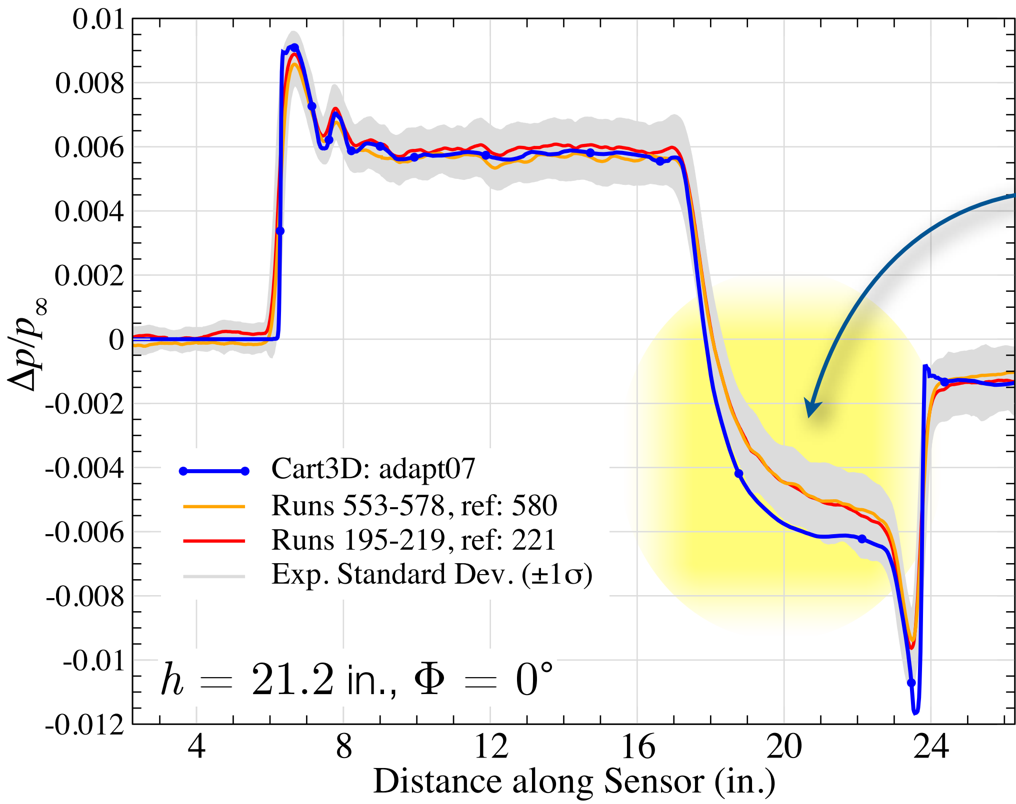

Differences in expansion were troubling since we have high confidence in solution

Seeb-ALR: Data Comparison

Comparison with experimental data, $M_\infty = 1.6$, $\alpha = 0°$

- Closest data at $h \approx 20.6$ in., $\alpha = -0.3°$, $\beta = -0.3°$
- Excellent agreement in peaks and on flat-top, some differences in expansion

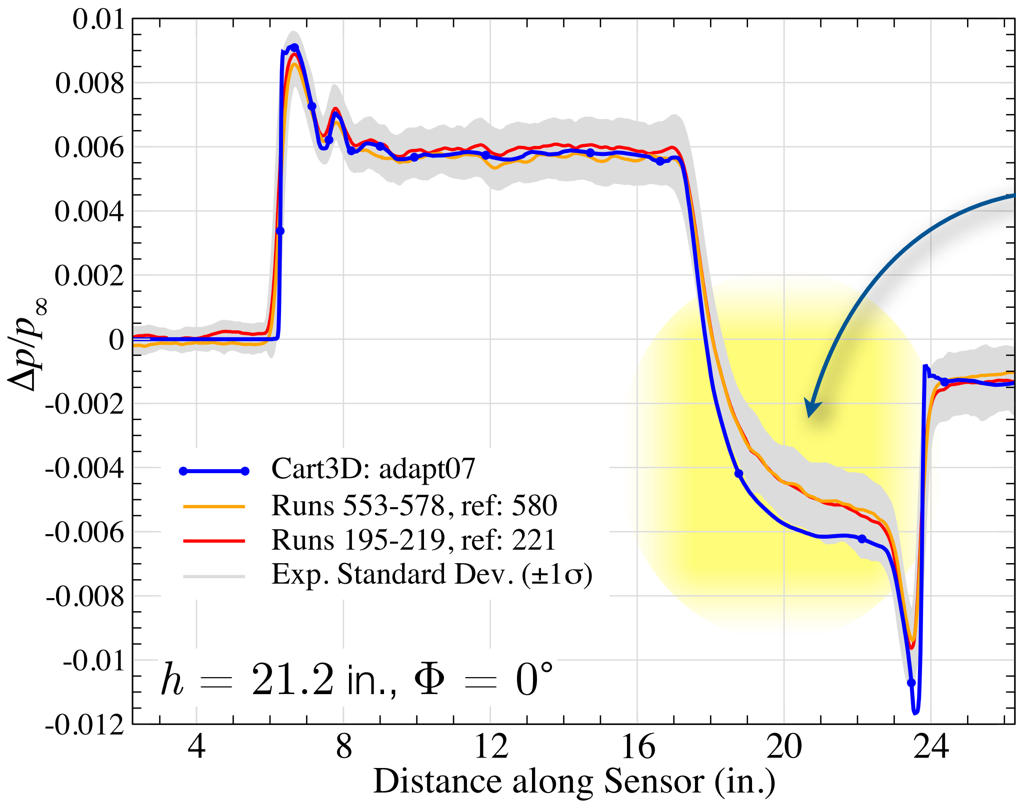

Differences in expansion were troubling since we have high confidence in solution

1. Re-measured model
2. Ran case with Seeb-ALR + pressure rail + tunnel wall

Seeb-ALR: Data Comparison

Simulation with Seeb-ALR + pressure rail + tunnel floor
Mid-traverse location for data @ $h = 20.6\,\text{in.}$

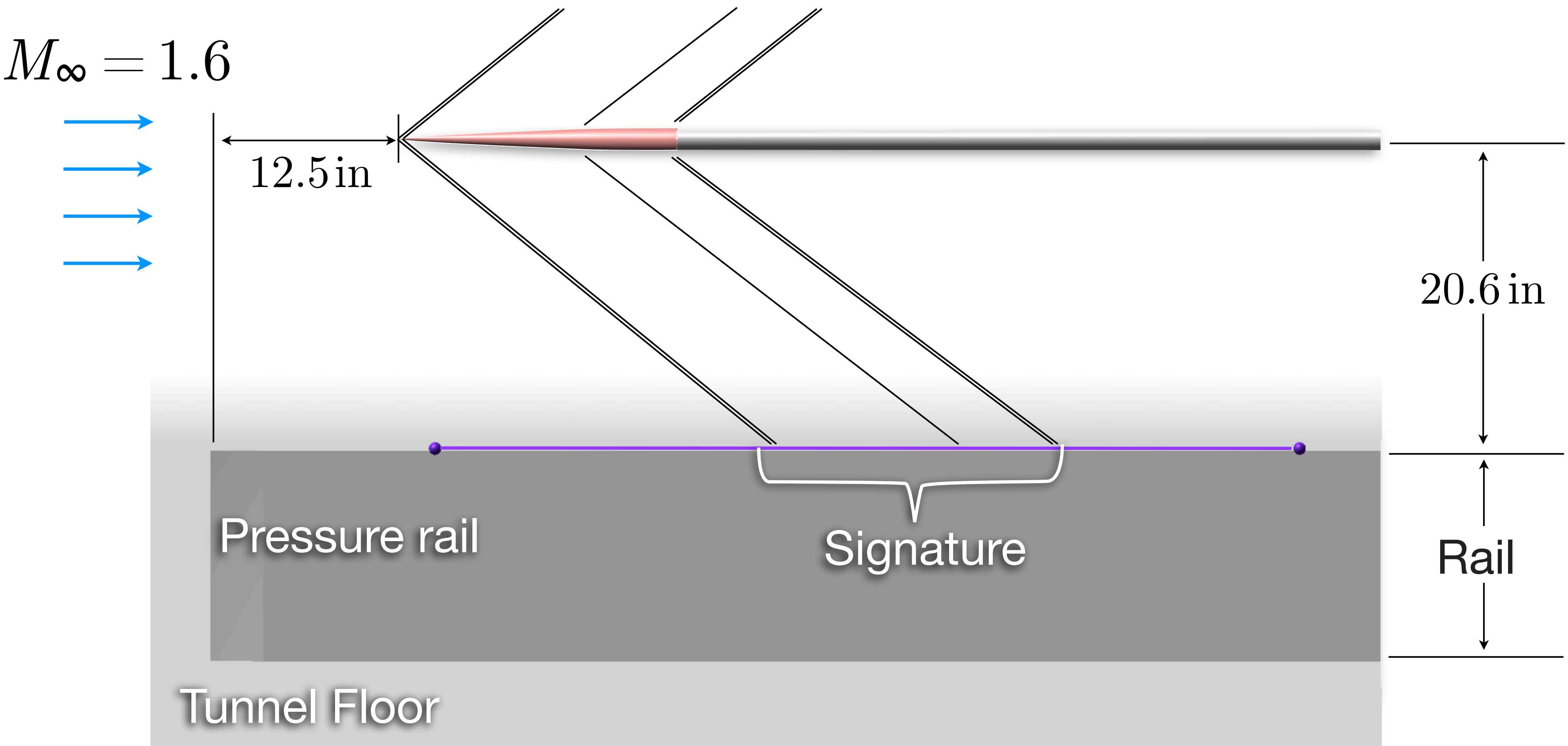

Seeb-ALR: Data Comparison

Simulation with Seeb-ALR + pressure rail + tunnel floor
Mid-traverse location for data @ $h = 20.6\,\text{in.}$

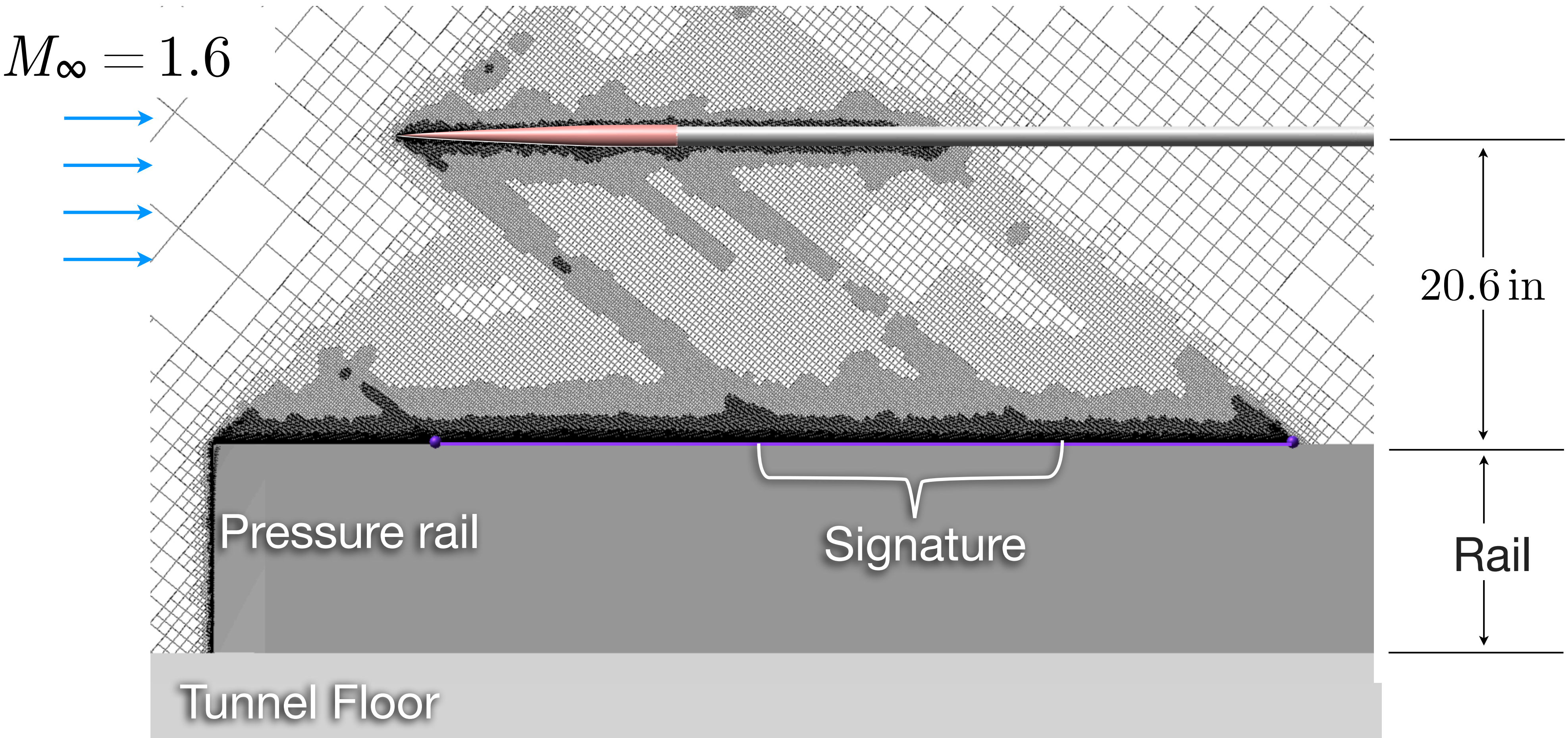

Seeb-ALR: Data Comparison

Simulation with Seeb-ALR + pressure rail + tunnel floor
Mid-traverse location for data @ $h = 20.6\,\text{in.}$

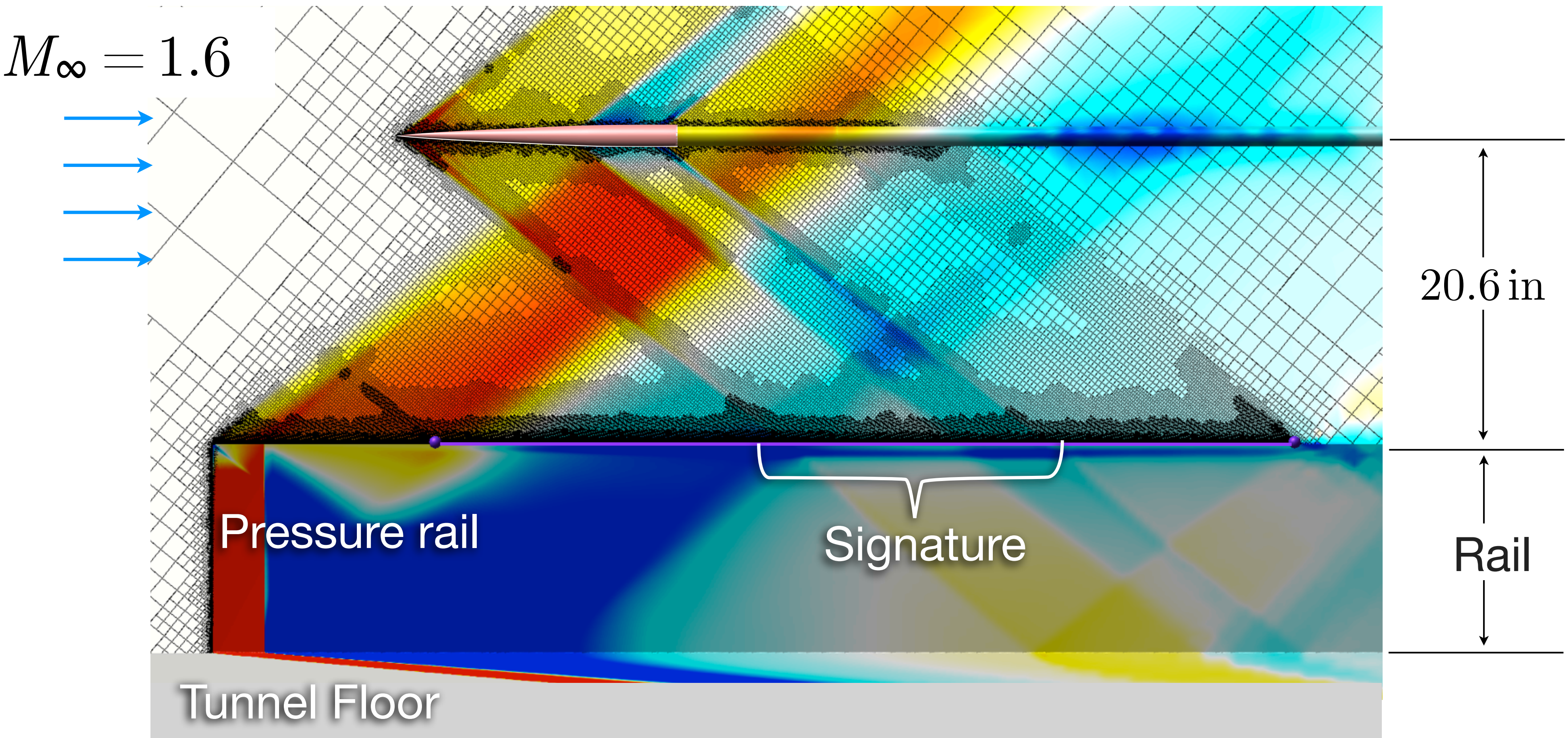

Seeb-ALR: Data Comparison

Simulation with Seeb-ALR + pressure rail + tunnel floor
Mid-traverse location for data @ $h = 20.6\,\text{in.}$

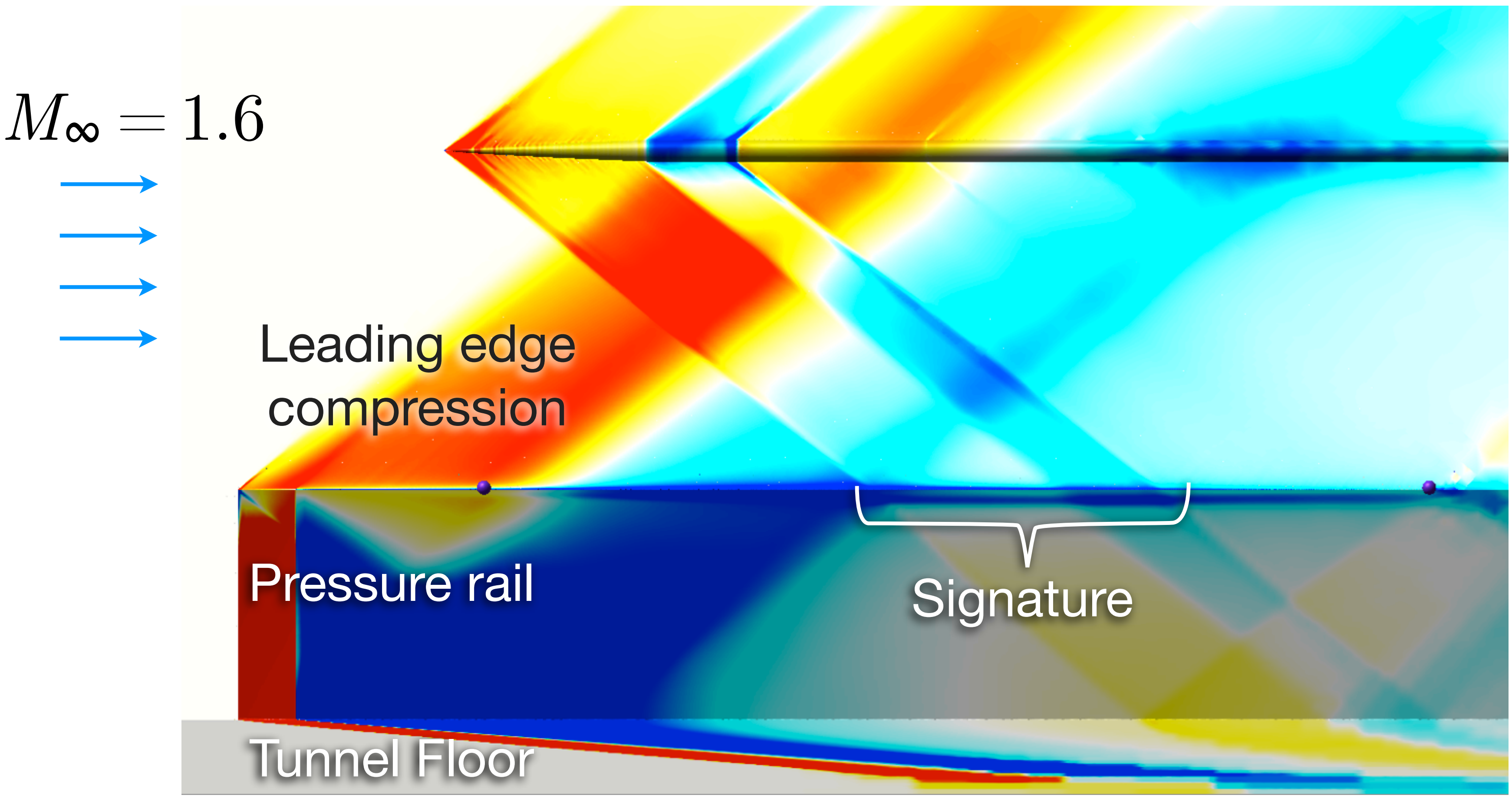

- Model positioned in middle of range of experimental traverse
- Leading edge compression interacts with model, relieving suction

Seeb-ALR: Data Comparison

Simulation with Seeb-ALR + pressure rail + tunnel floor
Mid-traverse location for data @ $h = 20.6\,\text{in.}$

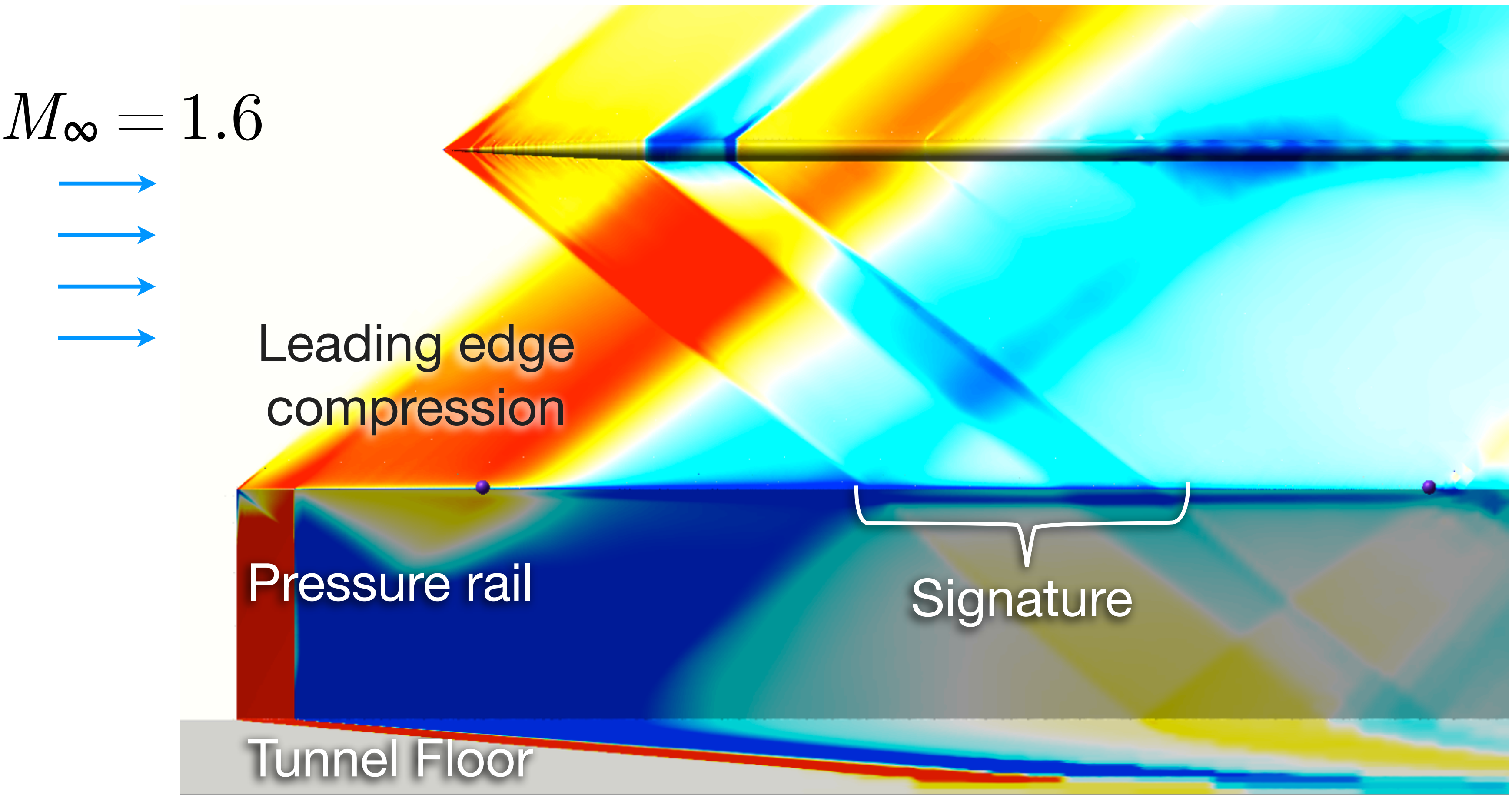

- Model positioned in middle of range of experimental traverse
- Leading edge compression interacts with model, relieving suction

Seeb-ALR: D

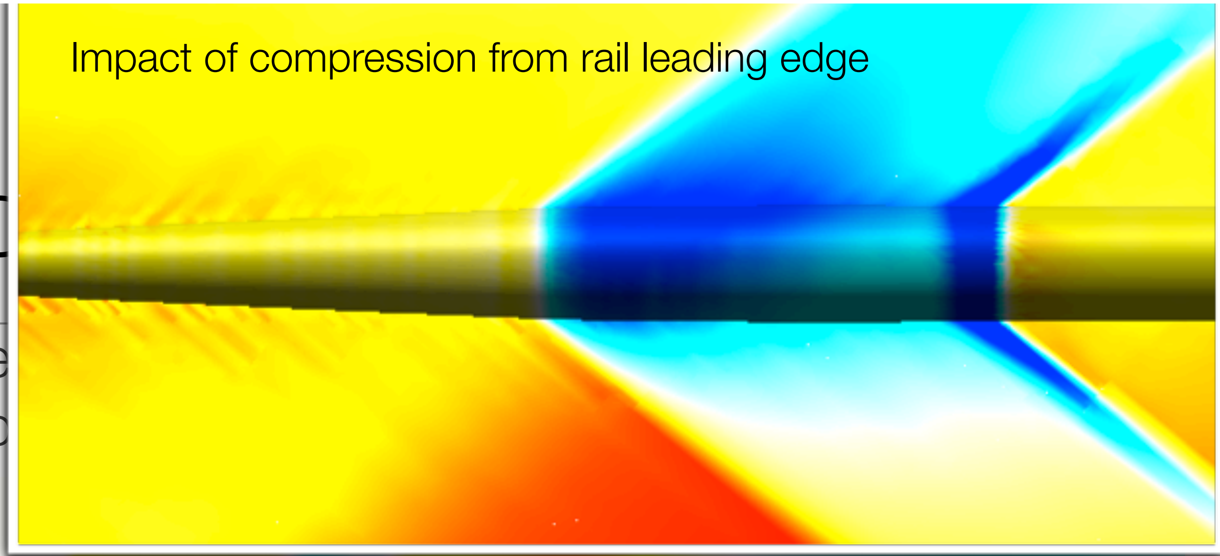

Simulation with See
Mid-traverse locatio

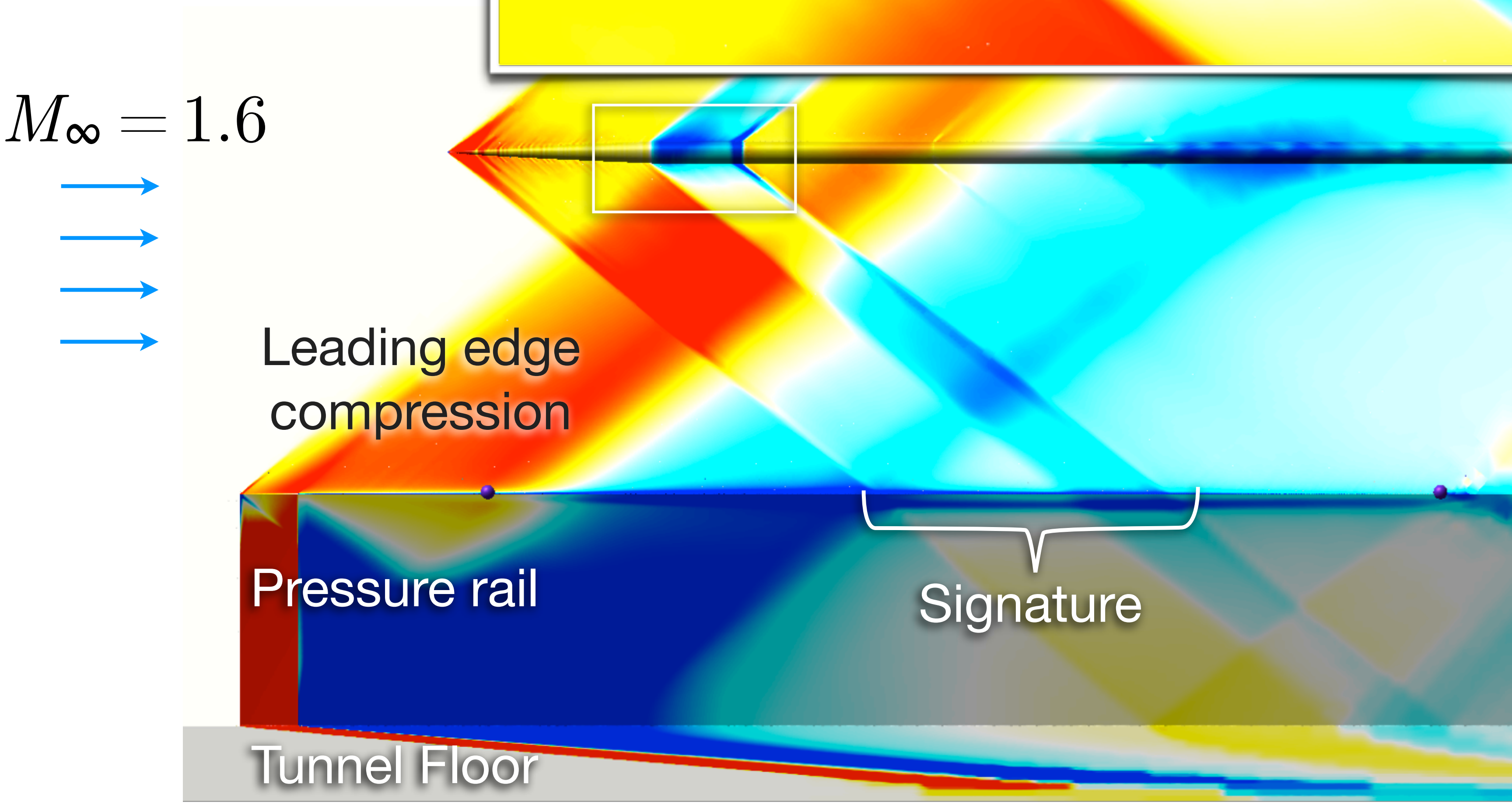

- Model positioned in middle of range of experimental traverse
- Leading edge compression interacts with model, relieving suction

Seeb-ALR: Data Comparison

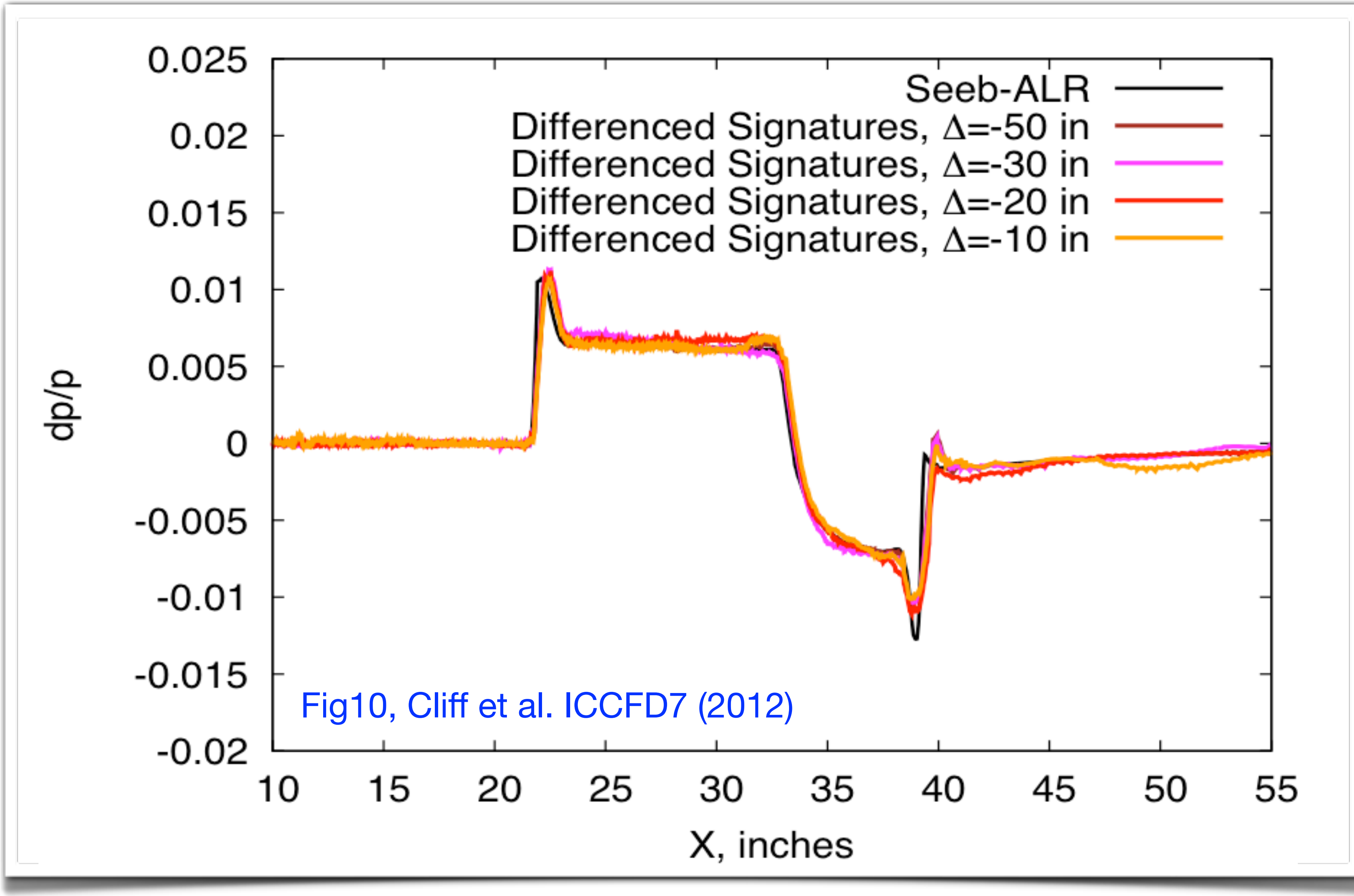

Seeb- n

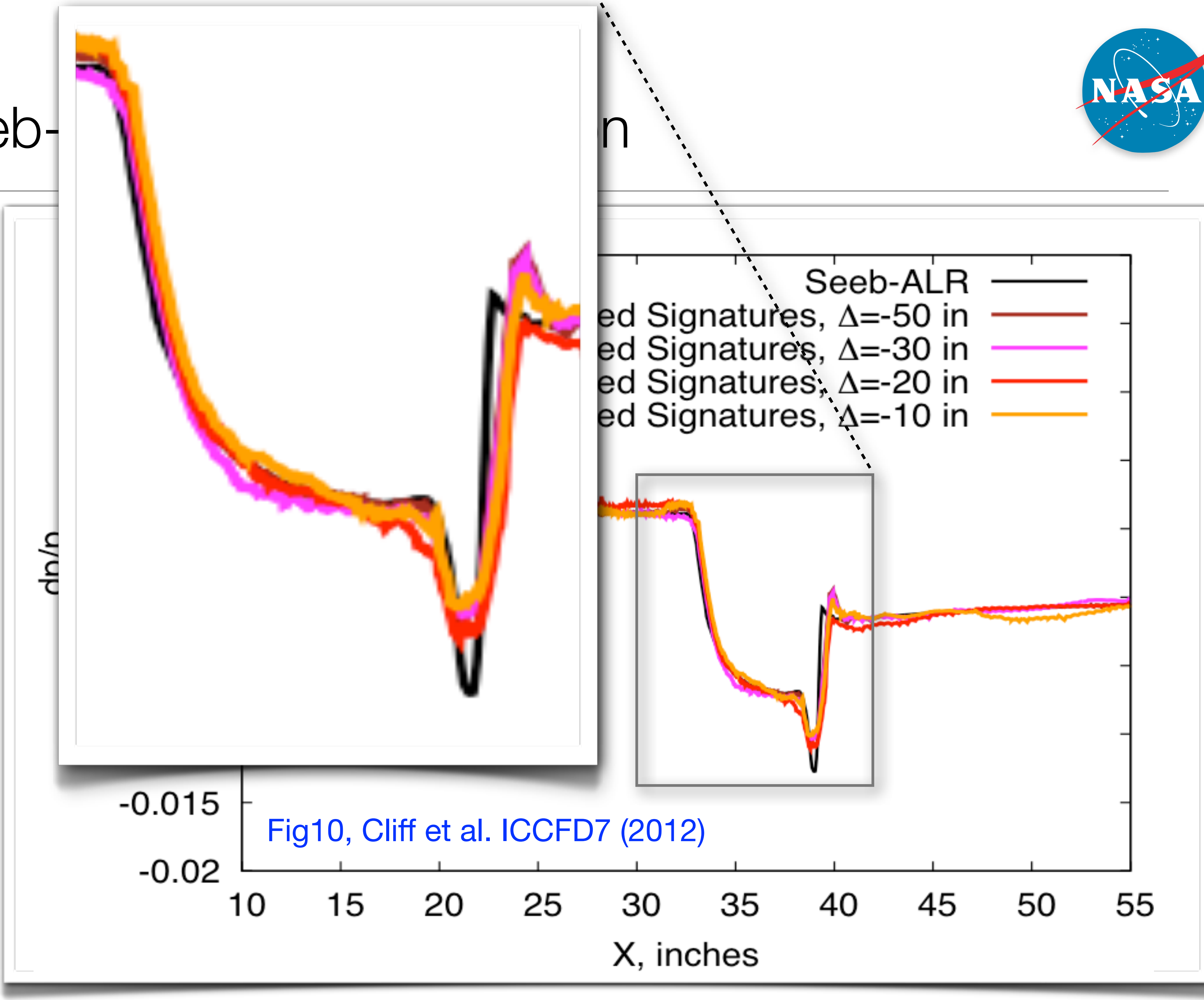

Fig10, Cliff et al. ICCFD7 (2012)

69° Delta Wing Body

$M_\infty = 1.7, \alpha = 0°$

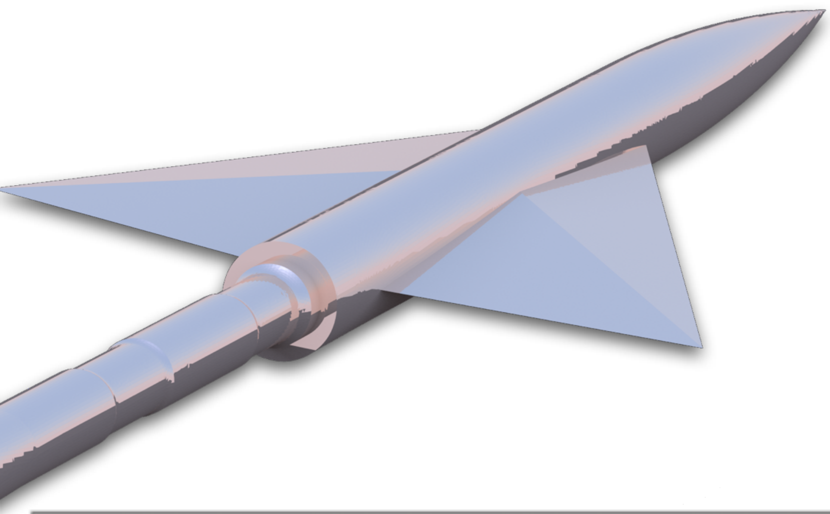

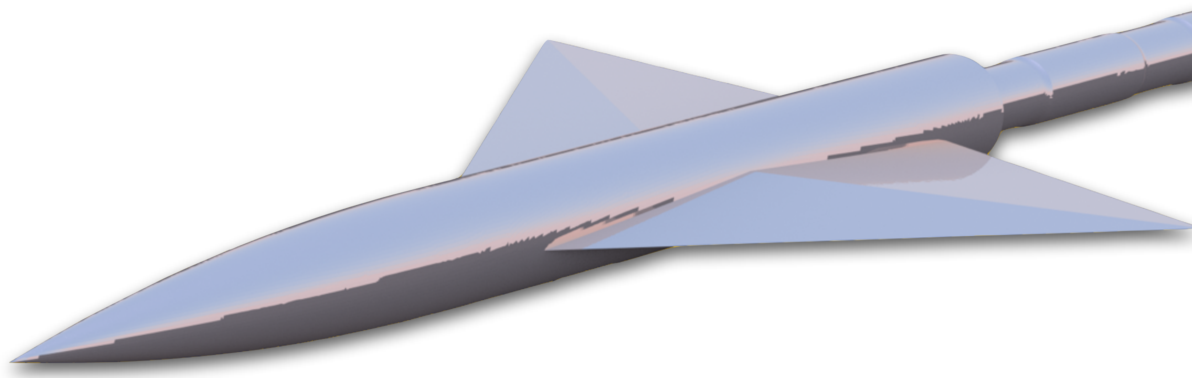

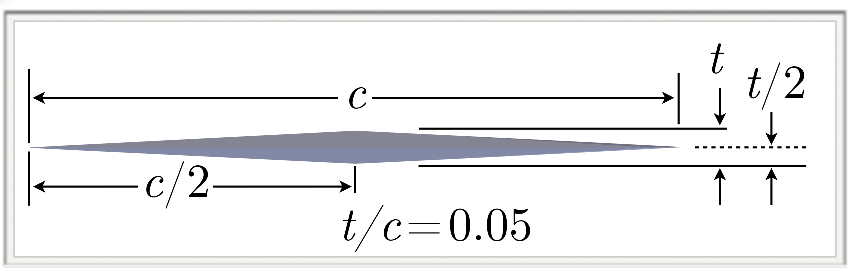

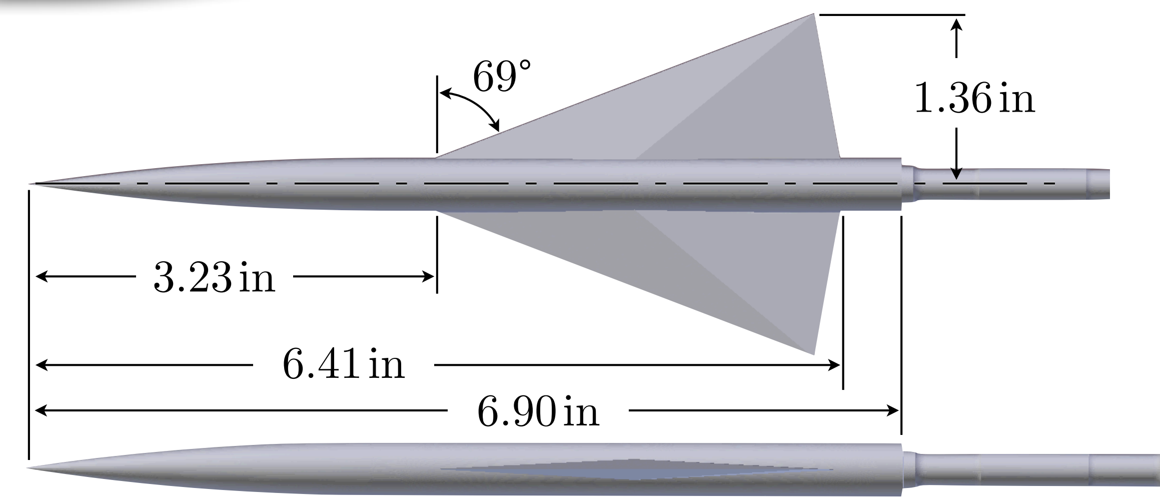

- Tangent-ogive-cylinder fuselage
- Delta wing with 5% thick diamond airfoil
- New sting fitted to original (1973) model from Hunton et al.

69° Delta Wing Body

$M_\infty = 1.7,\ \alpha = 0^\circ$

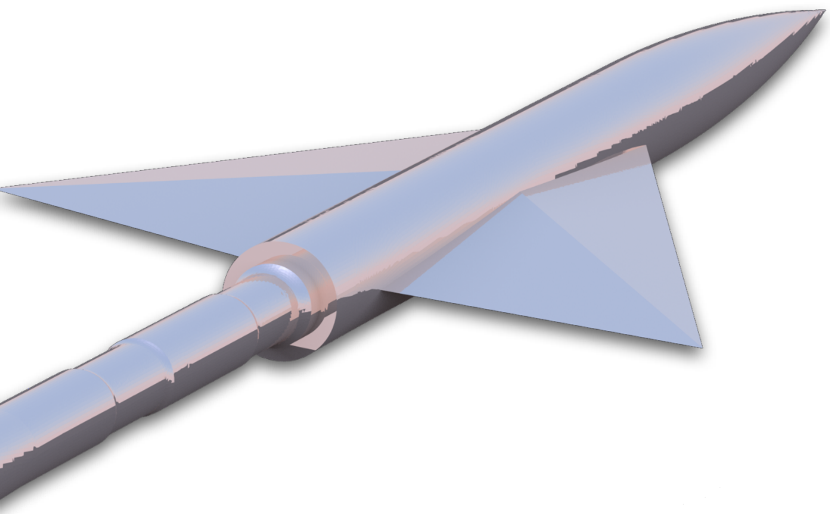

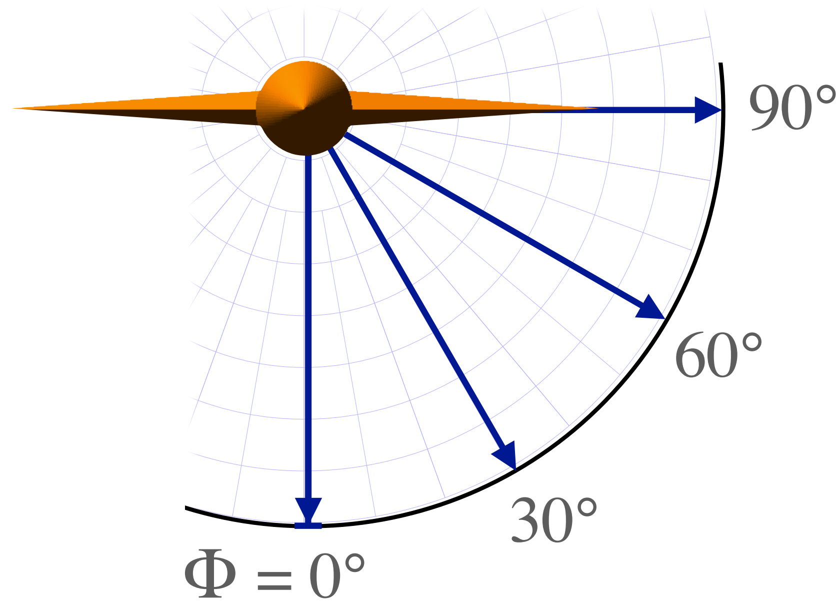

Required Pressure Signatures

- $\Phi = \{0^\circ, 30^\circ, 60^\circ, 90^\circ\}$
- $h = \{0.5, 21.2, 24.8, 31.8\}$ in.
- 10 sensors and extreme off-track angles

69° Delta Wing Body

$M_\infty = 1.7$

$\alpha = 0°$

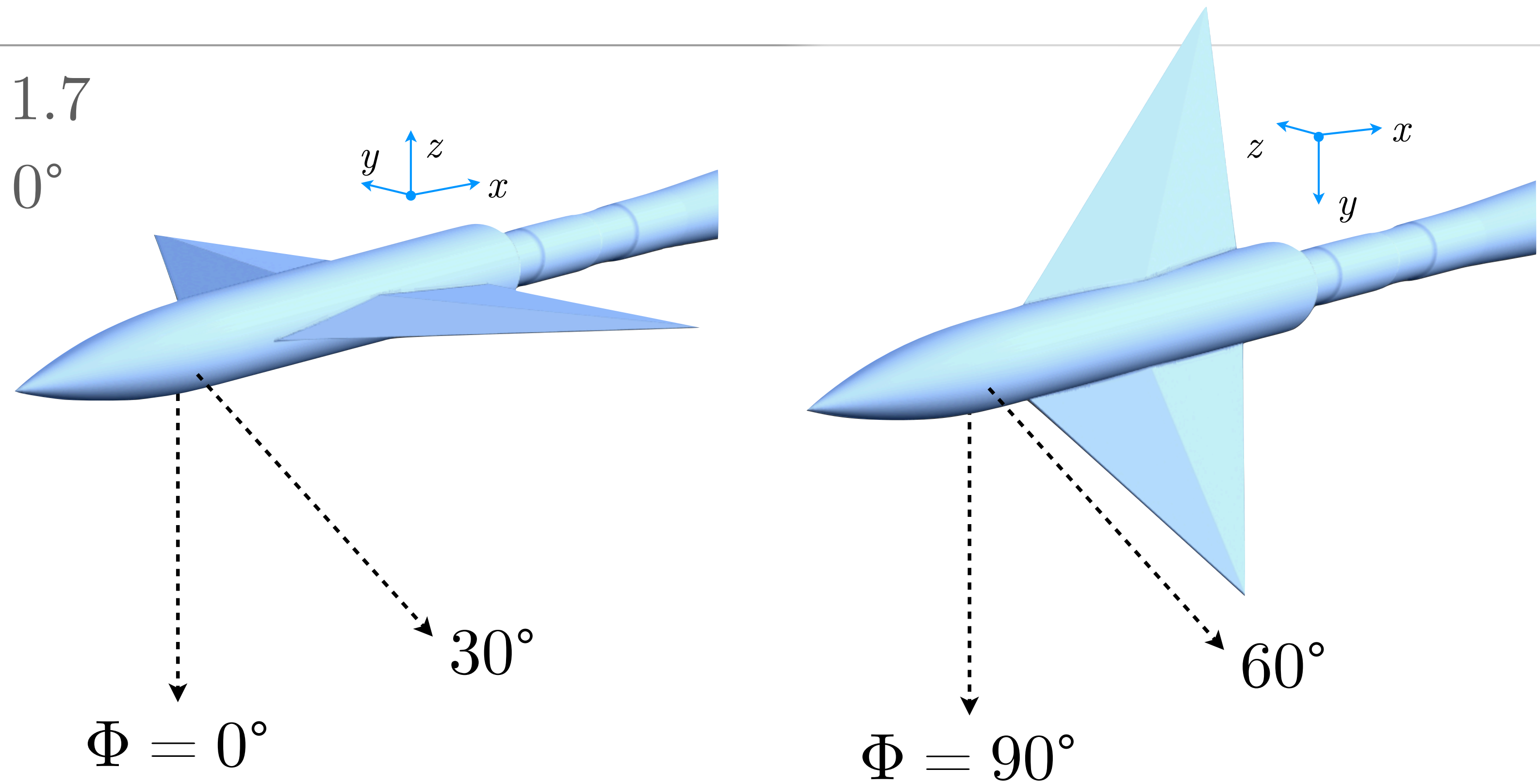

Setup as 2 cases

1. $\Phi = \{0°, 30°\}$ – Mesh rotated in pitch plane
2. $\Phi = \{60°, 90°\}$ – Mesh rotated in yaw plane

Case 2 – 69° Delta Wing Body

$M_\infty = 1.7$

$\alpha = 0^\circ$

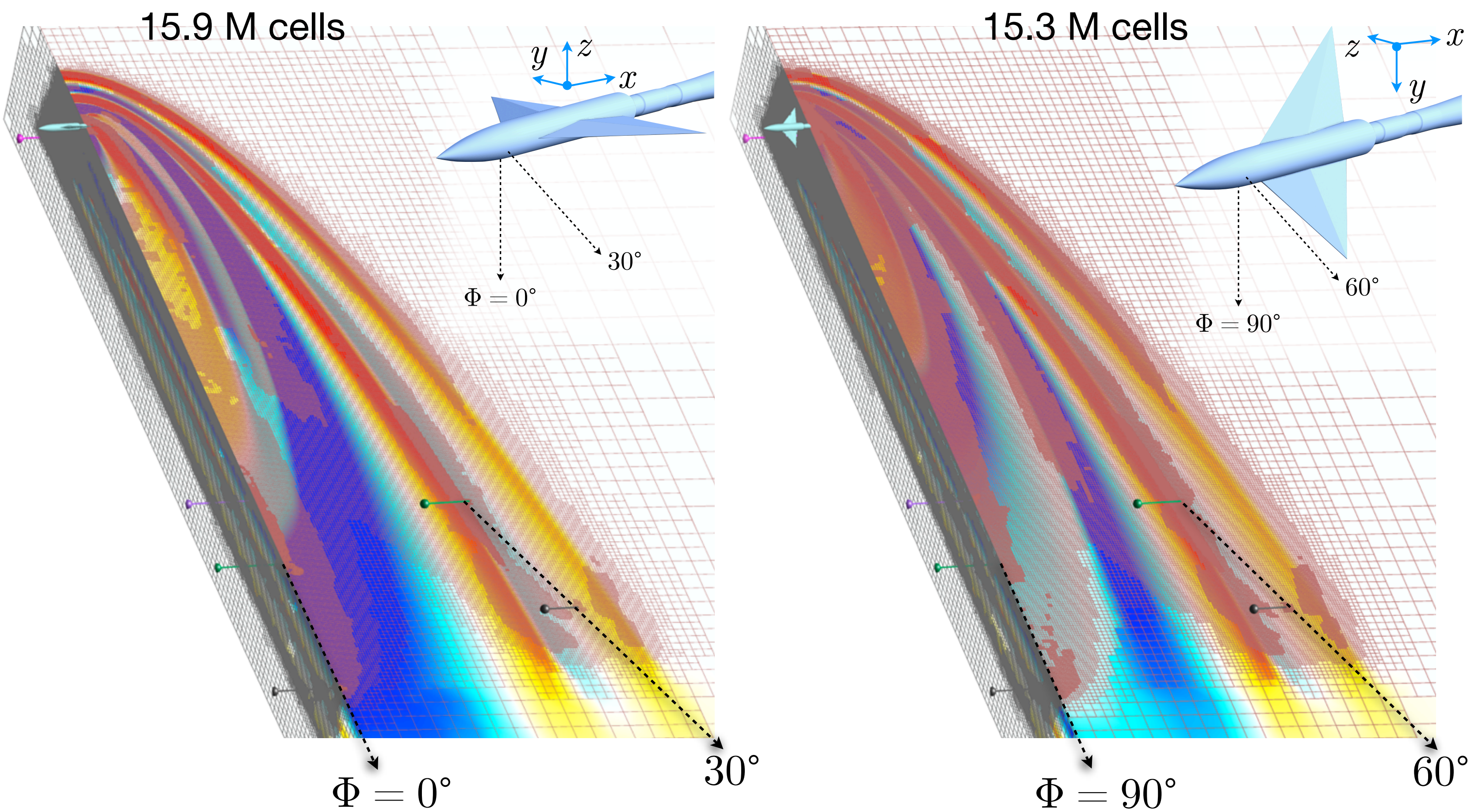

Setup as 2 cases

1. $\Phi = \{0^\circ, 30^\circ\}$ – Mesh rotated in pitch plane
2. $\Phi = \{60^\circ, 90^\circ\}$ – Mesh rotated in yaw plane

Case 2 – 69° Delta Wing Body

$M_\infty = 1.7$

$\alpha = 0°$

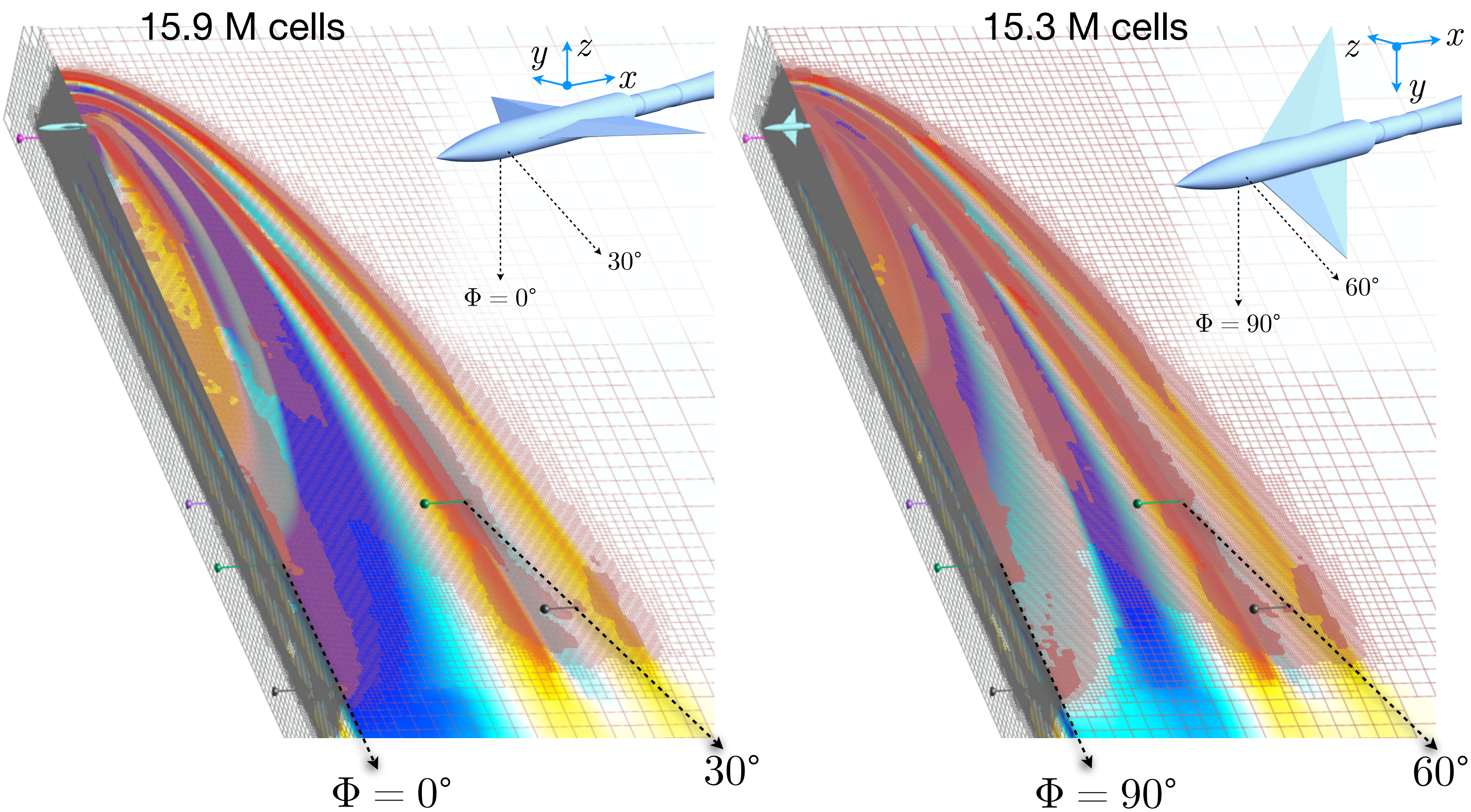

Resources

- Run on dual socket system w/ 20 cores
- (1 hr runtime) x 2
- 36 GB of memory (max)

69° Delta Wing Body: Mesh Convergence

- Results at 9th adaptation submitted to workshop
- Perform 2 more adaptations to assess degree of mesh convergence

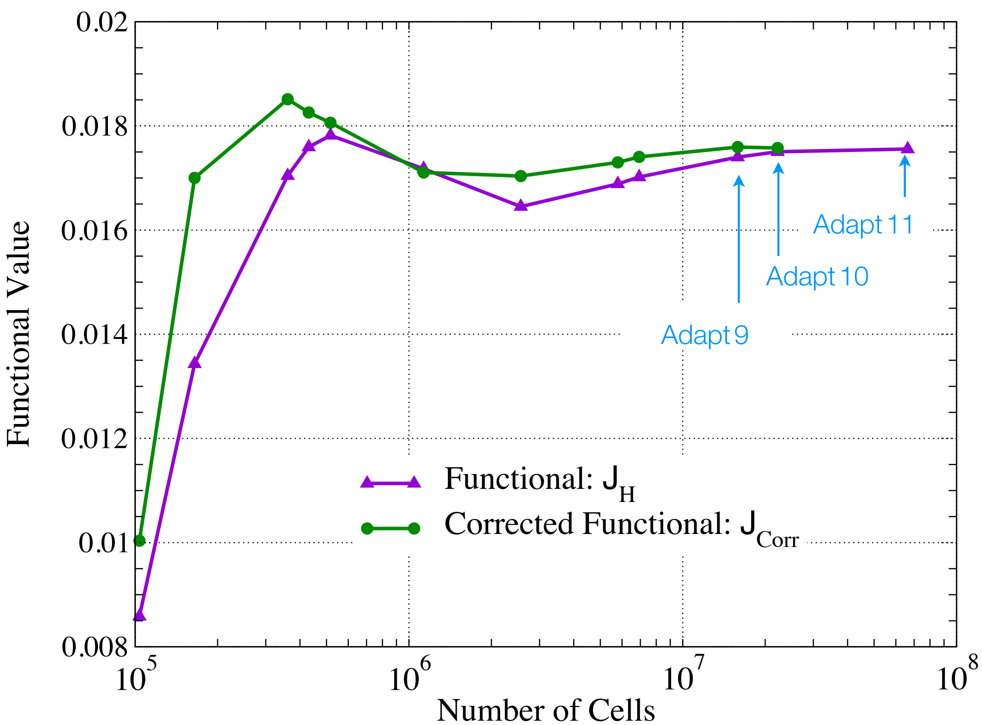

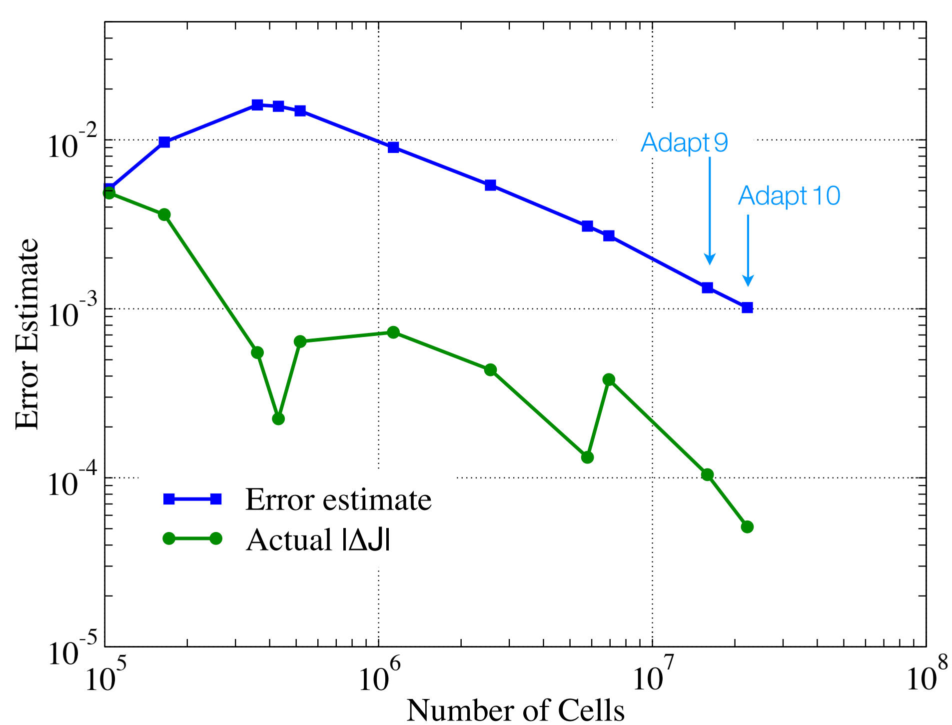

- Functional converges
- Correction *leads* functional
- Adjoint Correction vanishes

- Error-estimate bounds update |ΔJ|
- Remaining error converges asymptotically
- Very good convergence

69° Delta Wing Body: Signatures @ 24.8 in

$M_\infty = 1.7,\ \alpha = 0°$

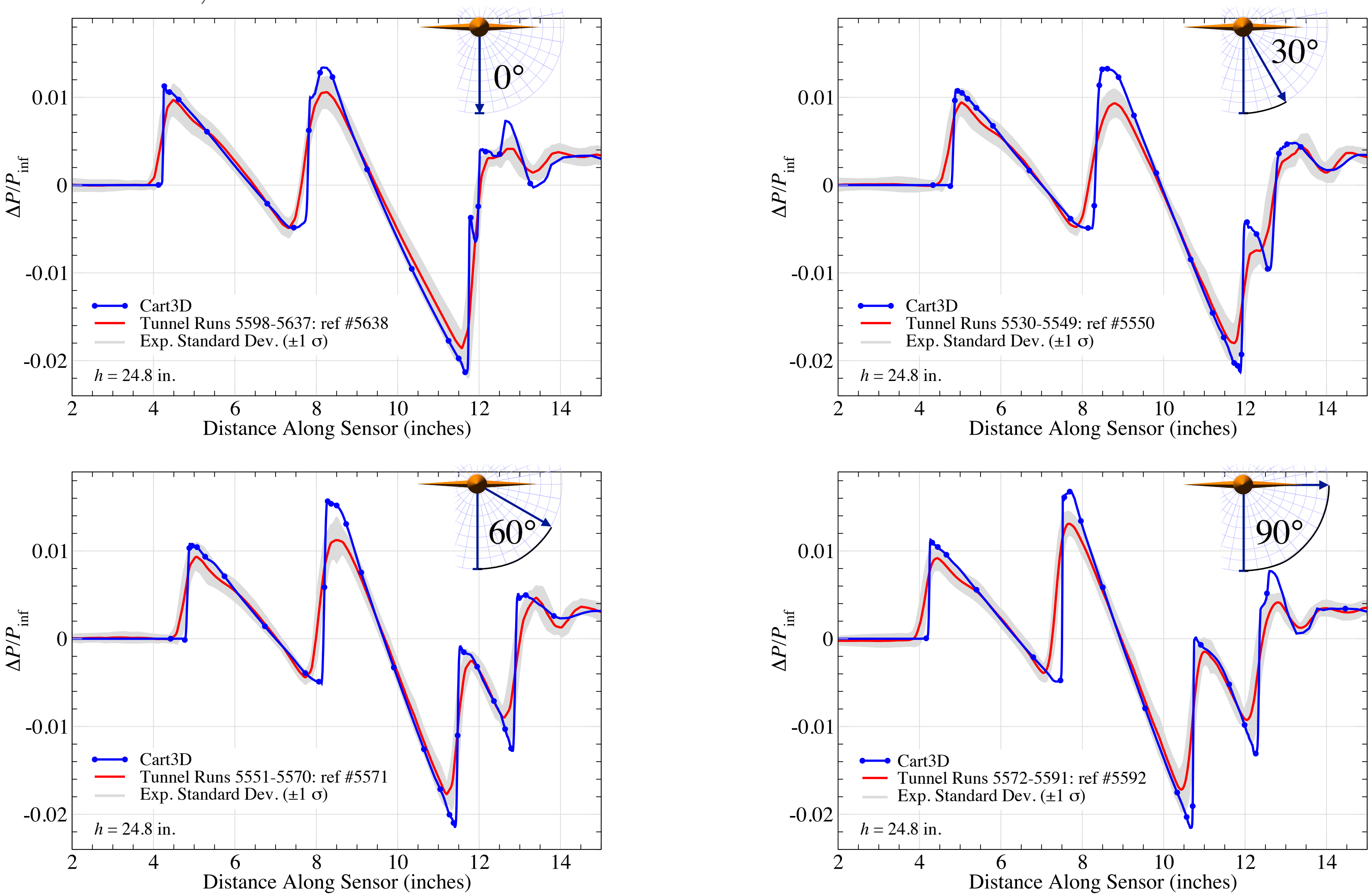

69° Delta Wing Body: Signatures @ 31.8 in

$M_\infty = 1.7, \alpha = 0°$

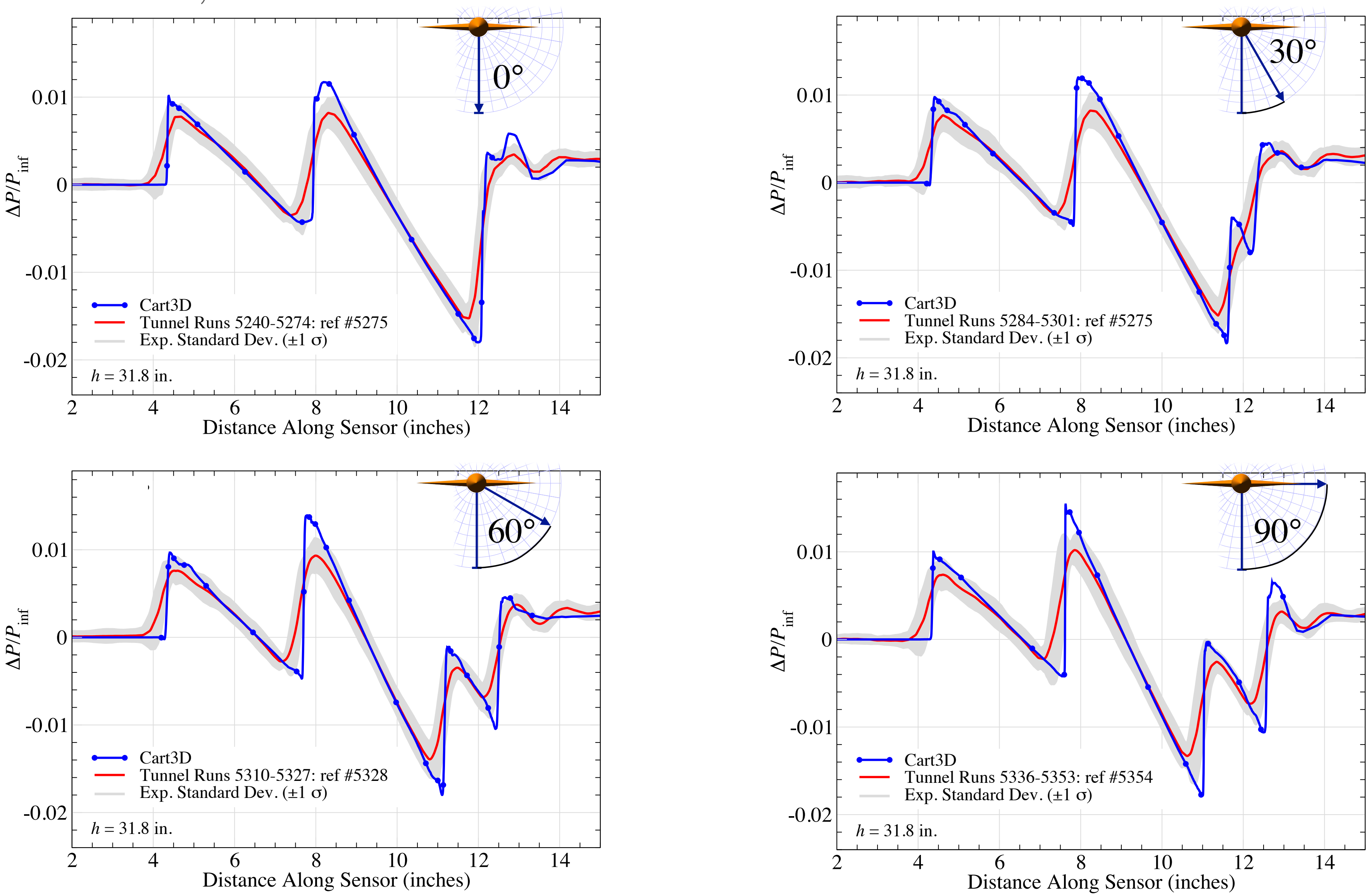

Lockheed Martin LM 1021

$M_\infty = 1.6, \alpha = 2.1°$

$L_{ref} = 22.40$ in
$S_{ref} = 33.18$ in^2
$M_\infty = 1.6$
$\alpha_{cruise} = 2.3°$
$C_{L\,cruise} = 0.142$

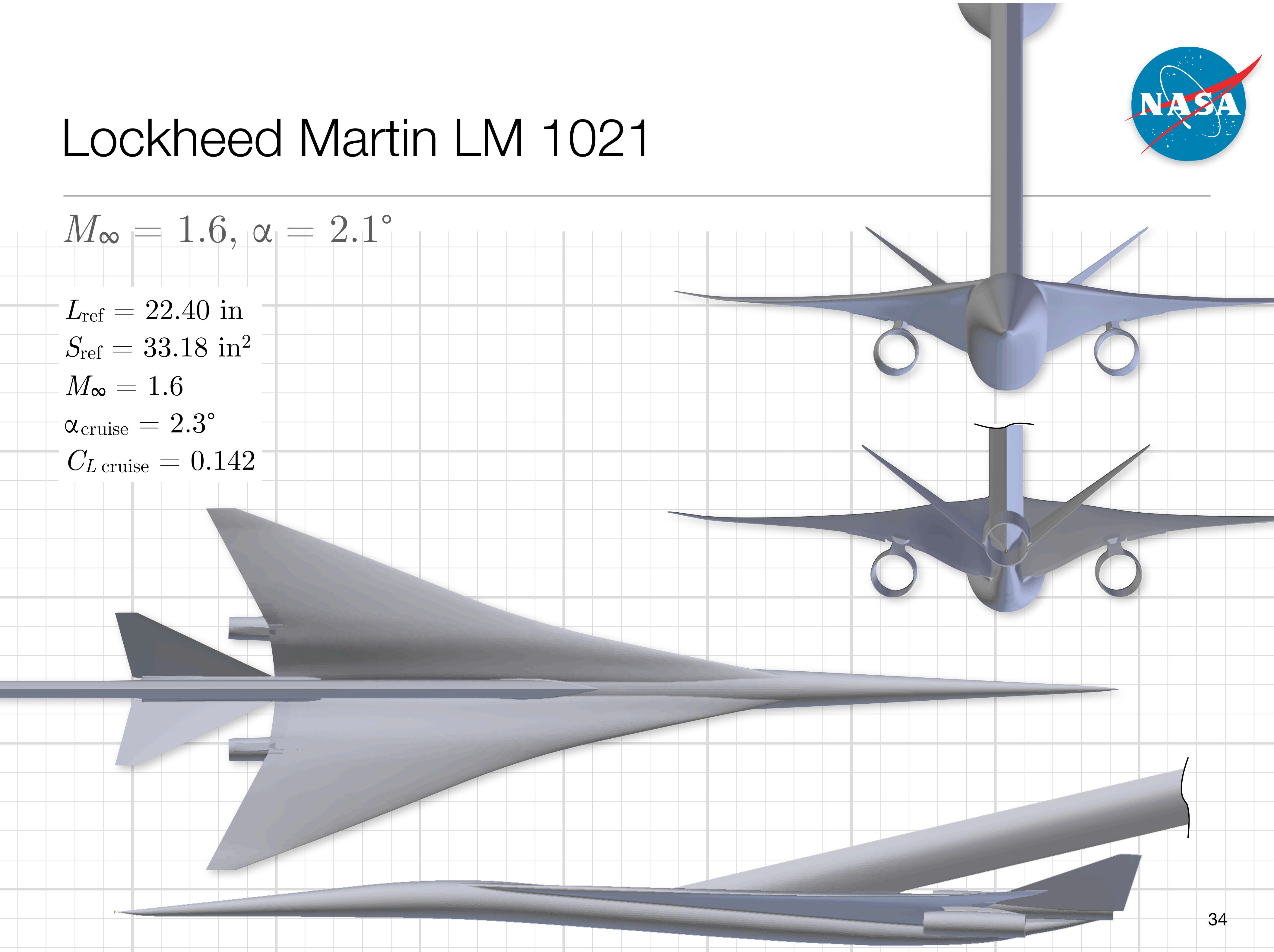

LM 1021: Conditions

$M_\infty = 1.6, \alpha = 2.1°$

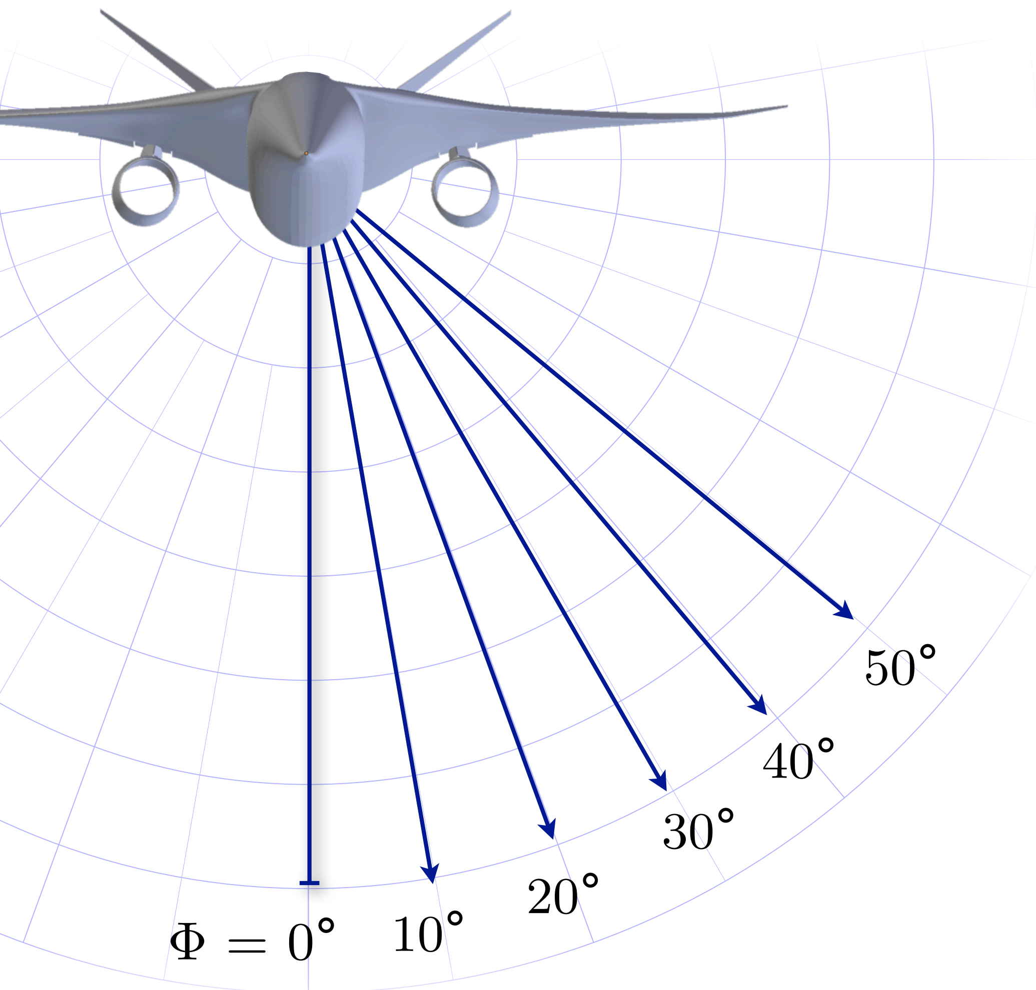

Extracted signatures at 30 locations

- h = {1.64, 2.65, 3.50, 5.83, 8.39} ft
- $\Phi = \{0°, 10°, 20°, 30°, 40°, 50°\}$
- Single simulation for all 30 signatures
- Net functional is combination of 30 sensors

$$\mathcal{J} = \sum_{i=1}^{M} w_i \mathcal{J}_i \qquad \text{with}$$

$$w_i = \frac{h_i}{L_{\text{ref}}}\left(1 + \frac{4}{\sqrt{2}} \sin \Phi_i\right)$$

Weighting accounts for

- Decrease in signal strength w/ increasing h
- Increase in resolution requirements with increasing Φ

LM 1021: Meshing

$M_\infty = 1.6,\ \alpha = 2.1°$

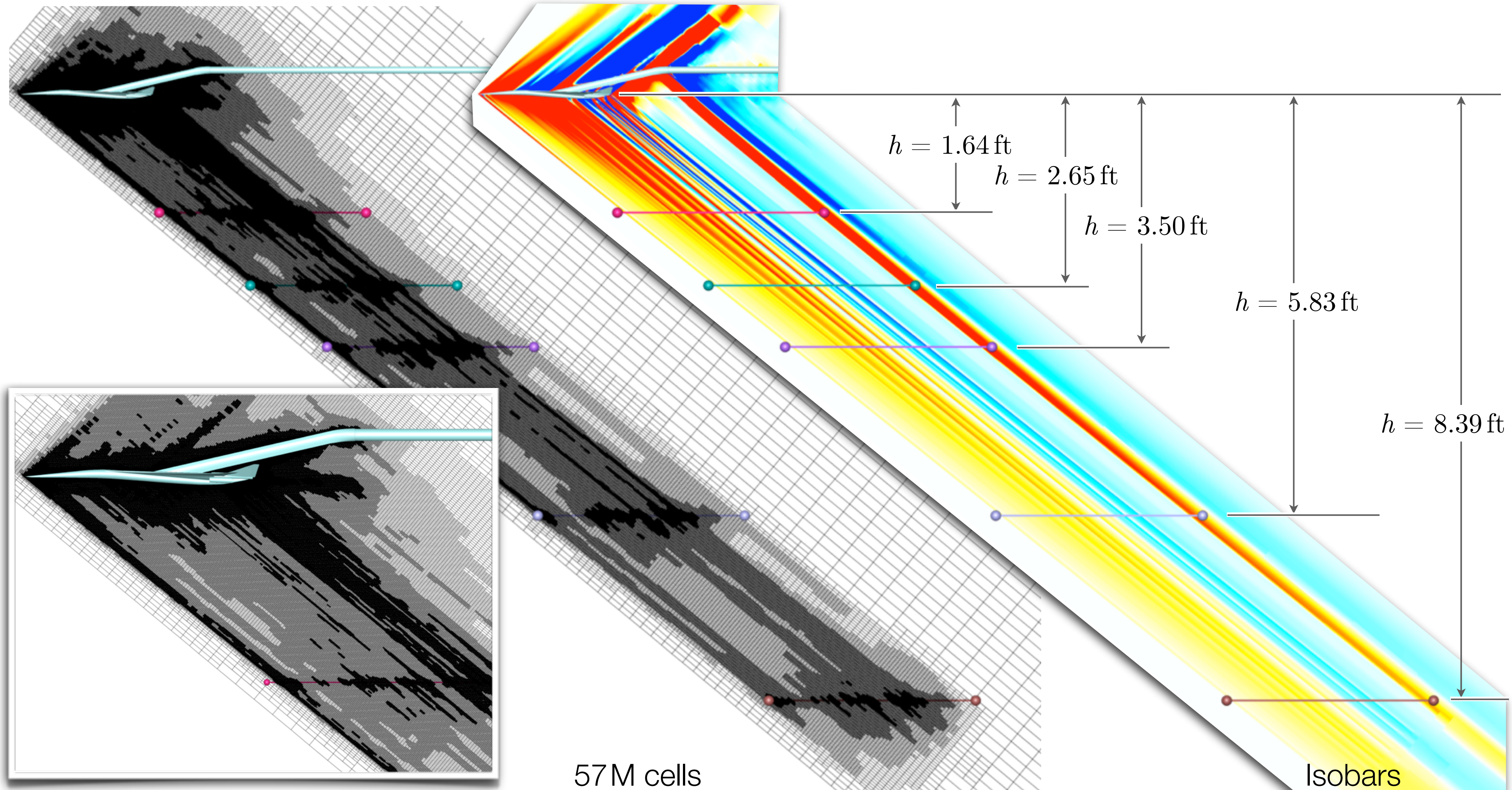

LM 1021: Meshing

$M_\infty = 1.6,\ \alpha = 2.1^\circ$

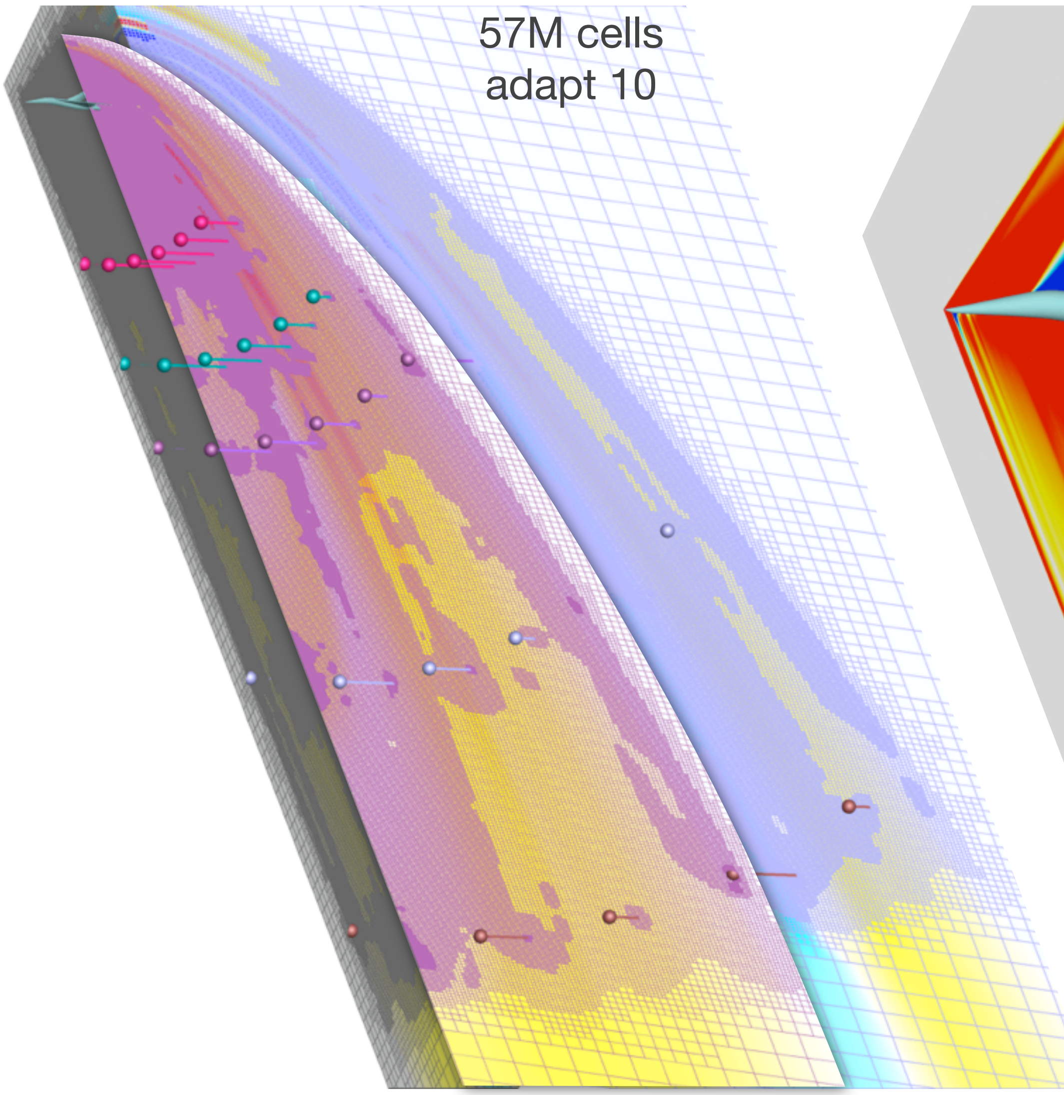

Isobars and mesh near body

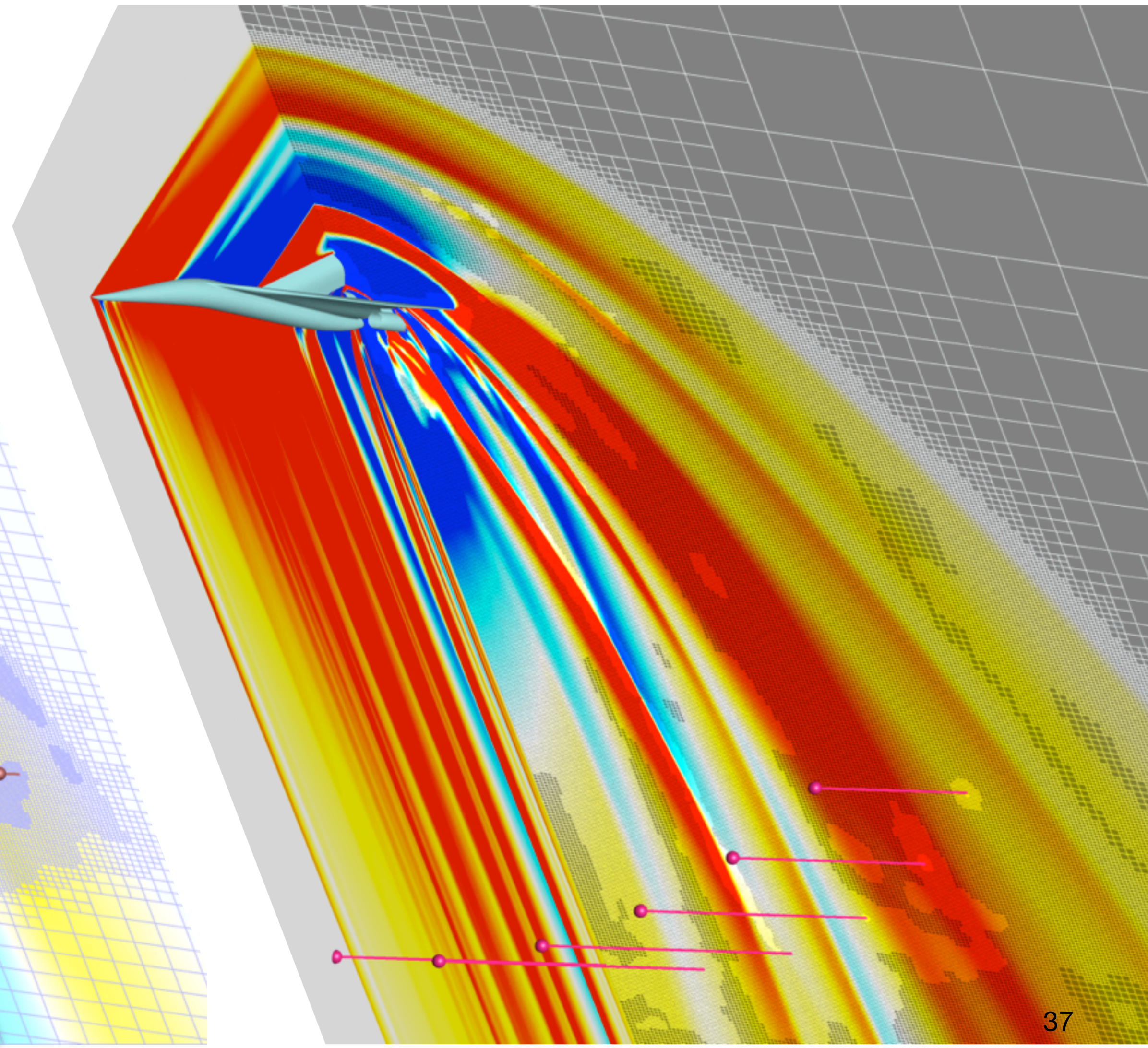

LM 1021: Resources

$M_\infty = 1.6, \alpha = 2.1^\circ$

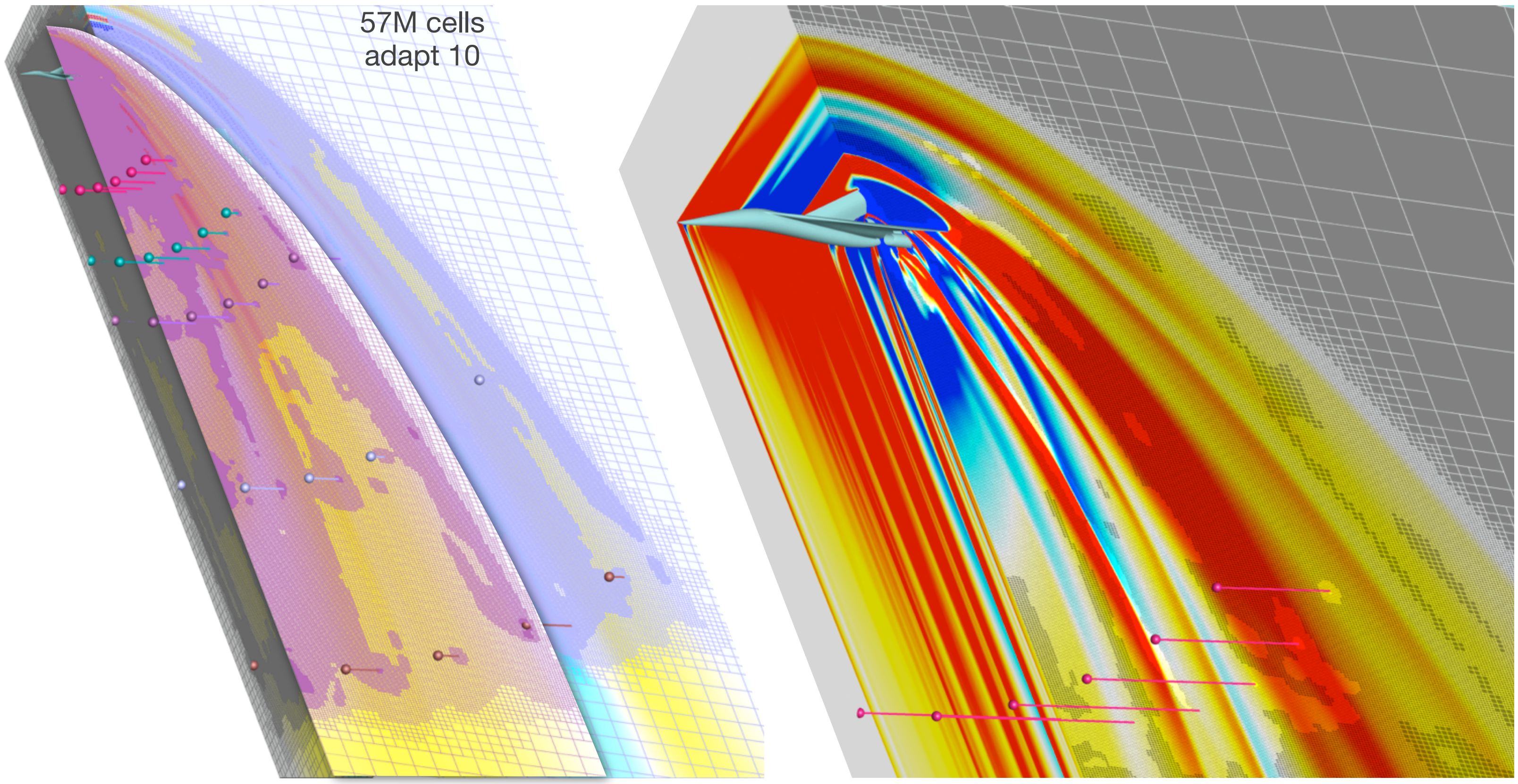

Resources

- Run on 96 Intel sandy bridge cores (NAS's Endeavour)
- 2 hr 20 mins runtime (61mins)
- 80 GB of memory (max)

LM 1021: Functional Convergence

- Results at 10th adaptation submitted to workshop
- Perform 2 more adaptations to assess degree of mesh convergence

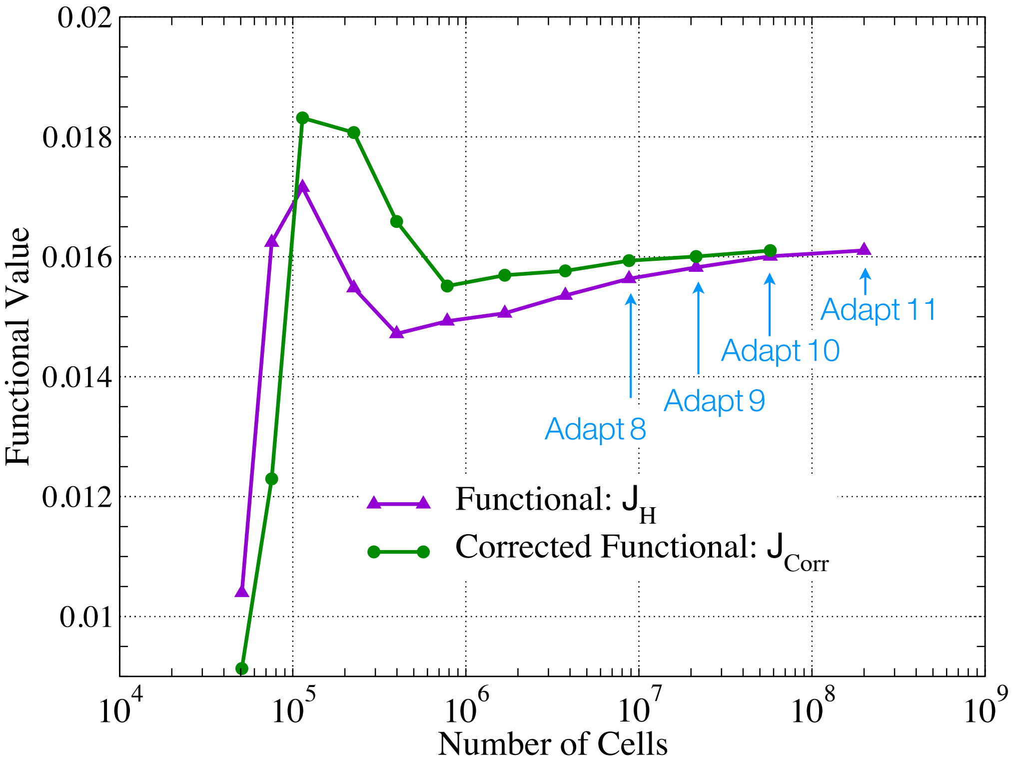

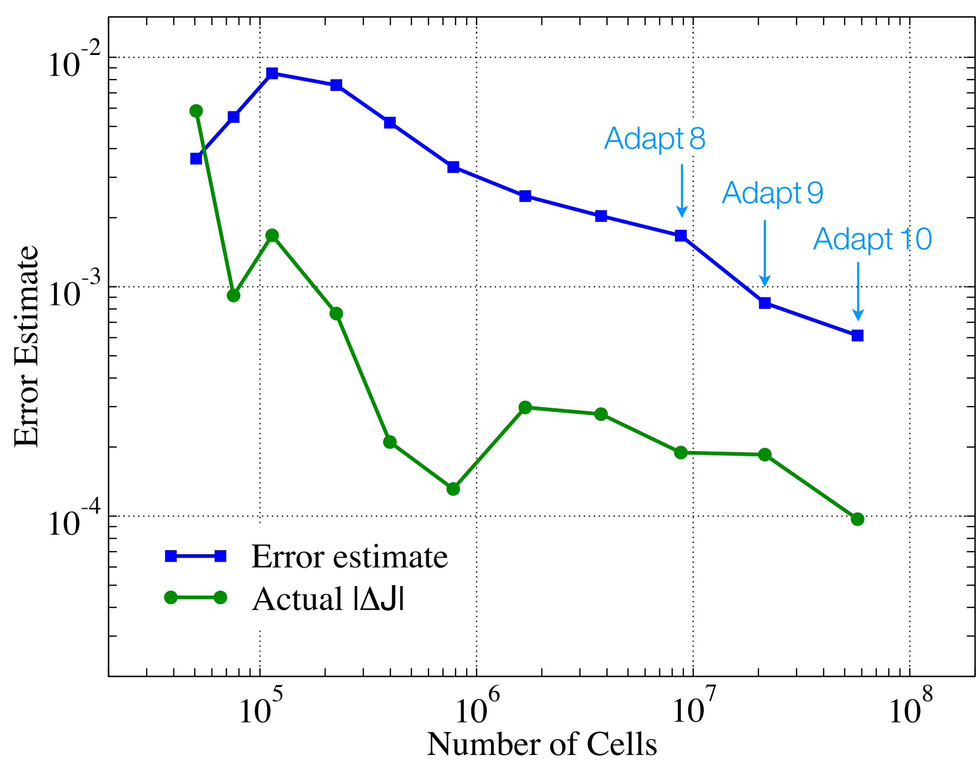

- Functional converges
- Correction *leads* functional
- Adjoint Correction vanishes

- Error-estimate bounds update |ΔJ|
- Remaining error converges asymptotically
- Very good convergence

LM 1021: Pressure field

$M_\infty = 1.6,\ \alpha = 2.1°$

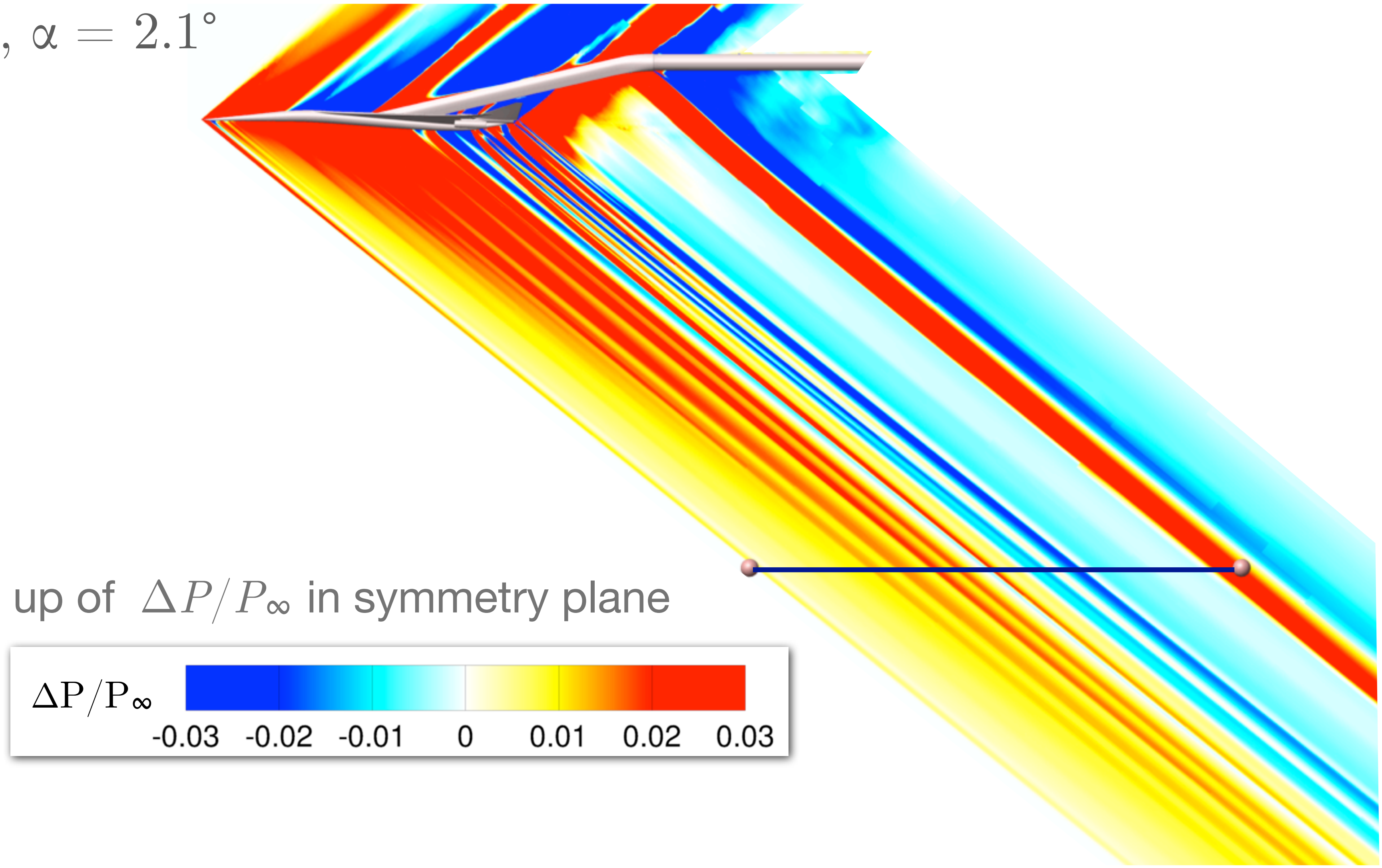

Close up of $\Delta P/P_\infty$ in symmetry plane

LM 1021: Pressure field

$M_\infty = 1.6, \alpha = 2.1°$

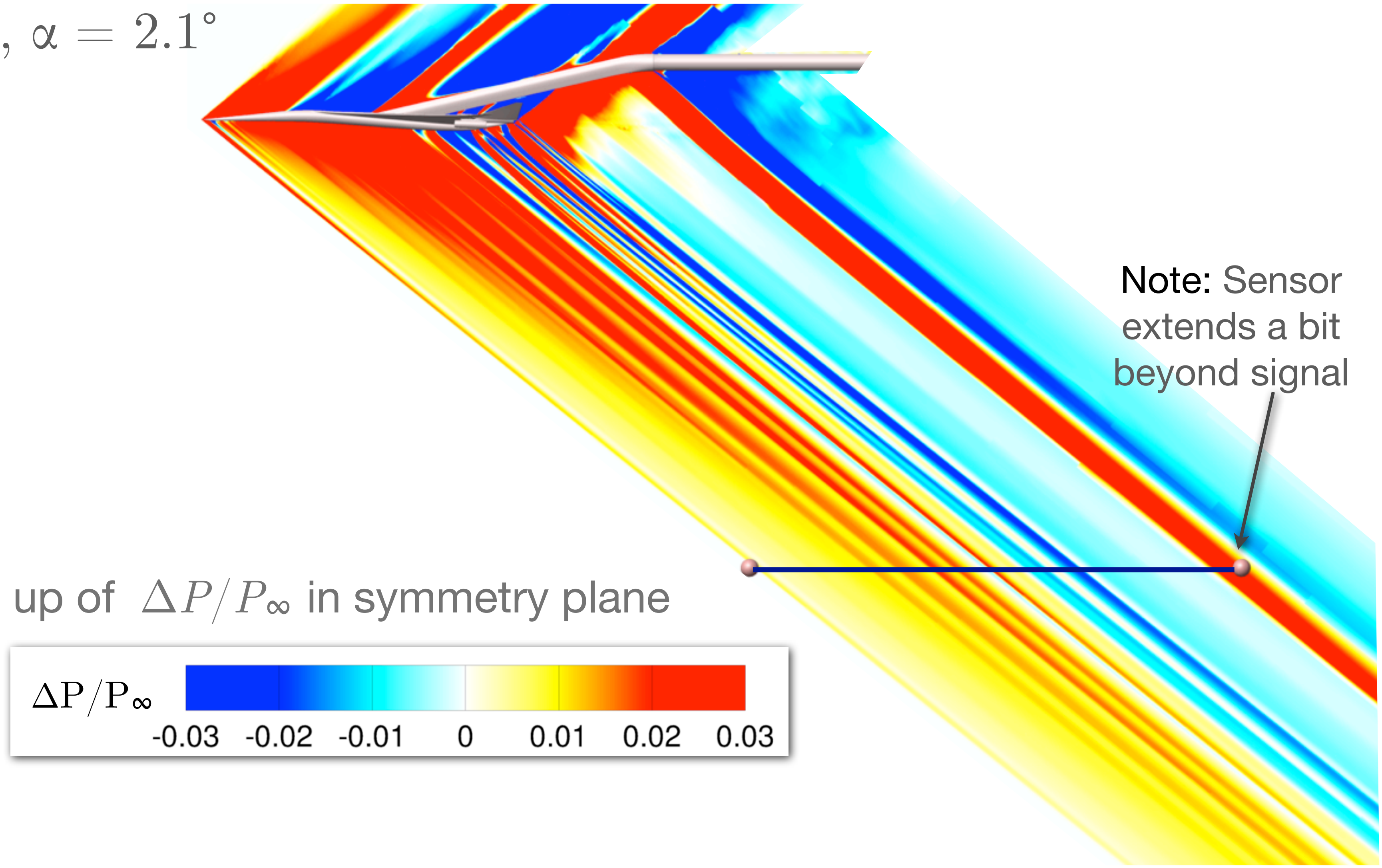

Close up of $\Delta P / P_\infty$ in symmetry plane

LM 1021: Pressure Carpets

$M_\infty = 1.6,\ \alpha = 2.1°$

- h = {1.64, 2.65, 3.50, 5.83, 8.39} ft
- $\Phi = \{0°, 10°, 20°, 30°, 40°, 50°\}$
- Construct pressure carpets by tessellating data along sensors at fixed h/L

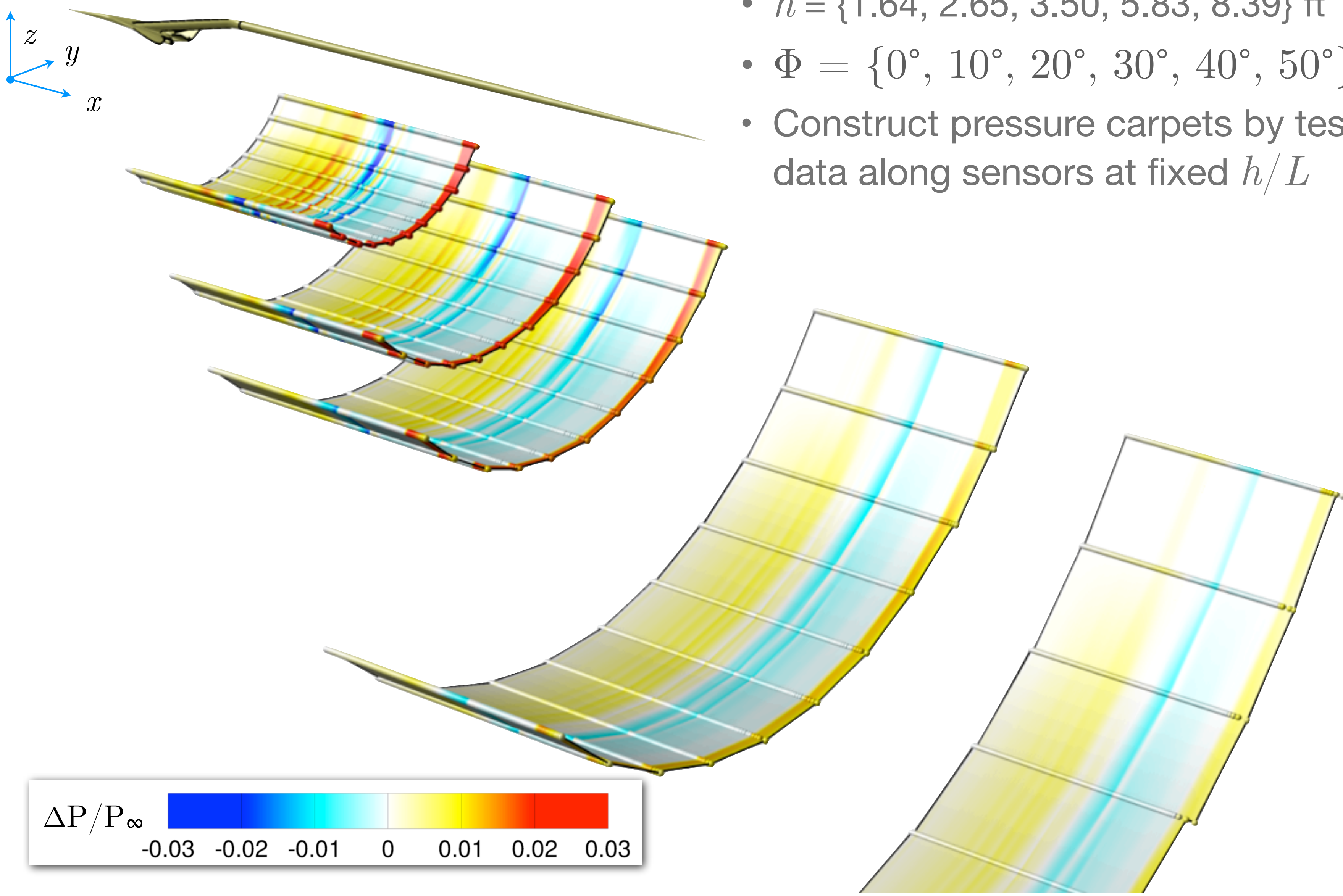

LM 1021: Pressure Carpets

$M_\infty = 1.6, \alpha = 2.1°$

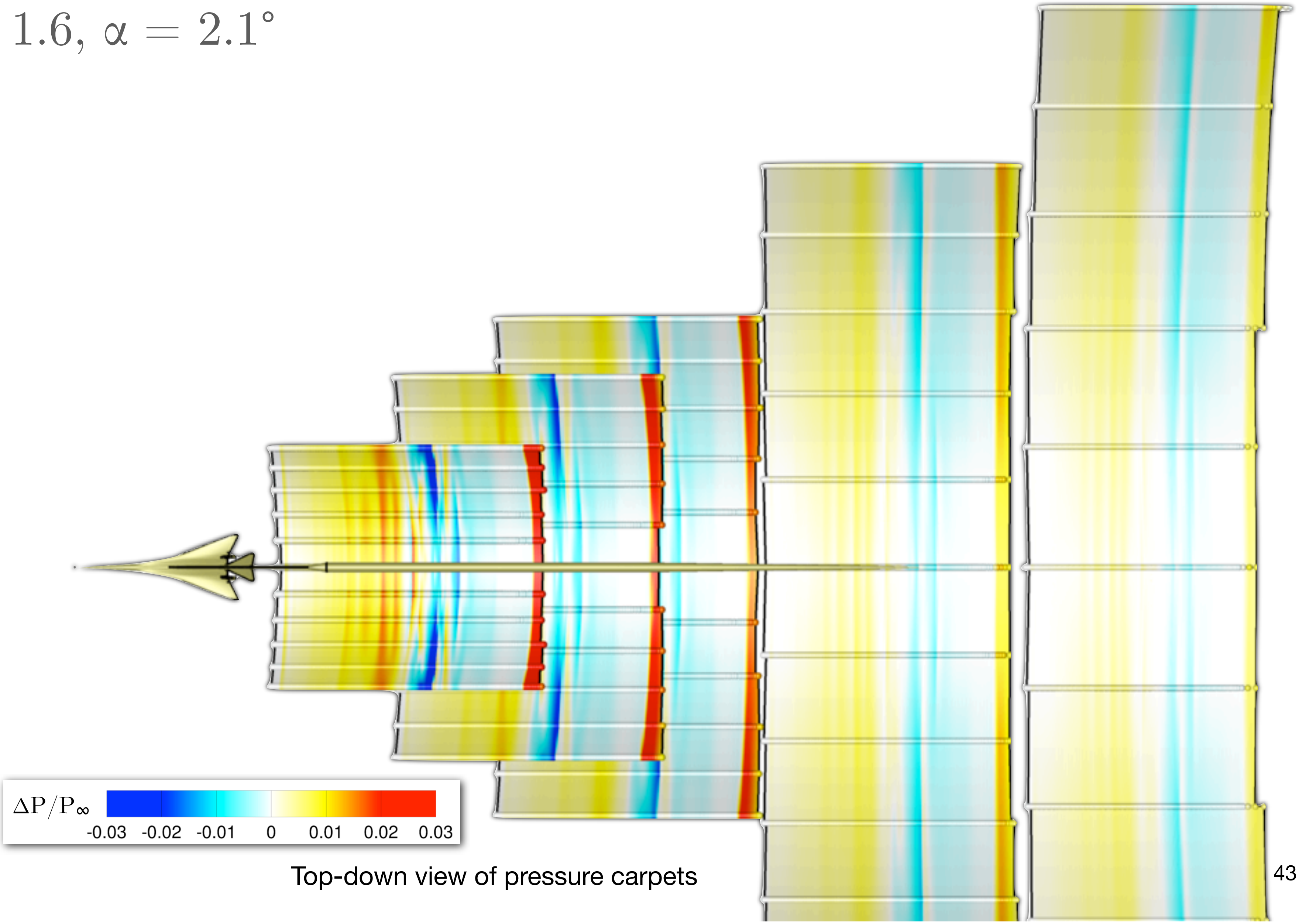

Top-down view of pressure carpets

LM 1021: Pressure Carpets

$M_\infty = 1.6,\ \alpha = 2.1°$

- Appears very quiet on-track

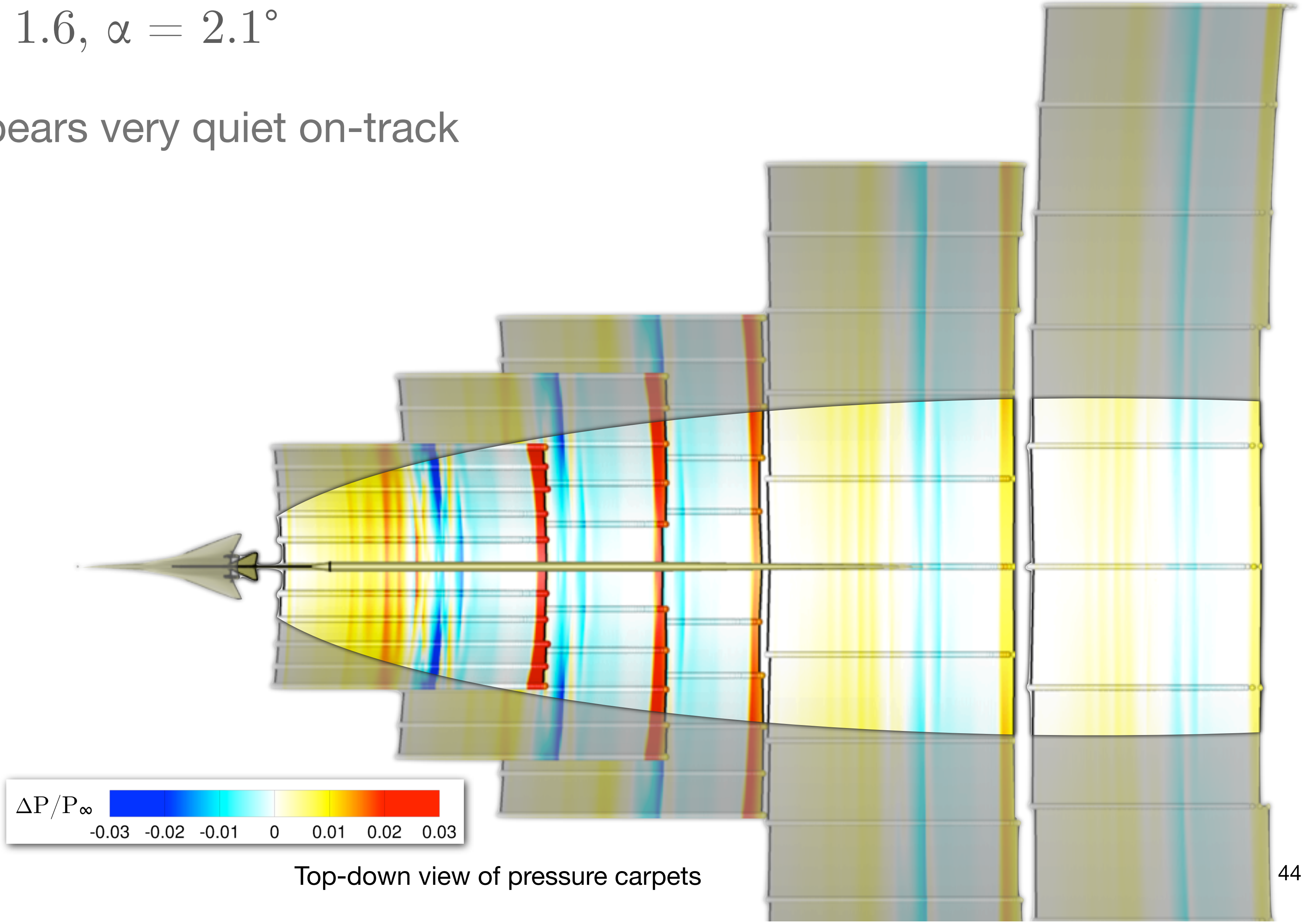

Top-down view of pressure carpets

LM 1021: Pressure Carpets

$M_\infty = 1.6, \alpha = 2.1°$

- Appears very quiet on-track
- Strong expansion off-track @ $\Phi > 10°$-$15°$
- Persists at large h and Φ

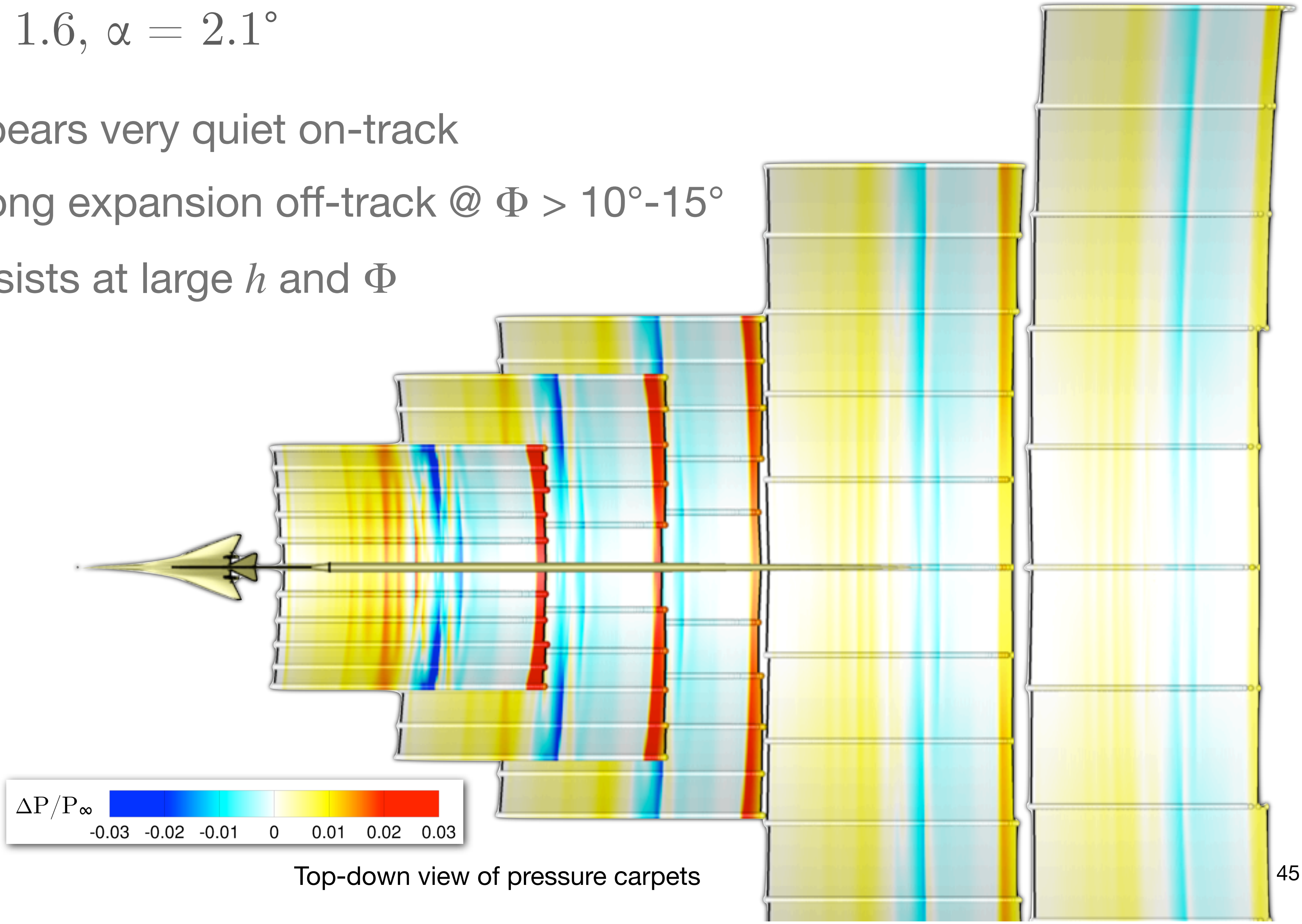

Top-down view of pressure carpets

LM 1021: Off-track Pressure Signature

$M_\infty = 1.6,\ \alpha = 2.1°,\ \Phi = 50°$

- Good agreement
- Difference in alpha may account for the slightly lower peaks

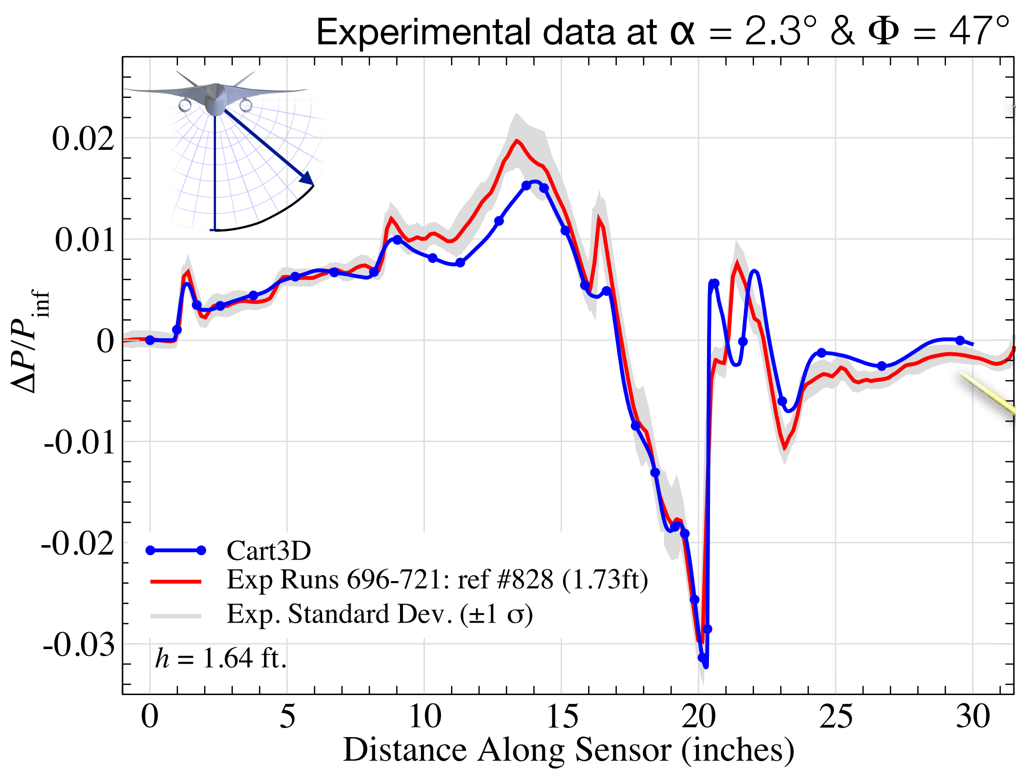

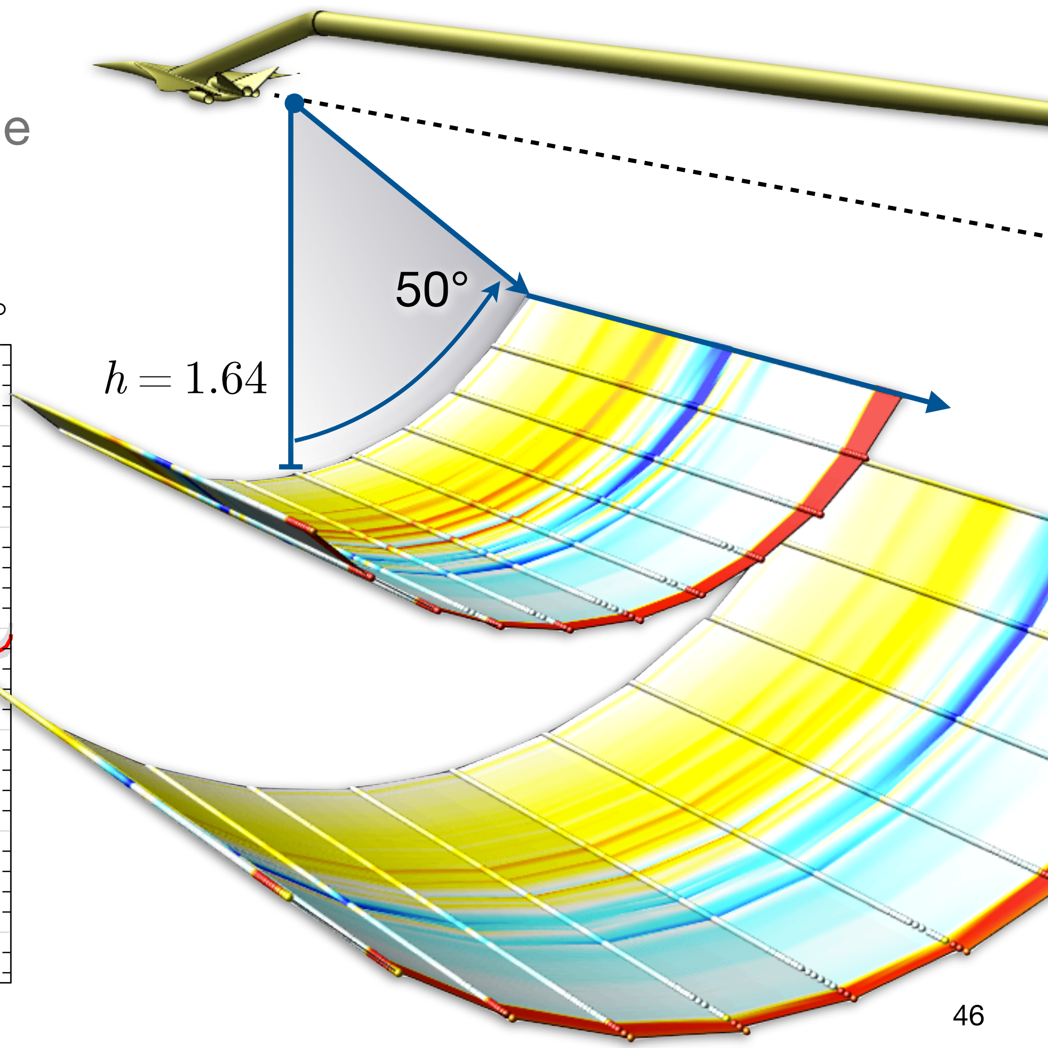

LM 1021: Off-track Pressure Signature

$M_\infty = 1.6,\ \alpha = 2.1°,\ \Phi = 20°$

Experimental data at α = 2.3°

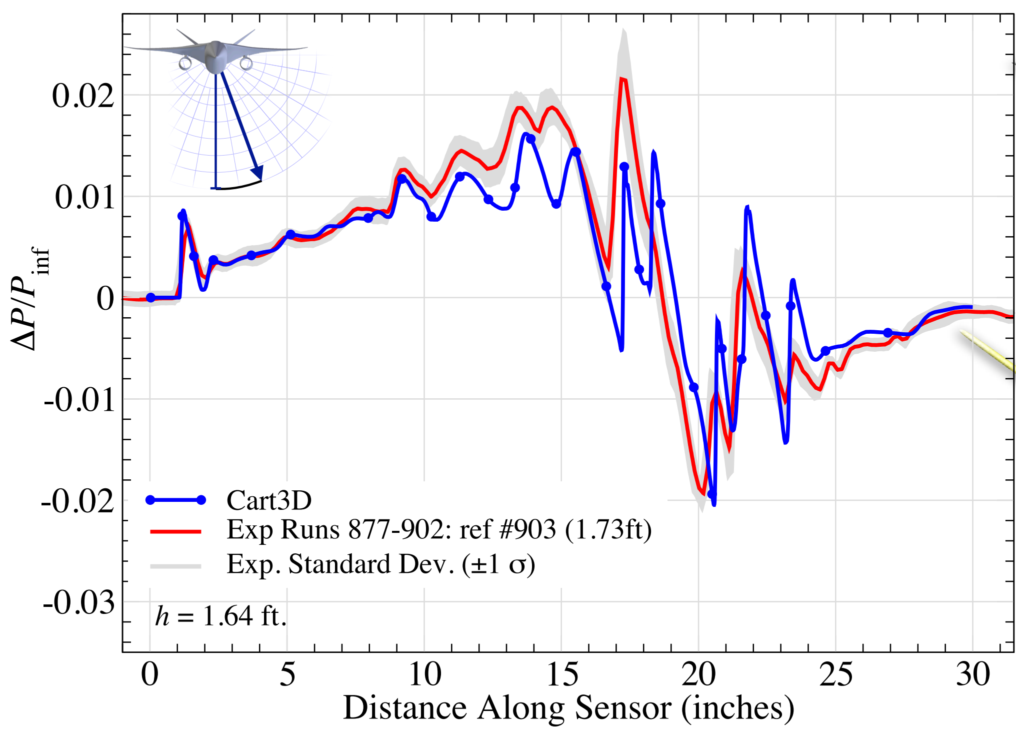

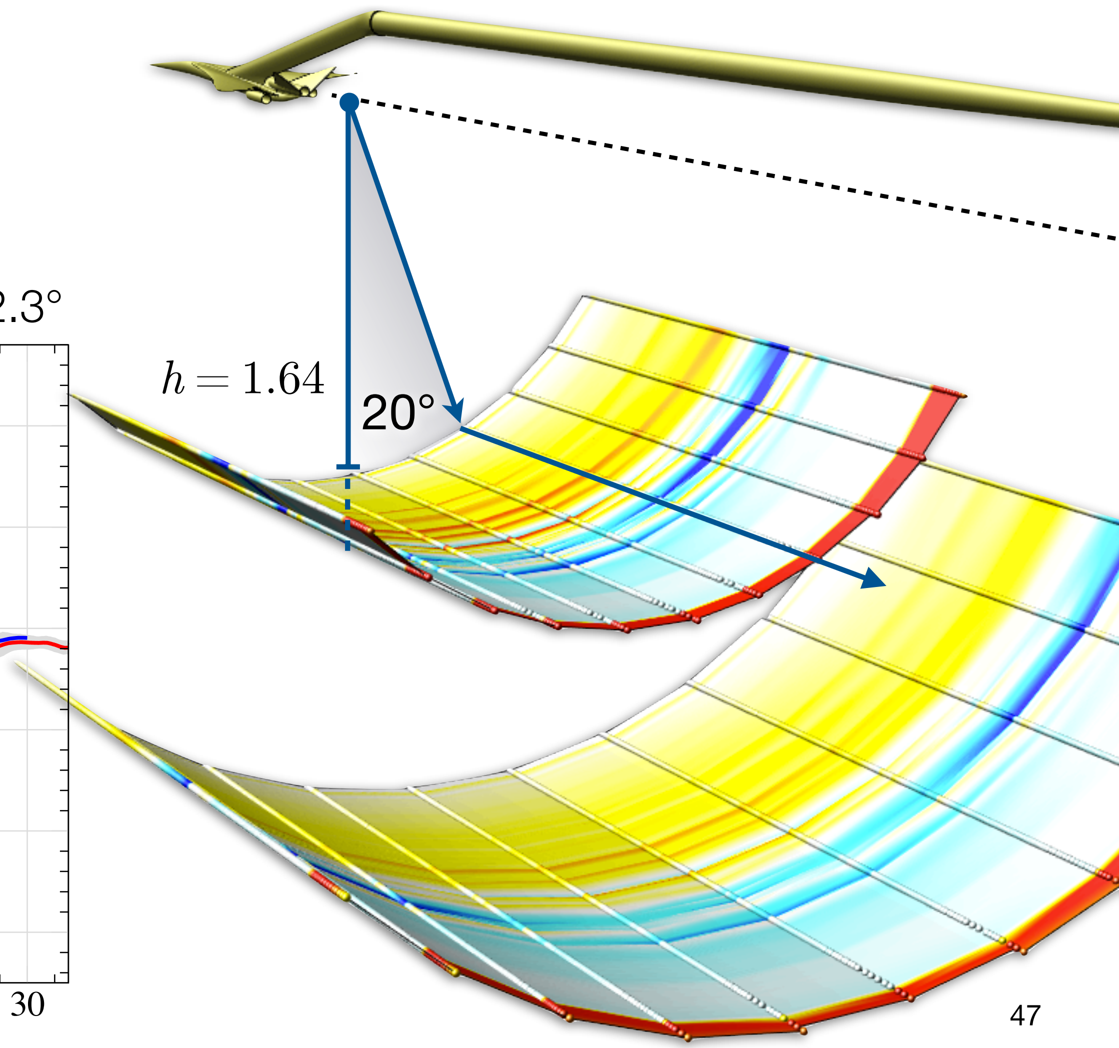

LM 1021: On-track Pressure Signature

$M_\infty = 1.6, \alpha = 2.1°, \Phi = 0°$

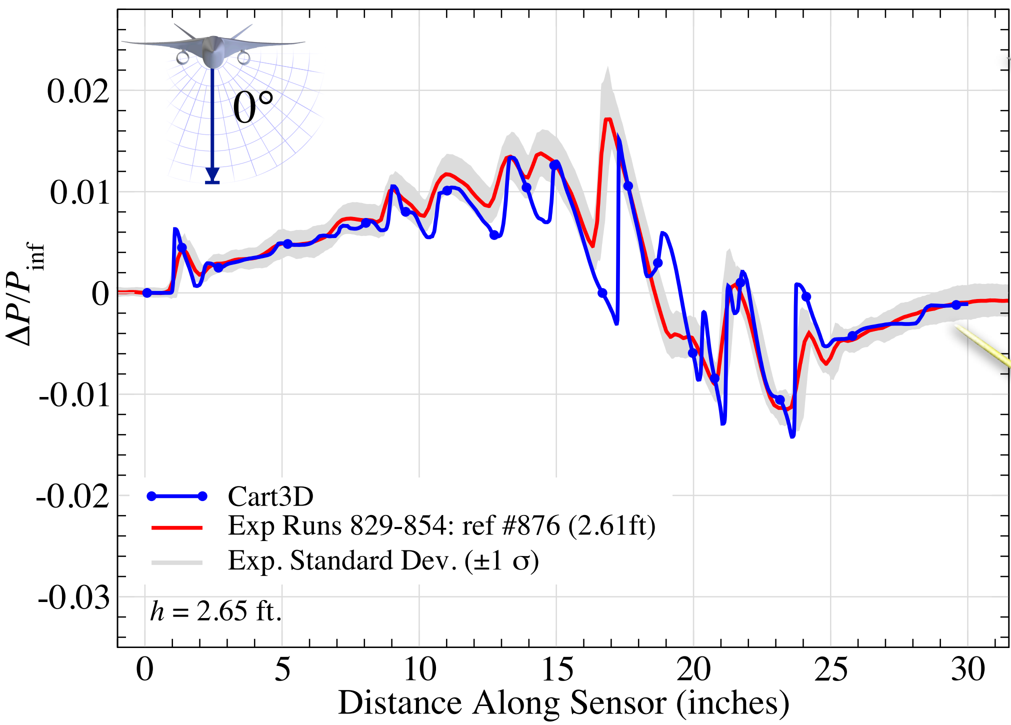

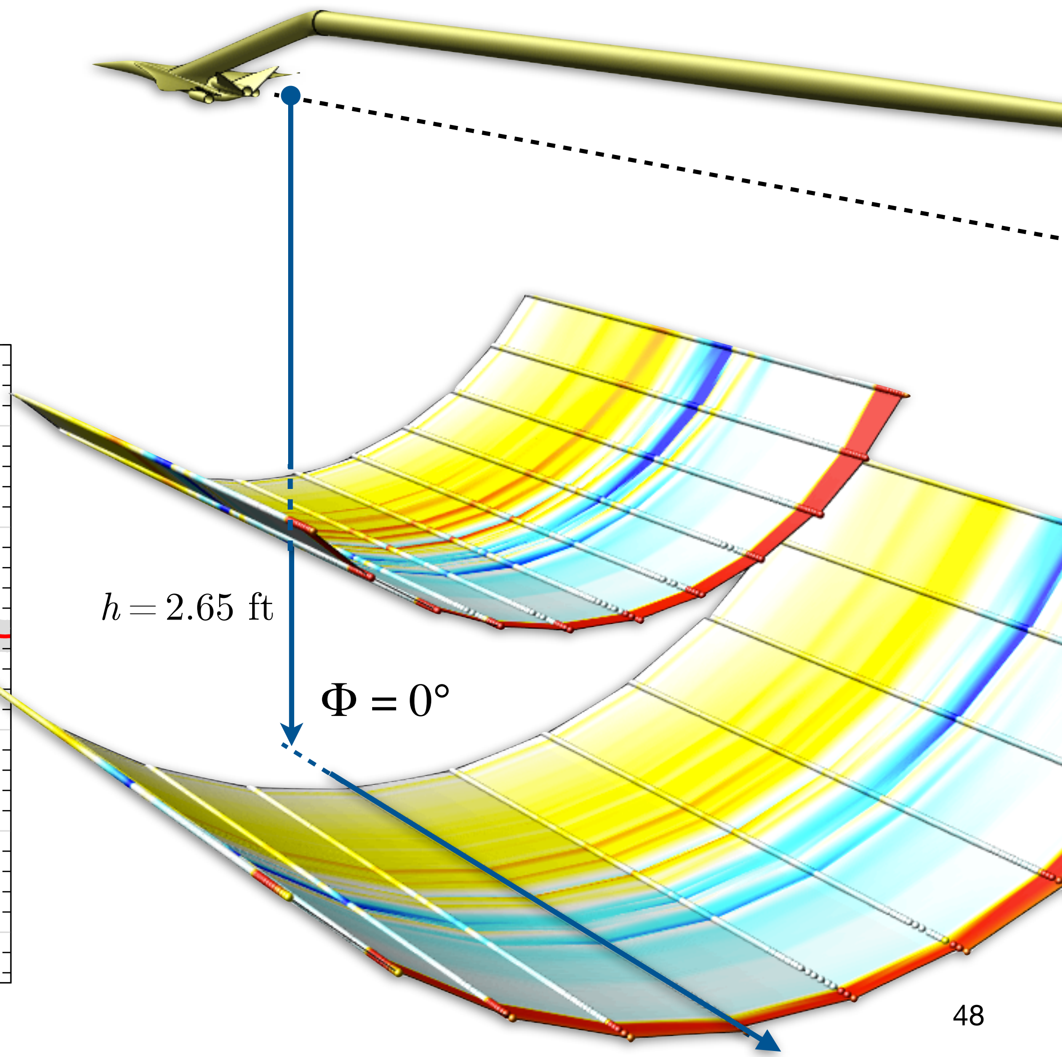

LM 1021: Investigation of On-track Discrepancy

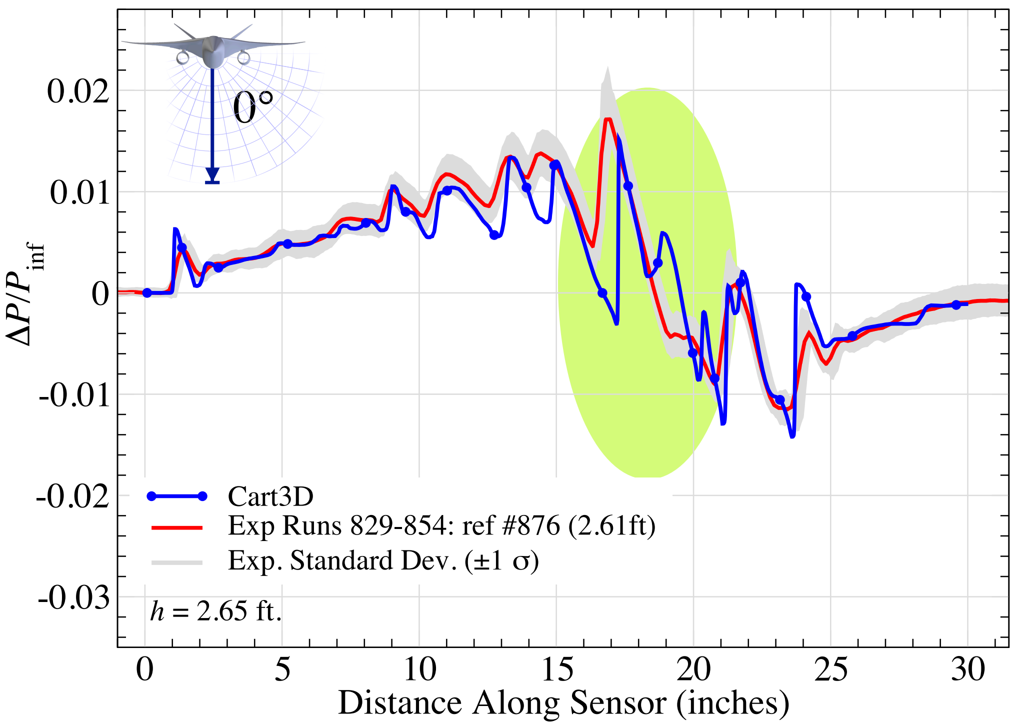

LM 1021: Investigation of On-track Discrepancy

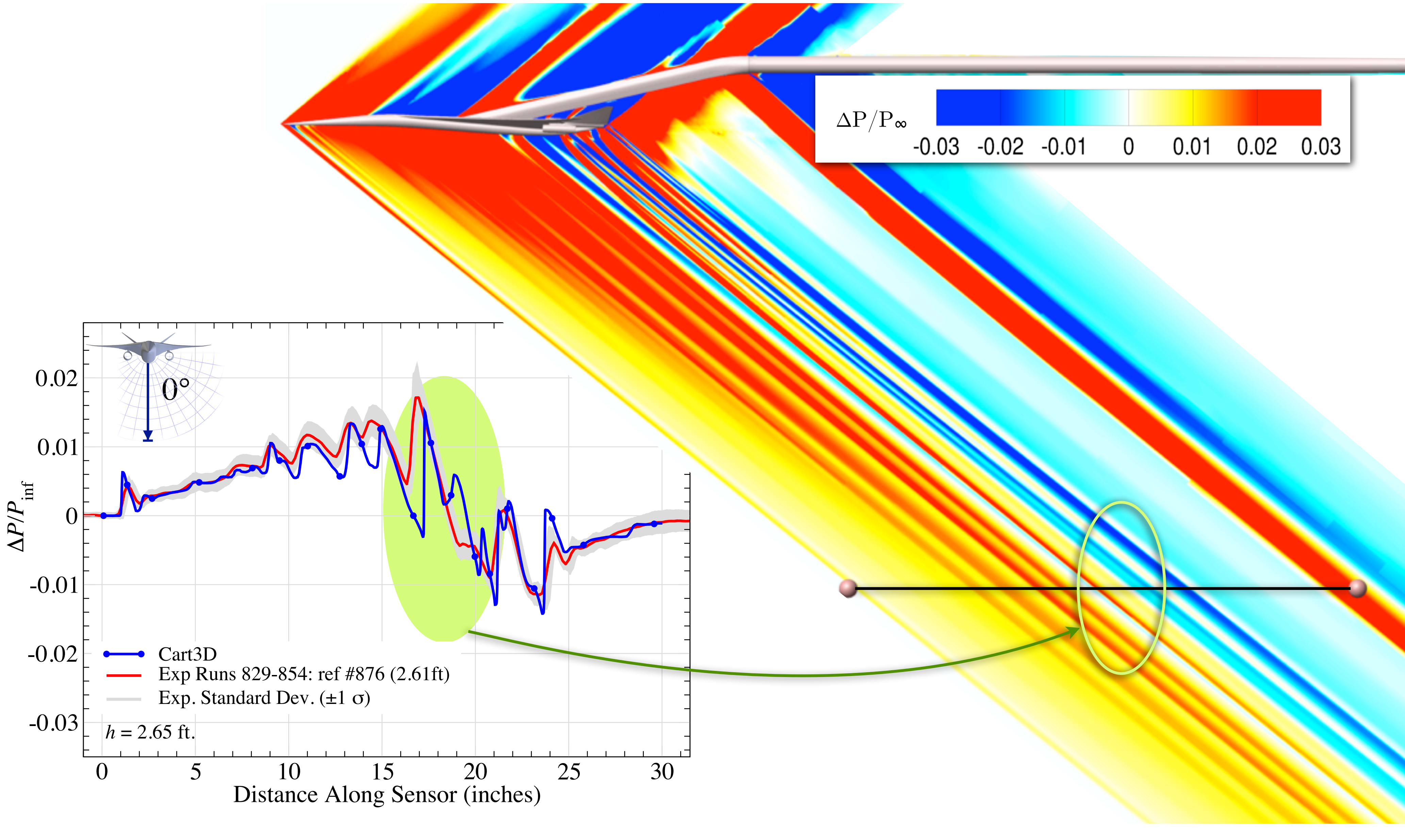

LM 1021: Investigation of On-track Discrepancy

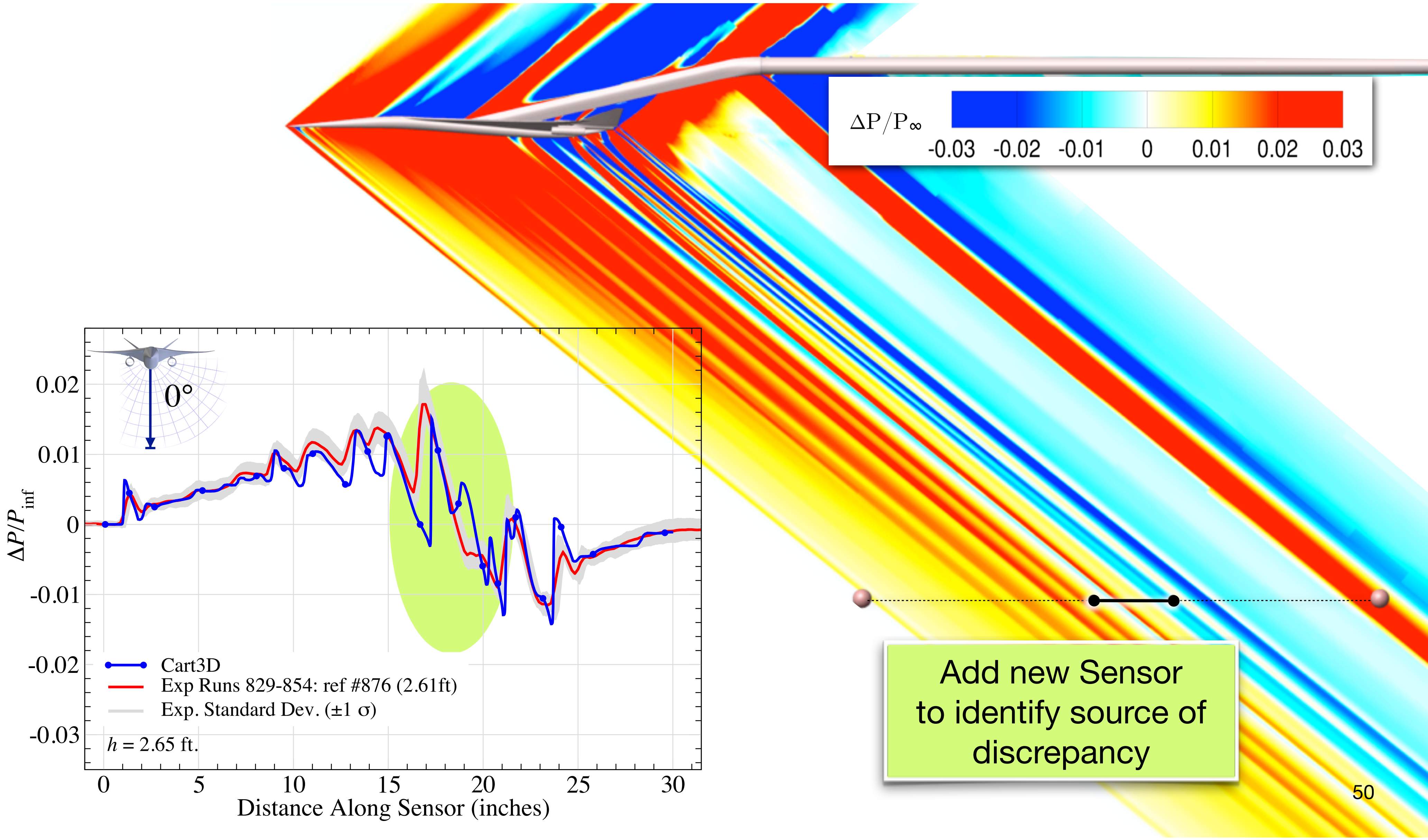

Add new Sensor to identify source of discrepancy

LM 1021: Investigation of On-track Discrepancy

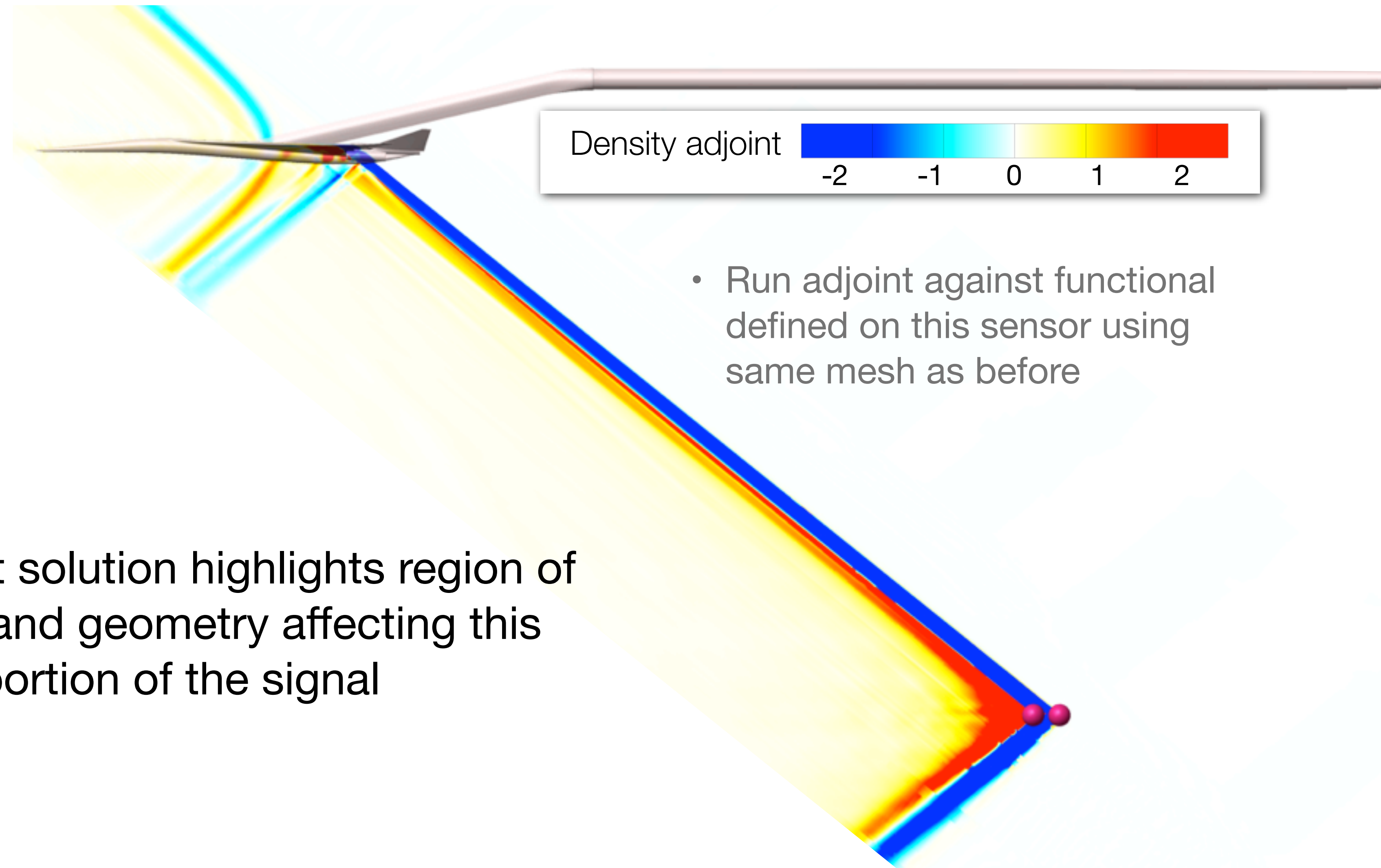

- Run adjoint against functional defined on this sensor using same mesh as before

The adjoint solution highlights region of the flow and geometry affecting this portion of the signal

LM 1021: Investigation of On-track Discrepancy

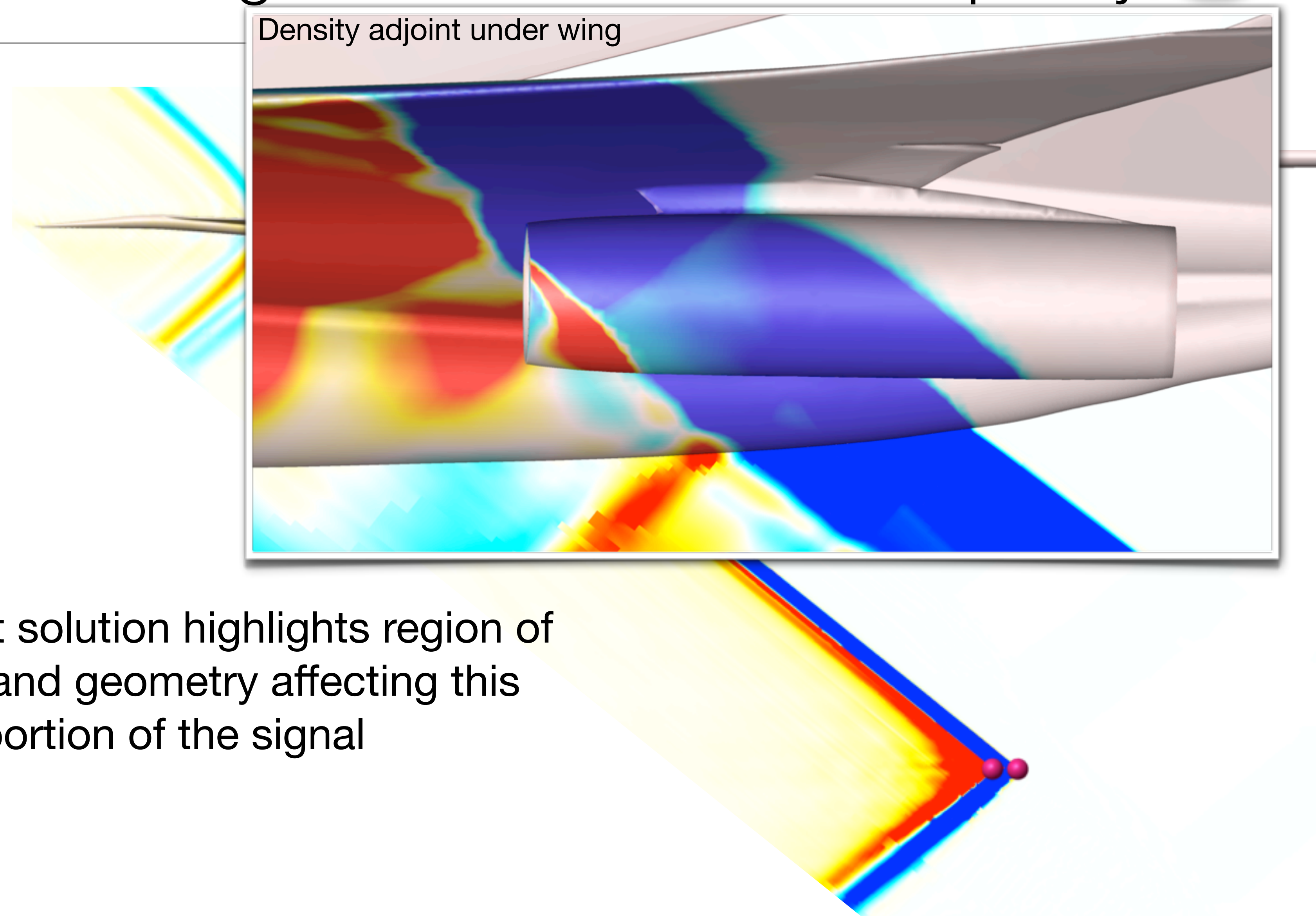

The adjoint solution highlights region of the flow and geometry affecting this portion of the signal

LM 1021: Investigation of On-track Discrepancy

- Adjoint tells us where to look...
- Investigate physics of tunnel flow
- Viscous results from USM3D
- Tunnel Re_L is ~100x lower than flight
- Boundary layer extends to nacelle

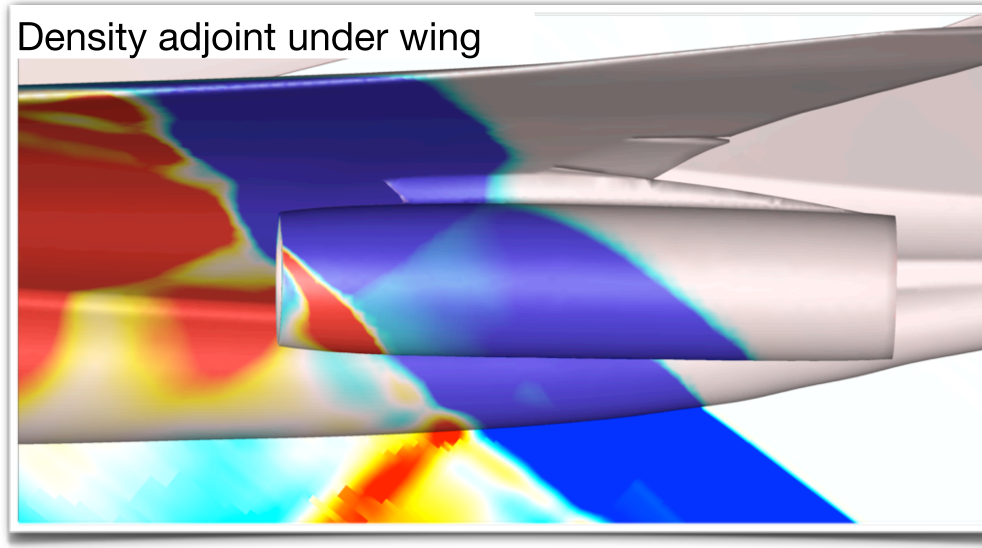

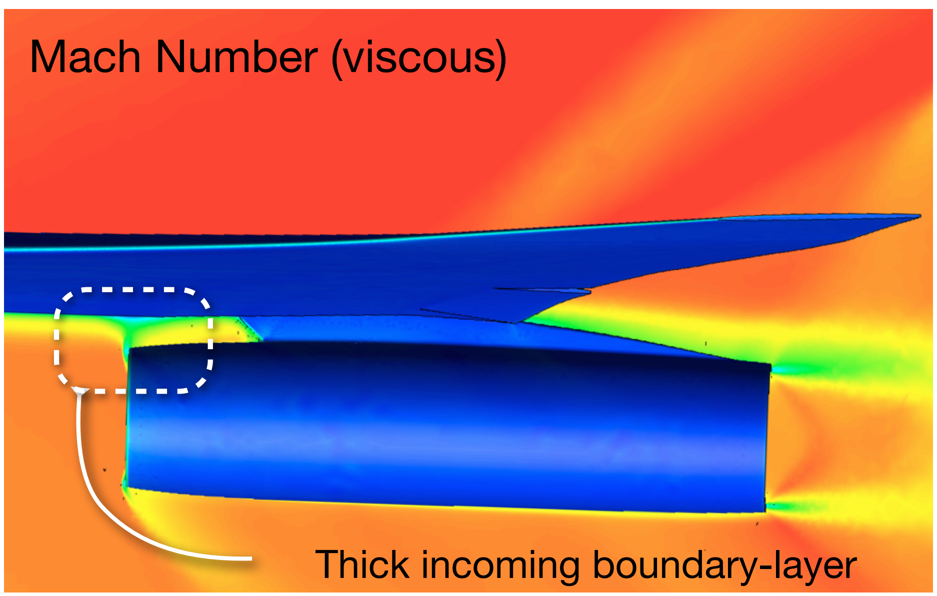

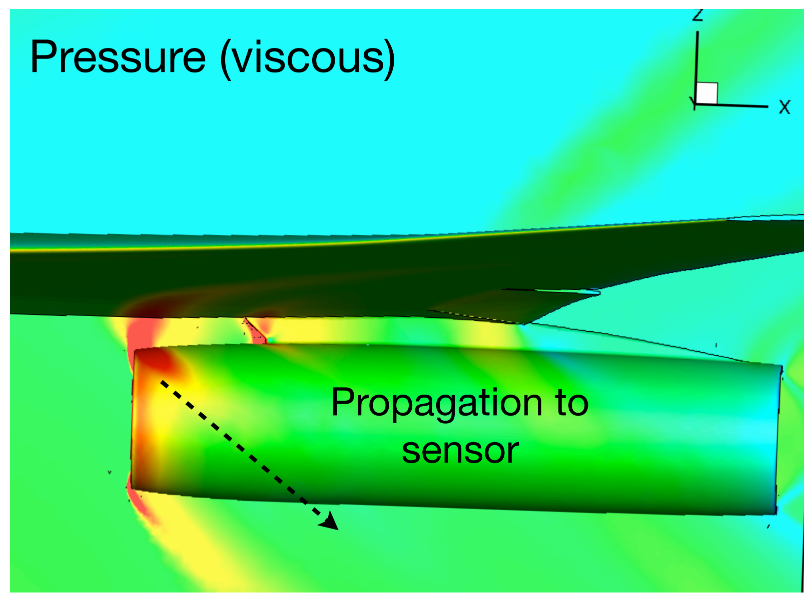

LM 1021: Investigation of On-track Discrepancy

- Compare viscous and inviscid
- Boundary layer extends to nacelle
- Inviscid has supersonic flow between underside of wing and nacelle
- Inviscid shock is delayed (oblique)
- 2nd peak comes from pylon

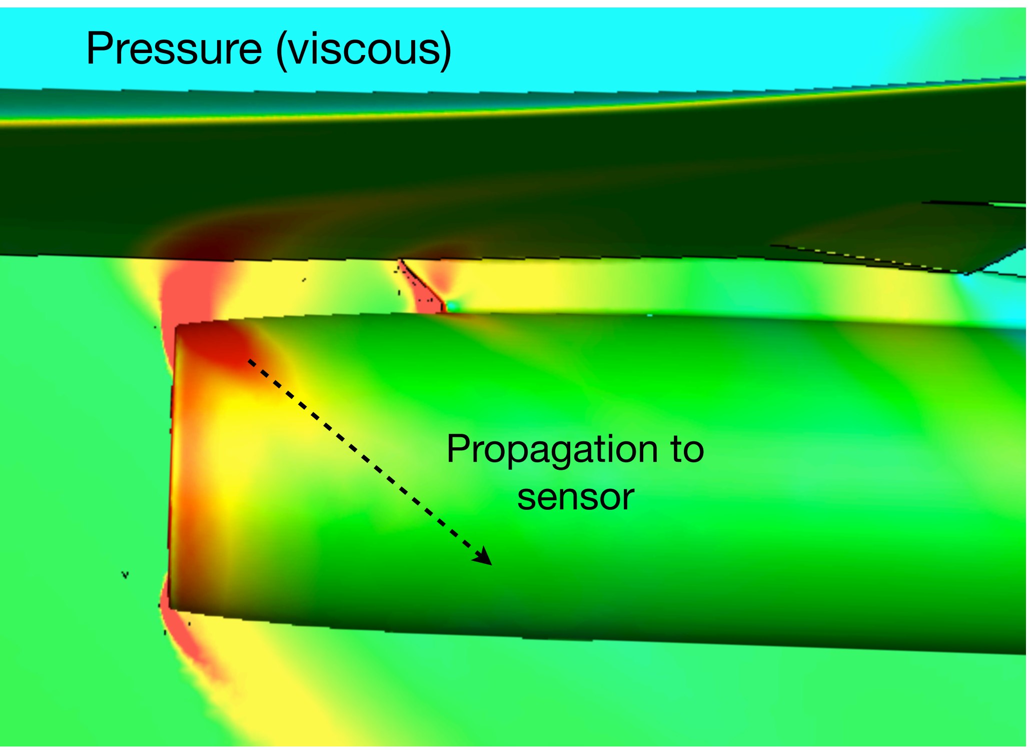

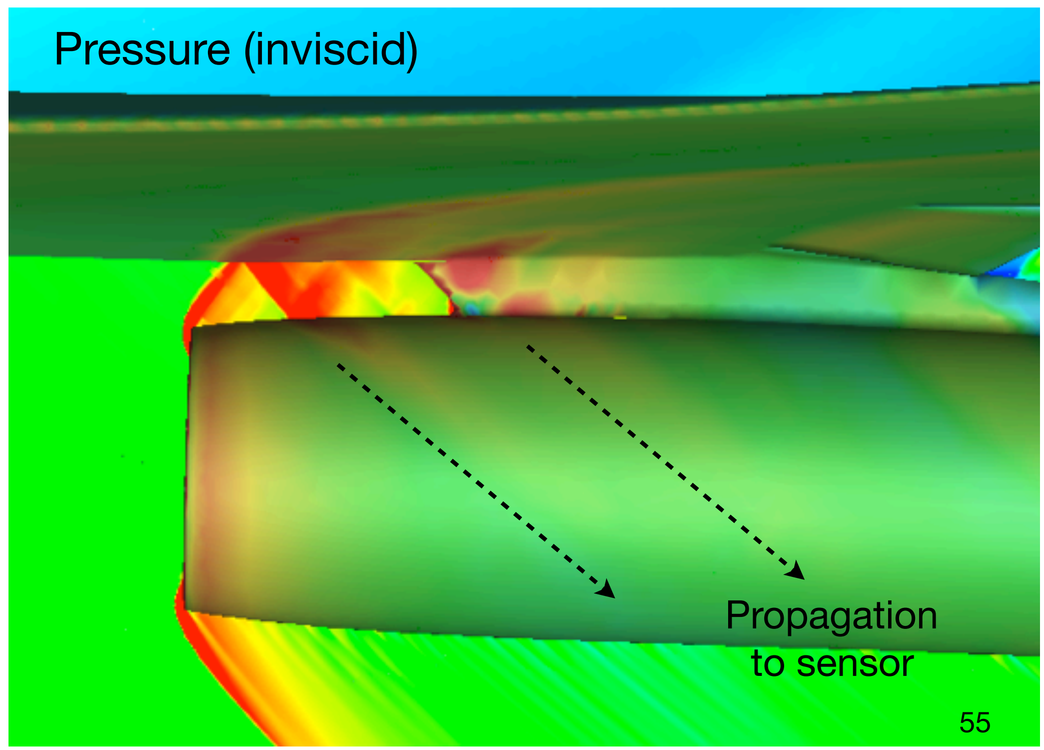

LM 1021: Investigation of

- Compare viscous and inviscid
- Boundary layer extends to nacelle
- Inviscid has supersonic flow between
- Inviscid shock is delayed (oblique)
- 2nd peak comes from pylon

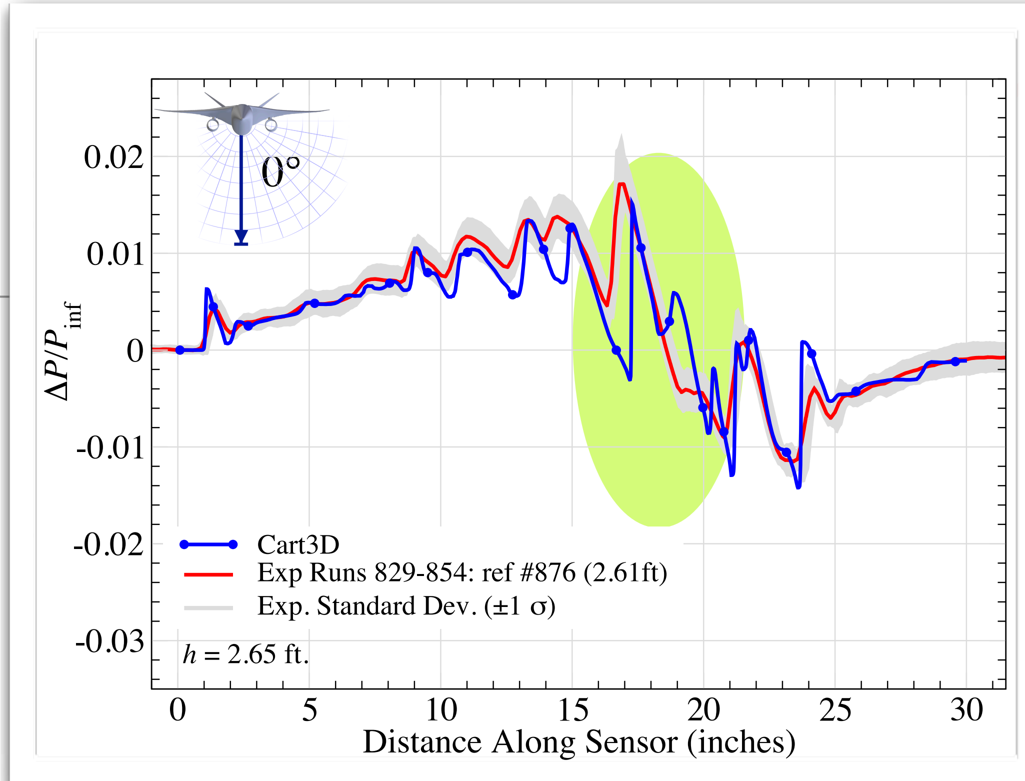

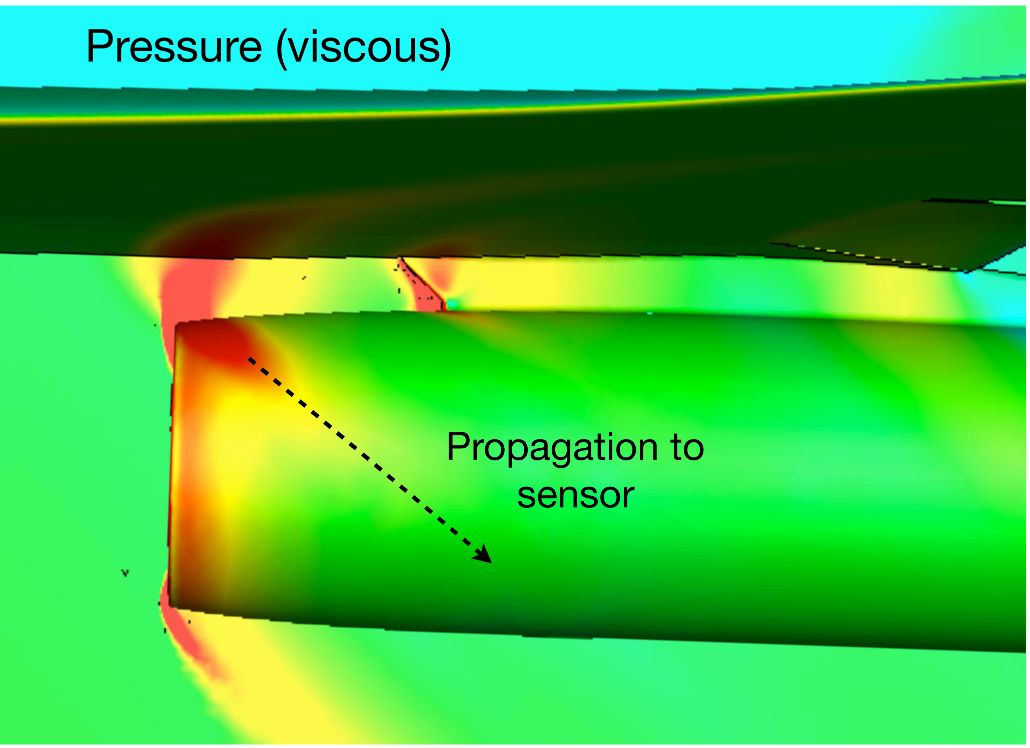

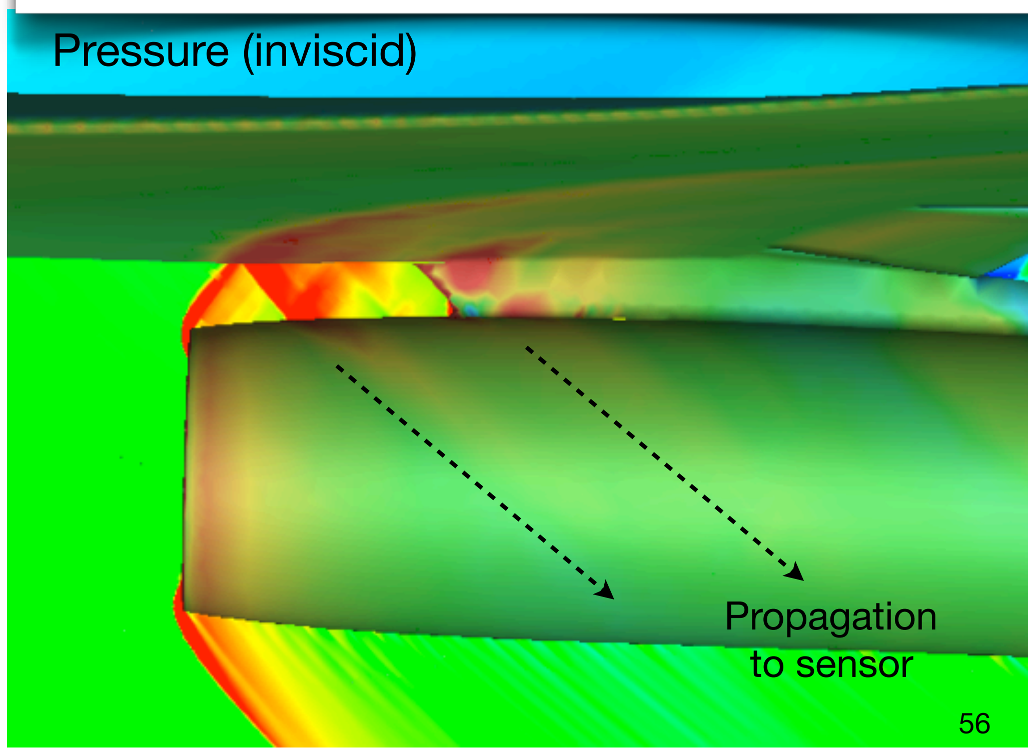

Summary

- Presented results for SEEB-ALR, DWB and LM 1021 using inviscid Cartesian method with
  - Automated meshing & adjoint-driven adaptation used for all cases
  - Presented evidence of mesh convergence

    (1) Pressure signature

    (2) Output Functional

    (3) Adjoint correction and error estimate
  - Computational resources
    - Seeb-ALR: ~1hr on a quad-core laptop in ~3.6 Gb
    - LM 1021: Under 2.5hrs on 96 cores in 80 Gb

Summary

- Presented results for SEEB-ALR, DWB and LM 1021 using inviscid Cartesian method with
  - Automated meshing & adjoint-driven adaptation used for all meshing
  - Presented evidence of mesh convergence
    - (1) Pressure signature
    - (2) Output Functional
    - (3) Adjoint correction and error estimate
  - Computational resources
    - Seeb-ALR: ~1hr on a quad-core laptop in ~3.6 Gb
    - LM 1021: Under 2.5hrs on 96 cores in 80 Gb
- Investigations
  - SEEB-ALR:
    - Showed that differences in main expansion are likely due to influence of rail leading-edge compression impacting shoulder of model
    - Results are consistent w/ earlier studies
  - LM 1021:
    - Good agreement off-track
    - Low tunnel Reynolds number results in differences in on-track signal
    - Showed a powerful technique using the adjoint-solver to trace specific regions of the signature to particular regions of the surface geometry and near-body flow

Summary

- Presented results for SEEB-ALR, DWB and LM 1021 using inviscid Cartesian method with
  - Automated meshing & adjoint-driven adaptation used for all meshing
  - Presented evidence of mesh convergence
    - (1) Pressure signature
    - (2) Output Functional
    - (3) Adjoint correction and error estimate
  - Computational resources
    - Seeb-ALR: ~1hr on a quad-core laptop in ~3.6 Gb
    - LM 1021: Under 2.5hrs on 96 cores in 80 Gb
- Investigations
  - SEEB-ALR:
    - Showed that differences in main expansion are likely due to influence of rail leading-edge compression impacting shoulder of model
    - Results are consistent w/ earlier studies
  - LM 1021:
    - Good agreement off-track
    - Low tunnel Reynolds number results in differences in on-track signal
    - Showed a powerful technique using the adjoint-solver to trace specific regions of the signature to particular regions of the surface geometry and near-body flow

Thanks!

- Fundamental Aeronautics High Speed Project for support & leadership
- Workshop Organizing committee
- Susan Cliff, Don Durston, David Rodriguez and Mathias Wintzer

Questions?